Final Interpretative Report on the Airborne Electromagnetic Survey of the Gilcrest and La Salle Areas of the Central Colorado Water Conservancy District

Photo by John Fingerlin

Jared Dale Abraham, MS
Principle Geophysicist

Theodore H. Asch, PhD
Research Geophysicist

James C. Cannia
Principle Geologist

Aqua Geo Frameworks, LLC
130360 County Road D
Mitchell, NE 69357

Paul G. Ivancie, CPG
Ivancie Geoscience, LLC
2717 S Monroe St
Denver, CO 80210

April 16, 2018

Executive Summary

Aqua Geo Frameworks, LLC. (AGF) is pleased to submit this report titled "*Final Interpretative Report on the Airborne Electromagnetic Survey of the Gilcrest and La Salle Areas of the Central Colorado Water Conservancy District*". The Central Colorado Water Conservancy District (CCWCD) commissioned a subsurface study to increase understanding of the South Platte River hydrogeology near Gilcrest and La Salle, Colorado. In particular, how the hydrostratigraphy in the near-surface which might be related to high groundwater levels in the area. AGF entered into an agreement with the CCWCD to collect, process, and interpret airborne electromagnetic (AEM) data, in conjunction with other available background information, to develop a 3D hydrogeologic framework of the Gilcrest project area, and to recommend future work to enhance groundwater management activities for managed aquifer recharge (MAR).

The scope of work for this project was as follows:

1. SCOPE OF WORK

1.1 AGF began project planning upon signing of the project between the parties. This work included flight plans, database development, and review of hydrogeologic and geologic work for the area. The CCWCD assisted in providing information such as power line maps, test hole databases, and related aquifer characteristic studies to AGF.

1.2 At the conclusion of the design process, the maximum line length for the Gilcrest AEM survey area was about 10 miles in length in the north-south direction and about 6 miles in the east-west direction. Flight lines were separated by up to 4 km and were as close as 250 m.

1.3 An AEM survey utilizing the SkyTEM304M system was flown over the CCWCD areas along reconnaissance-spaced flight lines and in the flight blocks.

1.4 Approximately 154 line-miles (250 line-kilometers) were acquired over the Gilcrest-La Salle AEM survey area on June 2nd-3rd, 2017. Status reports of the flying were provided to the Contract Representative of CCWCD on a daily basis, including the areas flown, production rates, and flight plan for the following day.

1.5 These flights were provided as preliminary AEM inversions on June 4th to 5th, 2017 and the final AEM data and inversions are included as a product attached to this data report. A preliminary data quality report was provided to CCWCD on June 16, 2017. A presentation to the CCWCD Board of Directors was given on September 19, 2017.

1.6 After final processing, 72.0 line-miles (116.6 line-km) of data were retained for the final inversions for the Gilcrest AEM survey area. This amounts to a data retention of 46.6%. This is due to the high level of infrastructure in the area. The final inverted georeferenced data are delivered to the CCWCD with this report. After inversion, AGF derived 2D sections, 3D electrical models, and interpreted geologic and hydrogeologic surfaces of the surveyed area.

1.7 AGF is providing a hydrogeologic framework report that includes maps of aquifer(s), maps of aquifer materials relationships to current test holes and production groundwater wells, estimates of water storage capacity, and maps of estimated potential recharge areas in the block flight areas. This report, as mentioned above, also includes all data (acquired, processed,

developed) files. The report is delivered in PDF digital format and the data in ASCII and native formats.

2. KEY FINDINGS

2.1 Boreholes - The borehole information was gathered from two sources: 1) Colorado Geological Survey (CGS) Gilcrest/LaSalle Pilot Project Hydrogeologic Characterization Report which contains information on 432 boreholes which the CGS has inspected and summarized lithologies; and 2) 62 additional wells from the Colorado Department of Water Resources (CO-DWR) database. In some cases, wells were extended into the bedrock units by reexamining the well information from the CO-DWR database. No boreholes within the AEM study area contained usable geophysical logs that were within the Quaternary materials. Some oil and gas wells had geophysical logs but logs were acquired below the depth of interest for this study.

2.2 Digitizing Interpreted Geological Contacts - Characterization and interpretation of the subsurface was performed in cross-section and derived surface grid formats. Contacts between the geologic units were digitized in 2D including: Quaternary (***Q***) and Cretaceous Laramie Formation (***Kl***), Cretaceous Fox Hills Sandstone (***Kfh)***, and Cretaceous Pierre Shale ***(Kp)***. The interpretive process benefited from the use of CGS and DWR borehole logs. Surface grids of the interpreted geologic formations were then produced. Each flight line profile with interpretation, including the ***Q*** aquifer lithology classes and ***Kl***, ***Kfh***, and ***Kp*** are included in the appendices as well as interpretative surface grids.

2.3 Resistivity/Lithology Relationship - Assessment of the sediment character in the ***Q*** deposits was conducted to determine the overall composition of the major categories used to define the aquifer and aquitards in the Gilcrest AEM survey area. Resistivity thresholds were used to characterize silt and clay (<16 ohm-m), sand and silt (16-23 ohm-m), sand and gravel (23-40 ohm-m), and gravel (>40 ohm-m). This allowed for the characterization of the ranges of resistivities present in the ***Q*** deposits.

2.4 Hydrogeological Framework of the Gilcrest AEM Survey Area - The AEM reveals considerable variability in the ***Q*** deposits across the Gilcrest survey area. The subsurface distribution of materials in the ***Q*** can be generally characterized in aquifer materials made up of mostly alluvial gravel, sand and gravel, and sand and silt with non-aquifer material made up of silt and clay. Due to an extensive silt and clay layer in the southern part of the study area which splits the ***Q*** deposits horizontally, an area of semi confined to confined conditions exist that affect wells in that area. The ***Q*** aquifer of the Gilcrest AEM survey area is potentially hydrologically connected to the Cretaceous units present in the area, most likely the ***Kfh*** units; the ***Kp*** acts as a deeper bedrock aquiclude for the area in most areas.

2.5 Potential Recharge Zones within the Gilcrest AEM Survey Area - Each Gilcrest AEM flight line was interpreted for potential aquifer recharge material at the first model layer (0-3 ft) as well as the following layers: 3-7 ft, 7-11 ft, 11-16 ft, 16-21 ft, and 21-26 ft. These layers are the most useful for understanding the potential for recharge from the land surface downward to the aquifers. Areas of gravel material will have the highest potential to transmit the largest amount of water to the groundwater system, with sand and gravel potentially transmitting slightly less water from whatever source, downward, as both units are permeable. Sand and silt zones will have lower potential to transmit water downward and the silt and clay will transmit minimal to

no water to the groundwater aquifer. The best information for illustrating this concept is where the flight lines are closely spaced, as there is a greater number of soundings in close proximity to each other providing greater detail.

3. Recommendations

Recommendations provided to the CCWCD in this section are based on the interpretation and understanding gained from the addition of the AEM data to existing information and from discussions with the CCWCD about their management challenges.

3.1 **Additional AEM Mapping** -The aquifer maps provided in this report represent the detailed hydrogeologic framework developed for the Gilcrest survey area. The detail provided in the hydrogeological interpretation of the survey area allowed for confident development of a hydrogeologic framework. The interpretations match well with the boreholes and the historic work in the area. While no additional high resolution AEM information is needed within survey area to resolve questions of resource management, it is recommended that additional areas of closely spaced lines or "block flights" be collected to develop detailed frameworks as needed in other areas. This would be particularly important if a detailed understanding of the near surface for recharge infrastructure or well field development is necessary. Surface geophysical, specifically EM or electrical, data acquisition could also be used to gain a detailed understanding of the near surface in small areas.

3.2 **Update the Water Table Map** - The groundwater data used in the analyses presented in this report use the 2017 water table map from the CGS. Additional water level measurement locations would improve the water table map if the mapped area is expanded to include all of the Gilcrest survey area and beyond. This is especially true on the north, west and south sides of survey area. Additional monitoring wells added to the network to understand the semi-confined and confined nature of the aquifers under the silt and clay layer on the south side would be beneficial.

3.3 **Siting new test holes and production wells** - The AEM framework maps and profiles provided in this report provide insight in 3D on the relationship between current boreholes and production groundwater wells. At the time of this report, the currently available lithology data for the Gilcrest area was used in building the framework maps and profiles. It is recommended that the results from this report be used to site new test holes and monitoring wells. Often test holes are sited based on previous work that is regional in nature. By utilizing the maps in this report, new drilling locations can be sited in optimal locations. The location of new water supply wells can also use the results in this report to guide development of sites. Planners should locate wells in areas of greatest saturated thickness with the best understanding of how the well production will be used in groundwater management related to CCWCD activities. Additional monitoring wells added to the network to understand the semi-confined and confined nature of the aquifers under the silt and clay layer on the south side would be beneficial.

3.4 **Aquifer testing and borehole logging** - Aquifer tests are recommended to improve estimates of aquifer characteristics. A robust aquifer characterization program is highly recommended at the state, District's and smaller entity levels. Aquifer tests can be designed based on the results of AEM surveys and existing production wells could be used in conjunction with three or more

installed water level observation wells. Additional test holes with detailed, functional, and well calibrated geophysical logging for aquifer characteristics are highly recommended. The lack of test holes with geophysical logs in the Gilcrest survey area did provide added complexity and uncertainty to the interpretation. Borehole geophysical logs would have made this investigation more robust. Examples of additional logging would be flow meter logs and geophysical logs including gamma, neutron, electrical, and induction logs. Detailed aquifer characteristics can be accomplished with nuclear magnetic resonance logging (NMR). This is a quick and effective way to characterize porosity and water content, estimates of permeability, mobile/bound water fraction, and pore-size distributions with depth. This is very cost effective when compared to traditional aquifer tests.

3.5 **Recharge Zones** - The Gilcrest hydrogeologic framework in this report provides a focus upon areas of recharge from the ground surface to the groundwater aquifer. The block flights of AEM data acquisition provide the most detailed information for understanding recharge throughout the Gilcrest survey area. It is recommended that additional AEM data be collected, or surface geophysical data utilizing closely-spaced lines for near-surface resolution as needed related to CCWCD activities. It is further recommended that future work integrate new soils maps with the results of this study to provide details on soil permeability, slope, and water retention to provide a more complete understanding of the transport of water from the land surface to the groundwater aquifer.

3.6 **Managed Aquifer Recharge** - The area which lies out of the silt and clay layer on the south side of Gilcrest may have the best potential for managed aquifer recharge. The unsaturated thickness map provided in the report is the best guide to looking for optimal sites when combined with the other information provided within the report. Detailed analysis for this purpose would need to be done to determine if this is a viable opportunity for the CCWCD. Additional AEM mapping within CCWCD would also locate similar locations. These detailed maps will benefit the CCWCD in locating and developing Managed Aquifer Recharge sites and would be beneficial for siting areas to provide storage and release of water for stream flow and other uses.

4. Deliverables

In summary, the following are included as deliverables:

- Raw EM Mag data Geosoft database and ASCII *.xyz
- SCI inversion Geosoft database and ASCII *.xyz
- Borehole Geosoft databases and ASCII *.xyz
- Interpretations Geosoft database and ASCII *.xyz
- Raw Data Files - SkyTEM files *.geo, *skb, *.lin
- ESRI ArcView and Geosoft grid files – surface, topo, etc.
- 3D fence diagrams of the CCWCD survey lines.
- 3D voxel models as ASCII *.xyz and *.gdb for the Gilcrest AEM survey areas
- KMZs for the Gilcrest AEM survey

Table of Contents

List of Figures

List of Tables

List of Abbreviations

2D	Two-dimensional
3D	Three-dimensional
$A*m^2$	Ampere meter squared
AEM	Airborne Electromagnetic
AGF	Aqua Geo Frameworks, LLC
ASCII	American Standard Code for Information Interchange
CCWCD	Central Colorado Water Conservancy District
CGS	Colorado Geological Survey
cm	Centimeter
CDSS	Colorado Decision Support System
CO-DWR	Colorado Department of Water Resources
COGCC	Colorado Oil and Gas Conservation Commission
CWCB	Colorado Water Conservation Board
dB/dt	Change in amplitude of magnetic field with time
DEM	Digital Elevation Model
DOI	Depth of Investigation
DGPS	Differential global positioning system
FT	Fourier Transform
GIS	Geographic Information System
gpm	Gallons per minute
HEM	Helicopter Electromagnetic
Hz	Hertz (cycles per second)
IGRF	International Geomagnetic Reference Field
Km/km	Kilometers
KMZ/kmz	Keyhole Markup language Zipped file
Kfh	Cretaceous Fox Hills Sandstone
Kl	Cretaceous Laramie Formation
Kp	Cretaceous Pierre Shale
LCI	Laterally-Constrained Inversion
LiDAR	Light Detecting and Ranging
m	Meters
MAG	Magnetic (data); Magnetometer (instrument)
MAR	Managed Aquifer Recharge
MCG	Minimum curvature gridding
N	North
NAD83	North American Datum of 1983
NAVD88	North American Vertical Datum of 1988
NED	National Elevation Dataset
NMR	Nuclear Magnetic Resonance
NRD	Natural Resources Districts
nT	Nano-Tesla
OM	Geosoft Oasis montaj
Ohm-m	Ohm-meter
PA	Profile Analyst
PFC	Primary Field Compensation
PLNI	Power Line Noise Intensity

Q	Quaternary
Qal	Quaternary alluvial deposits
Qe	Quaternary eolian deposits
Qpc	Quaternary Piney Creek Alluvium
Qpp	Quaternary Post-Piney Creek Alluvium
Qsw	Quaternary slope wash deposits
Qt	Quaternary terrace deposits
Qtb	Quaternary Broadway Alluvium
QA/QC	Quality Assurance/Quality Control
RMF	Residual Magnetic Field
R	Range
Rx	Receiver
S	South
SCI	Spatially-Constrained Inversion
SPDSS	South Platte Decision Support System
STD	Standard Deviation
TDEM	Time-Domain Electromagnetic
TEM	Transient Electromagnetic
T	Township
Tx	Transmitter
USGS	United States Geological Survey
UTM	Universal Transverse Mercator
W	West
X	Positive in the easting direction of the Cartesian coordinate system
XYZ	ASCII file type
Y	Positive iin the northing direction of the Cartesian coordinate system
Z	Positive in the “up” vertical direction in Cartesian coordinate system

1 Introduction

The Central Colorado Water Conservancy District (CCWCD) required a detailed hydrogeological framework of the area around Gilcrest and La Salle, Colorado in order to understand the groundwater system in the area. CCWCD contracted Aqua Geo Frameworks, LLC (AGF) to implement an Airborne Electromagnetic (AEM) survey of selected areas in the vicinity of Gilcrest and La Salle, Colorado (Figure 1-1). Specifically, CCWCD would like to gain knowledge of the distribution of aquifer materials and their relations to high groundwater levels in the area. The existence of a near surface clay layer in the Quaternary sediments that fill the South Platte River basin are known from borehole descriptions and previous reports from the Colorado Geologic Survey (Barkmann et al., 2014). What is not known is the continuity of the silt and clay layers between the boreholes and their spatial geographic relationship to the valley. A map showing the overlap of the Barkmann et al. (2014) study and the AEM survey area is presented in Figure 1-2.

Use of AEM technology to map and evaluate groundwater resources has gained momentum over the last 20 years in the United States and abroad. The state of Nebraska has been on the forefront of implementing AEM for water resources management over the last decade with projects across the state in a variety of geologic settings. Specifically, for the Platte River system, previous work for the South Platte, North Platte, and Twin Platte Natural Resources Districts have mapped areas of the North Platte, South Platte, and Platte rivers in areas of western Nebraska (AGF, 2017; Hobza et al., 2014; Abraham et al., 2011). These studies provided detailed information on the elevation of the base of aquifer and the Quaternary alluvial materials associated with the Platte River system.

The AEM survey data was acquired June 2 – 3, 2017 and totaled approximately 155 line-miles (~250 line-km) (Figure 1-3). A preliminary report on the AEM survey containing the QA/QC results and the preliminary laterally-constrained inversion (LCI) results were presented to CCWCD on June 16, 2017. The final inversions and interpretation of the survey data began in February 2018. Spatially-constrained Inversions (SCI) were performed on the data to derive an electrical resistivity earth-model. That model was then interpreted to provide a 3D hydrogeological framework of the survey area utilizing borehole lithology and other geological and hydrogeological inputs.

The results of the AEM survey provides near continuous geographic coverage of the subsurface in the project area within the block flight area near Gilcrest and reconnaissance level information along the flight lines outside the block flight area. The survey provided a 3D representation of the Cretaceous bedrock and Quaternary sediments separated into four distinct lithology classes including: Silt and Clay; Sand and Silt; Sand and Gravel; and Gravel and their relationship to the water table. The 3D representation also provides the relationship between the hydrogeologic framework showing the aquifers of the area and the test holes and production wells of the area and information on the groundwater recharge of the area from overlying soils and constructed recharge basins used by the CCWCD.

This investigation should enhance CCWCD's understanding of the subsurface in detail to best improve current and future water management planning and activities.

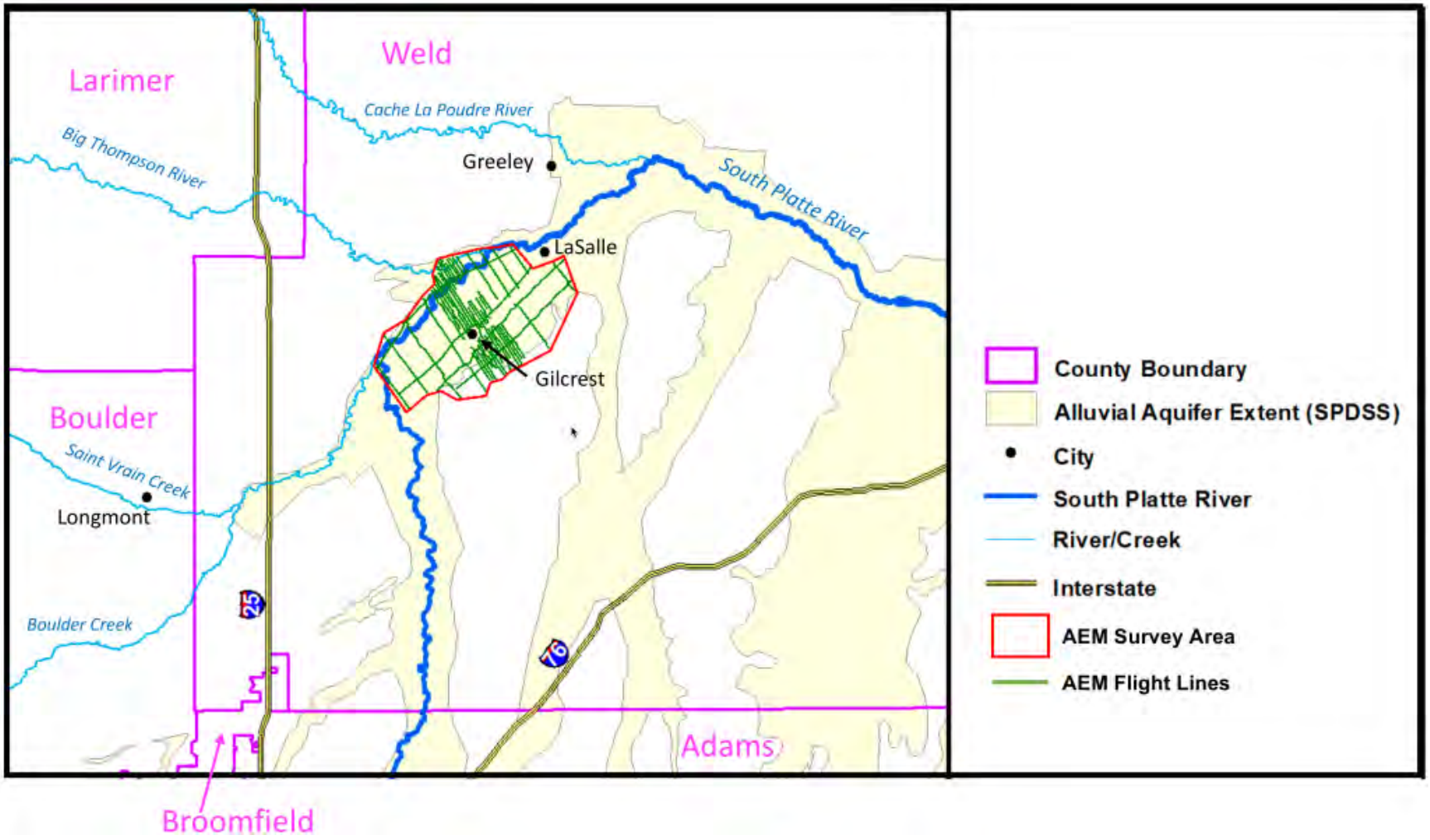

Figure 1-1. General location map of the AEM survey and flight lines within the Central Colorado Water Conservancy District, Weld County, Colorado along the South Platte River centered on the town of Gilcrest. The map is also showing the major surface water features and the alluvial aquifer extent from the South Platte Decision and Support System (SPDSS) (base map modified from Barkmann et al., 2014)

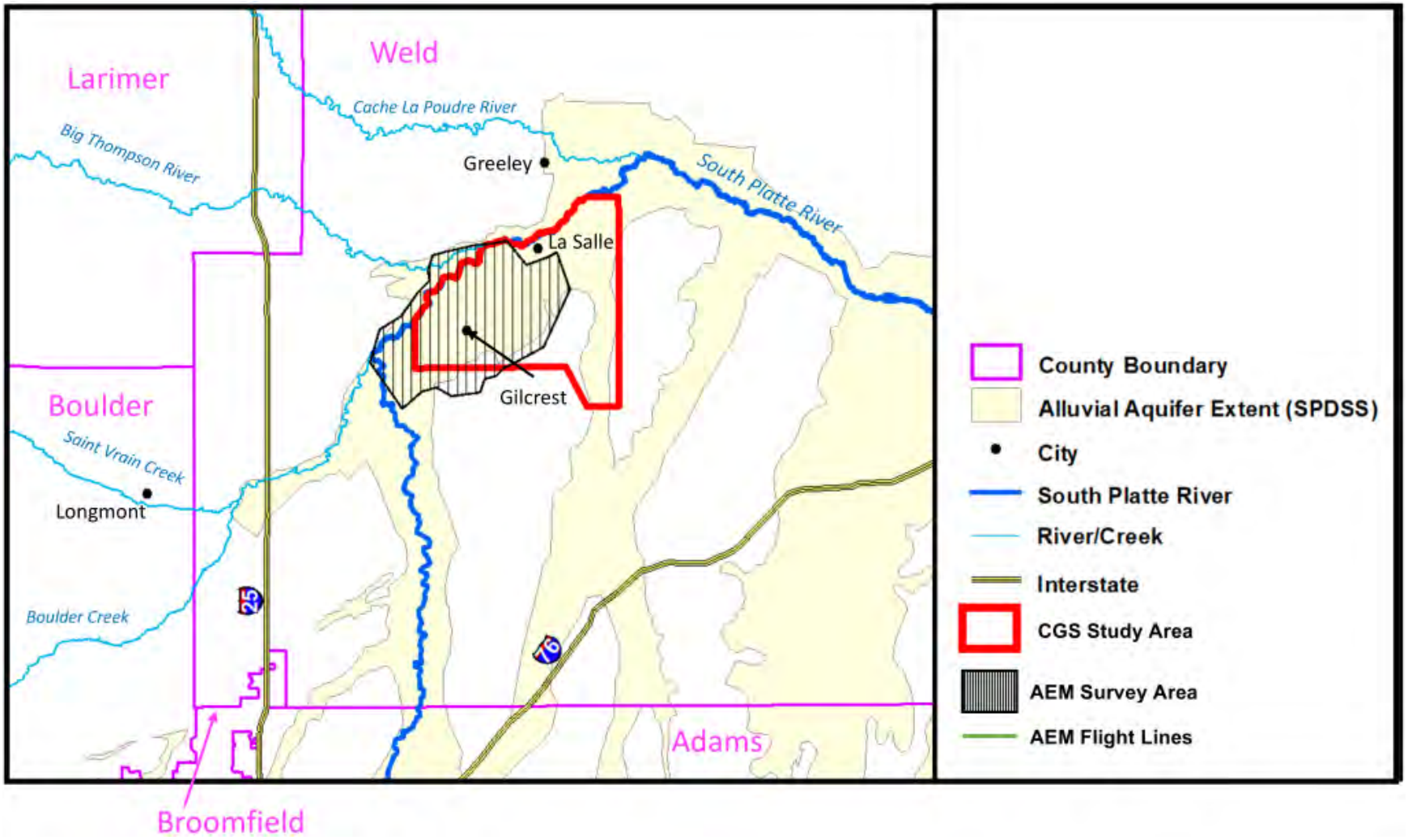

Figure 1-2. General location map of the AEM Survey within the Central Colorado Water Conservancy District, Weld County, Colorado along the South Platte River centered on the town of Gilcrest and the Colorado Geological Survey Gilcrest/LaSalle Pilot Project area (Barkmann et al., 2014). The map is also showing the major surface water features and the alluvial aquifer extent from the South Platte Decision and Support System (SPDSS) (base map modified from Barkmann et al., 2014)

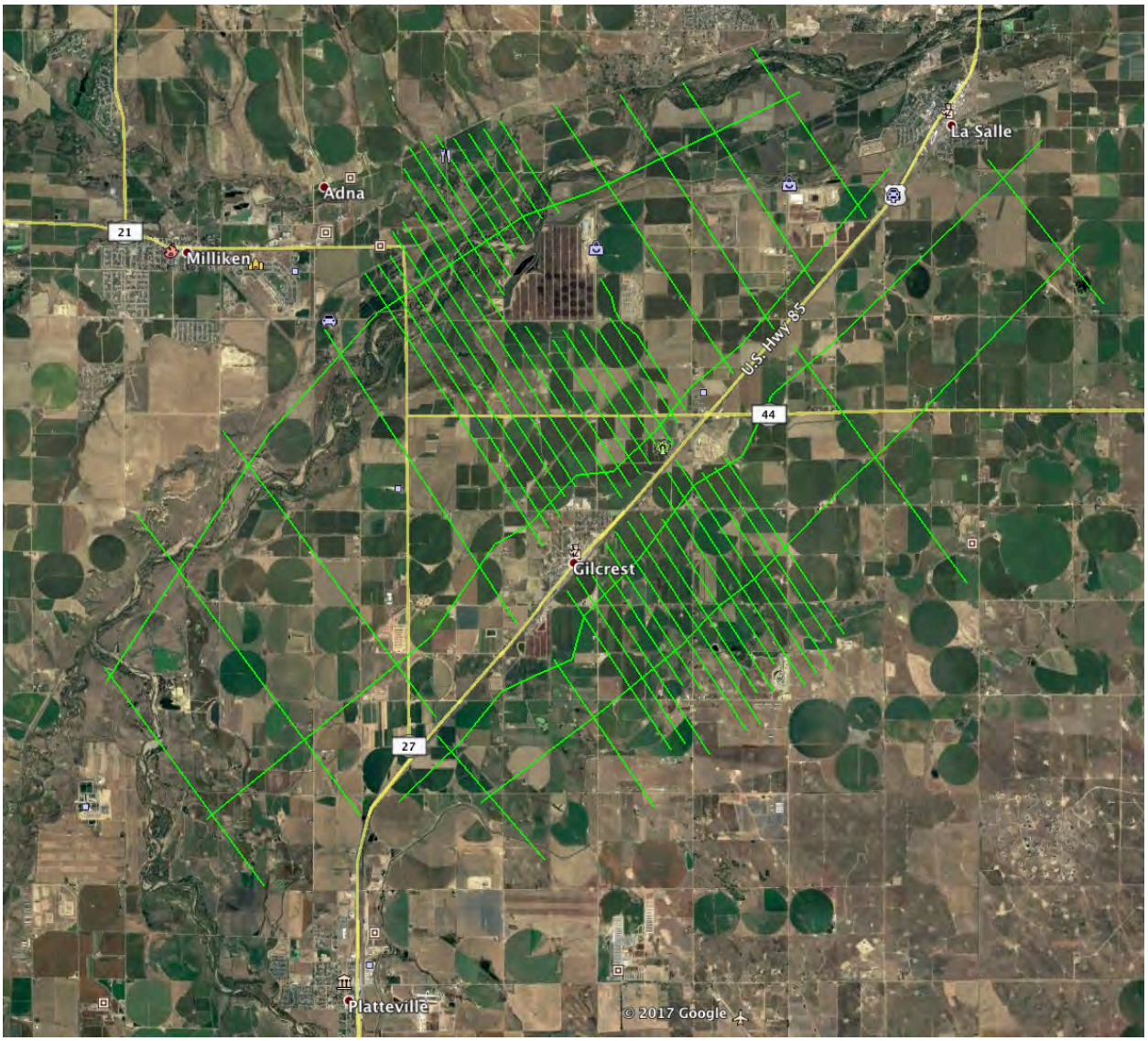

Figure 1-3. Google Earth image of the AEM survey lines around Gilcrest, Colorado.

2 Geological and Hydrogeological Setting

Various sources of background information were used to interpret the AEM data, which is discussed in Section 5.

2.1 Background Geology

2.1.1 South Platte River Basin

The alluvial deposits of the South Platte River Basin consist of primarily sand and gravel with finer grain floodplain deposits in the valley floor areas. The alluvium in the major tributaries and the main stem comprises a continuously connected aquifer system. The alluvial aquifer is in hydraulic communication with the surface water system throughout most of the basin. The extensive development of irrigation with surface water diversions and groundwater pumping results in gaining conditions for the majority of streams since percolation of applied irrigation water raises water levels. The maximum thickness of alluvial deposits increases in a downstream direction on the main stem, with saturated thickness of 20 to 40 feet at the upstream extent near Denver, to more than 200 feet near Julesburg, Colorado. Saturated aquifer thickness is typically lower in tributary streams (CDM Smith, 2013).

2.1.2 South Platte Alluvial Valley – Gilcrest/LaSalle Area

The AEM survey area is in Weld County, Colorado, which includes the towns of Gilcrest and LaSalle in the South Platte River valley. The study area lies in the northern portion of the Denver Basin and on the south flank of the Greeley Arch. The survey includes the South Platte River alluvial valley, consisting of the South Platte River floodplain and bounded by adjacent upper alluvial terraces. The South Platte alluvial aquifer underlies most of the floodplain and varies from zero to more than 100 feet thick. The South Platte alluvial aquifer is a heterogeneous geologic unit composed of interbedded gravel, sand, silt, and clay. Highly permeable coarse-grained material dominates the central portion of the aquifer and is interbedded with lenses of less permeable fine-grained material. The alluvial aquifer fills a channel incised into bedrock of the Upper Cretaceous Laramie Formation (***Kl***) and underlying Cretaceous Fox Hills Sandstone (***Kfh***). On the aquifer flanks, sheet wash deposits derived from the fine- grained Laramie Formation or loess form low-permeability deposits locally overlain by sand and loess (Barkmann et al., 2014).

2.1.3 Survey Area Geologic Units

The bedrock formations listed below only outcrop in limited extent within the study area; however, these units underlie the eolian and alluvial deposits.

Cretaceous Laramie Formation (***Kl***) – The upper part, 600-650 feet thick, is mostly gray claystone, shale, sandy shale, and scattered lenticular beds of sandstone and lignite. The lower part, about 75 to 120 feet thick, is light-gray to light yellowish-gray sandstone and sandy shale interbedded with clay, shale, and several beds of coal.

Cretaceous Fox Hills Sandstone (***Kfh***) – The upper part consists of cross-bedded tan sandstone. ***Kfh*** grades downward into brown, fine-grained silty sandstone interbedded with gray fissile shale. Locally it may contain thin coal beds. The thickness of this unit is about 300 to 500 feet.

Cretaceous Pierre Shale (***Kp***) -Marine shale mainly deposited in outer and deeper marine environments. The ***Kp*** deposits are intercalated with shallow to coastal marine sediments (Dechesne et al., 2011). The contact between the ***Kfh*** and underlying Pierre Shale is gradational consisting of sandstone interbedded with shale and shale becoming more prevalent at greater depth. Though the ***Kp*** does not outcrop in the study area, this formation comprises the lower-most confining unit among the hydrogeologically significant strata present.

Overlying the bedrock is a series of unconsolidated geologic units that comprise the South Platte alluvial aquifer in the study area. These geologic units influence the groundwater flow, aquifer productivity, and groundwater levels.

Slope Wash Deposits (***Qsw***) – This unit is a modification based on mapping by Smith et al. (1964) who describes slope wash as consisting of gravel and sand interbedded with clay and silt feathering out against upland areas, but lapping onto, and interlayering with, stream deposited valley fill deposits. Slope wash deposits are likely mobilized from uplands by precipitation resulting in sheet flow events and deposited below on gentler slopes.

Unnamed 3rd Level Terrace (***Qt3***) – This unit is based on physiographic evaluation of the study area and is mapped by Smith et al. (1964) as present in the western and southwestern portion of the Study Area.

Eolian Deposits (***Qe***) – (windblown clay, silt [loess], and sand) Light-brown to reddish-brown to olive-gray deposits of windblown clay, silt, and sand mainly as sand dunes in the east half of the area but also as a blanket of loess between the Front Range and the South Platte River. Loess is as much as 15 feet thick but generally is less than 3 feet thick; sand dunes are as much as 50 feet thick but generally are less than 15 feet thick.

Post-Piney Creek Alluvium (***Qpp***) – Dark-gray humic, sandy to gravelly alluvium. This unit underlies flood plains of major streams and terraces less than 10 feet above stream level. Thickness is from 5 to 15 feet.

Piney Creek Alluvium (***Qpc***) – Dark-gray humic sandy to gravelly alluvium containing organic matter. Underlies terraces whose surfaces are 10 to 20 feet above a nearby flood plain. Areas underlain by this formation along the South Platte River were partly flooded in 1965, again in 1973, and very likely in 2013).

Broadway Alluvium (***Qtb***) – Sand and gravel deposited by the South Platte River and its tributaries. Well-sorted and well-stratified sand and fine gravel. Along the South Platte River, Broadway Alluvium is as much as 125 feet thick but averages approximately 35 feet thick (Barkmann et al., 2014).

2.1.4 South Platte River Alluvial Valley Surficial Deposits

The South Platte alluvial aquifer consists of Quaternary-age unconsolidated alluvial deposits filling a paleo-channel incised into Upper Cretaceous-age mudstones and sandstones of ***Kl*** and ***Kfh***. The alluvial aquifer deposits consist of gravel, sand, silt and distinct silt and clay layers generally deposited by flowing water. These deposits are comprised primarily of material from the eroding mountains to the west where the main rivers and streams originate. Local ephemeral streams and slope wash contribute material eroded from the mudstone-dominant ***Kl*** and coarse-grained material from older high terrace deposits. The topography and unconsolidated sedimentary deposits of the South Platte River Basin record a gradual progression of incision overprinted by cycles in alluvial sediment supply. These cycles are associated with periods of glacial advance and retreat (Lindsey et al., 2005) and have resulted in a series of terraces flanking the modern stream course. The lowest terraces lie closest to the river and are youngest in age and are flanked by older terraces that step upward in elevation away from the river. All of these terraces are believed to overlie and be hydraulically connected with the alluvial aquifer. Locally, eolian sand and loess blanket both alluvium and bedrock. In other places, slope wash deposits consisting of fine-grained sediments spill from hillsides across lower terraces. Eolian and slope wash deposit thicknesses are generally 20 feet or less. (Barkmann et al., 2014)

2.1.5 Bedrock Topography and Geology

Bedrock formations in the Gilcrest area have only limited exposure due to a blanket of eolian deposits in the uplands and valley fill deposits in the alluvial valley. The bedrock surface topography underlying the alluvial valley is irregular and asymmetrical. This buried topography consists of a broad paleovalley incised by buried paleochannels. The bedrock geology underlying the alluvial aquifer consists of ***Kl*** and ***Kfh*** subcrops dipping gently to the southeast. This subcrop pattern is based on a projection from the subsurface using geophysical logs combined with surface outcrop patterns (Dechesne et al., 2011).

2.1.6 Borehole and Regional Mapping Data

Borehole data compiled beyond the 2014 Gilcrest Study database consisted of mainly well permits and related lithologic and stratigraphic logs. The borehole information was gathered from the following sources: Colorado Division of Water Resources (CO-DWR) Hydrobase (CO-DWR, 2018) and well records section, and the Colorado Water Conservation Board (CWCB) South Platte Decision Support System (SPDSS) alluvial aquifer GIS data set (CWCB, 2018). Colorado's Decision Support System (CDSS) was developed by CWCB with CO-DWR cooperation for each of Colorado's major water basins (Barkmann et al., 2014). The SPDSS GIS data set includes a collection and compilation of geologic and hydrologic data and collection of new data. Much of this data was from the USGS hydrologic atlases (Robson et al., 2000a; Robson et al., 2000b) for the South Platte alluvial aquifer which were incorporated into the SPDSS data set. The atlases provided general guidance on previous regional interpretation of the South Platte alluvial aquifer thickness, bedrock surface, and water table elevation.

There were few geophysical logs available in the project area. Geophysical log picks and logs were accessed using the CDSS online groundwater (geophysical logs) tools section. The database included log picks for tops and bases of the ***Kl***, ***Kfh***, and ***Kp*** bedrock formations derived from Colorado Oil and Gas Conservation Commission (COGCC, 2018) records and geophysical database. The CDSS online tools section provided a useful platform for comparing top and base data for the deeper Cretaceous bedrock picks across the study area.

A 288 foot geophysical log, *21011-F*, from a regional cross section M-M' (Barkmann et al., 2011) was utilized to provide context for the ***Kfh*** electrical section in the T3N R66W area (Figure 2-1). The log was one of the few geophysical records in the study area which was a contact resistance log and was of limited use. Regional cross section E-E' from Topper et al. (2017) was reviewed for stratigraphic context. The cross section incorporated area geophysical logs in the interpretation of the Quaternary alluvium and deeper Cretaceous bedrock formations.

2.2 Hydrology

Originating high in the Rocky Mountains, the main stem of the South Platte River and its many tributaries descend through high, glaciated mountain valleys before incising deep canyons through the foothills. Well known tributaries include the Big Thompson, Cache la Poudre rivers, and St. Vrain Boulder, Clear, and Cherry creeks. From Colorado, the South Platte River continues east to join the North Platte River at North Platte, Nebraska.

Ground water within the alluvial aquifers of the South Platte River basin is in hydraulic connection with the surface water, and therefore tributary to the surface water system. The alluvial aquifer system is generally unconfined and under water-table conditions. Infiltration from precipitation, irrigation, canal seepage, and pond seepage recharge the alluvial aquifers whereas ground water tends to discharge to the main channel of the river. Groundwater discharge to the river channel creates base flow to the river. The overall water balance in the alluvial aquifer system is complex and changes as the volume of water in storage in the aquifer varies with changes in water levels over time. Where the Denver Basin bedrock aquifers subcrop beneath the alluvium, they are in hydraulic connection with, and discharge into, the alluvial aquifers of the lower South Platte River basin (Topper et al., 2003)

Locally, in the Gilcrest area the shallow aquifer ranges in altitude from about 4780 in the southern area of the survey to about 4660 feet in the South Platte River valley near La Salle. Groundwater flows from areas of high water-table altitude toward areas of low water-table altitude along paths that are generally perpendicular to the water-table contours (Figure 2-2). Groundwater flows from upland areas toward stream valleys and thence, down the valleys or down the paleovalleys. Groundwater flows down the valley and toward the stream where the water may seep into the stream. Thus, the Saint Vrain creek and the South Platte River are gaining streams though most of the study area. Most of the groundwater in the study area that is not withdrawn by wells or consumed by evapotranspiration eventually flows to the South Platte River and leave the area as streamflow, canal flow, or as underflow through the unconsolidated sediments of the South Platte Valley near La Salle (Robson et al., 2000a). Groundwater flow in the central portion of the survey area is generally subparallel to the South Platte River, and throughout the entire study area has a strong northward flow component. Groundwater will

preferentially flow through the areas of highest transmissivity and can be expected to be highest through the transmissive sands and gravels in paleochannels. Constrictions of the high transmissivity zone, imposed by bedrock highs or low-permeability sediments, will limit the aquifer's capacity to transmit groundwater (Barkmann et al., 2014).

Irrigated agriculture plays an important role in the survey area's water balance. The survey area includes irrigation reservoirs, canals, and numerous ditches. In addition to surface water diversions, agricultural groundwater pumping from the highly productive alluvial aquifer plays an important role in the survey area hydrology, with many production wells capable of producing more than 1,000 gallons per minute (gpm). Several seepage canals traverse the low-lying flood plain to provide drainage in areas of historic high-water table conditions near the South Platte River. In addition to irrigation and seepage from reservoirs and ditches, which percolates into the aquifer, many ponds for augmentation recharge have been constructed within the survey area (Barkmann et al., 2014).

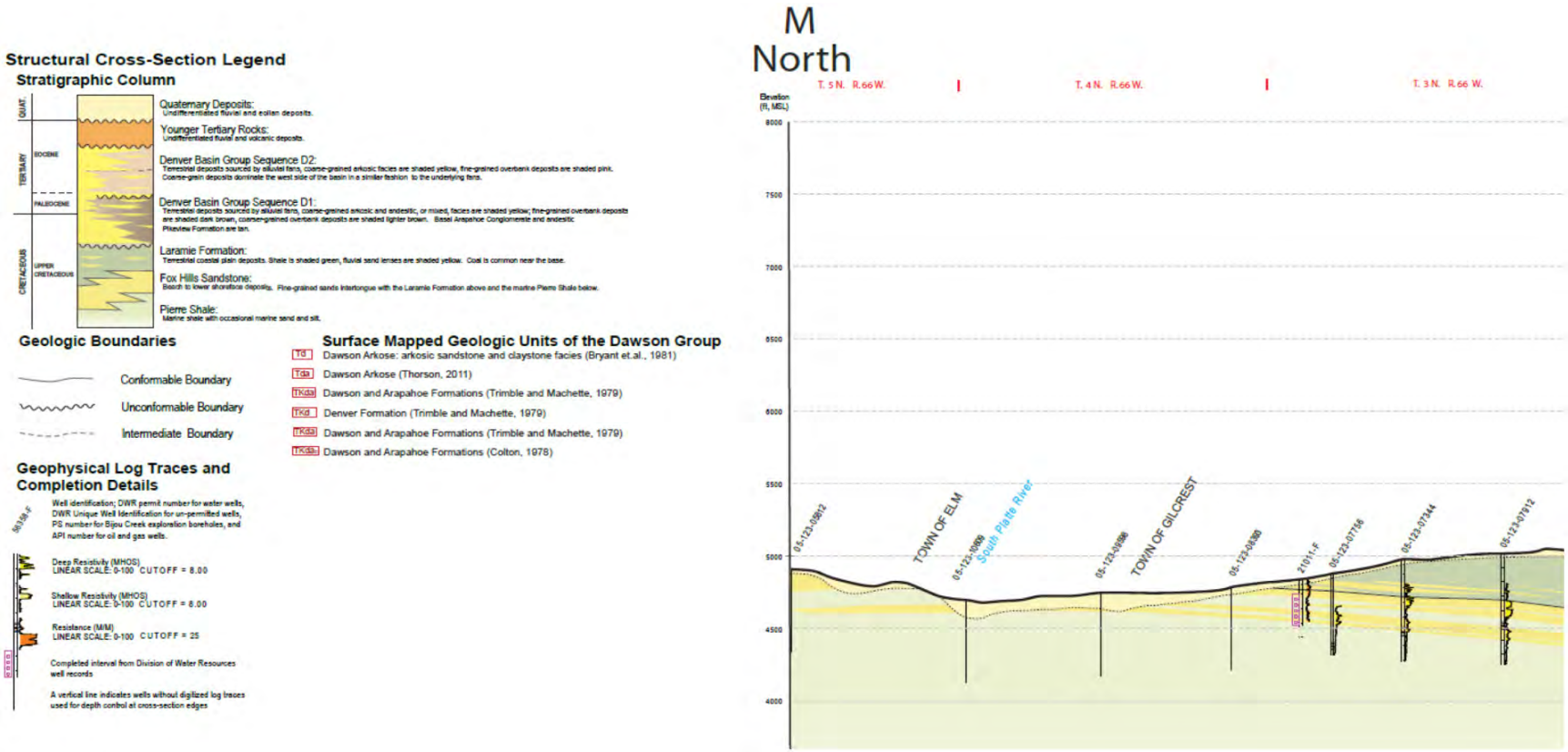

Figure 2-1. Northern end of the Cross-section M-M' from Barkmann et al. (2011) showing the area near Gilcrest, CO (Modified from Barkmann et al., 2011)

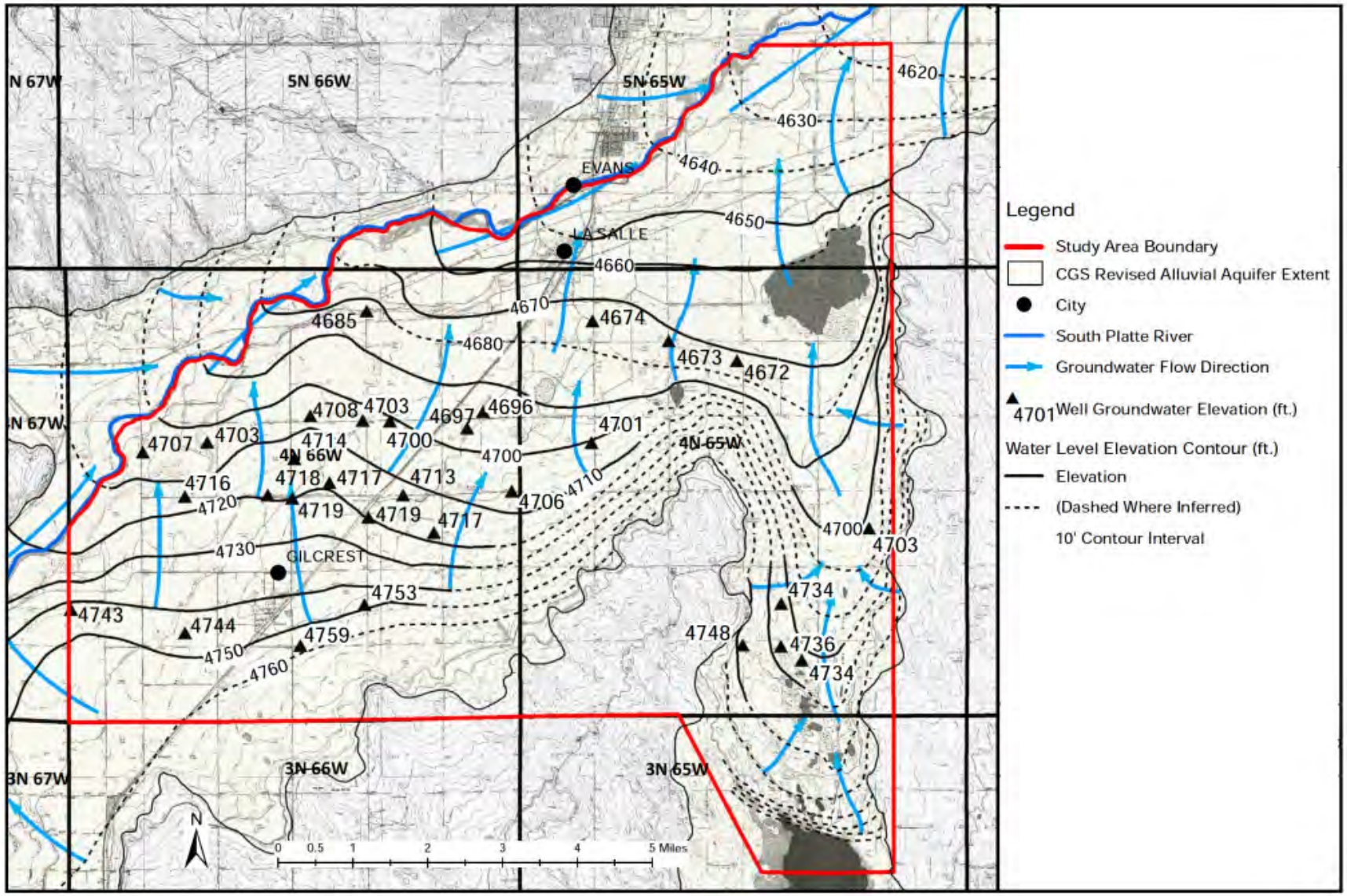

Figure 2-2. Map of the Spring 2012 water table and groundwater flow direction in the Gilcrest area. Modified from Barkmann et al. (2014).

3 Additional Background Information

Various sources of background information were used to interpret the AEM data, which is discussed in Section 5.

3.1 Borehole Data

Borehole data for this project consisted of lithologic logs. The borehole information was gathered from two sources: 1) CGS Gilcrest/LaSalle Pilot Project Hydrogeologic Characterization Report (Barkmann et al., 2014) which contains information from 432 boreholes that the CGS has inspected and summarized lithology; and 2) 62 additional wells from the CO-DWR database (CO-DWR, 2018) these lithologies were summarized similarly as Barkmann et al. (2014) with the exception of including the descriptions of the bedrock units' (***Kl***, ***Kfh***, and ***Kp***) lithologies (i.e. sandstone, shale, siltstone, and limestone). In some cases, wells identified in Barkmann et al. (2014) were extended into the bedrock units by reexamining the well information from the CO-DWR database. No boreholes within the AEM study area contained geophysical logs that were within the ***Q*** and contained calibrated resistivity logs. Some oil and gas wells had geophysical logs but were below the depth of investigation in this study.

The locations of all of the boreholes used within this study (494) are indicated in Figure 3-1.

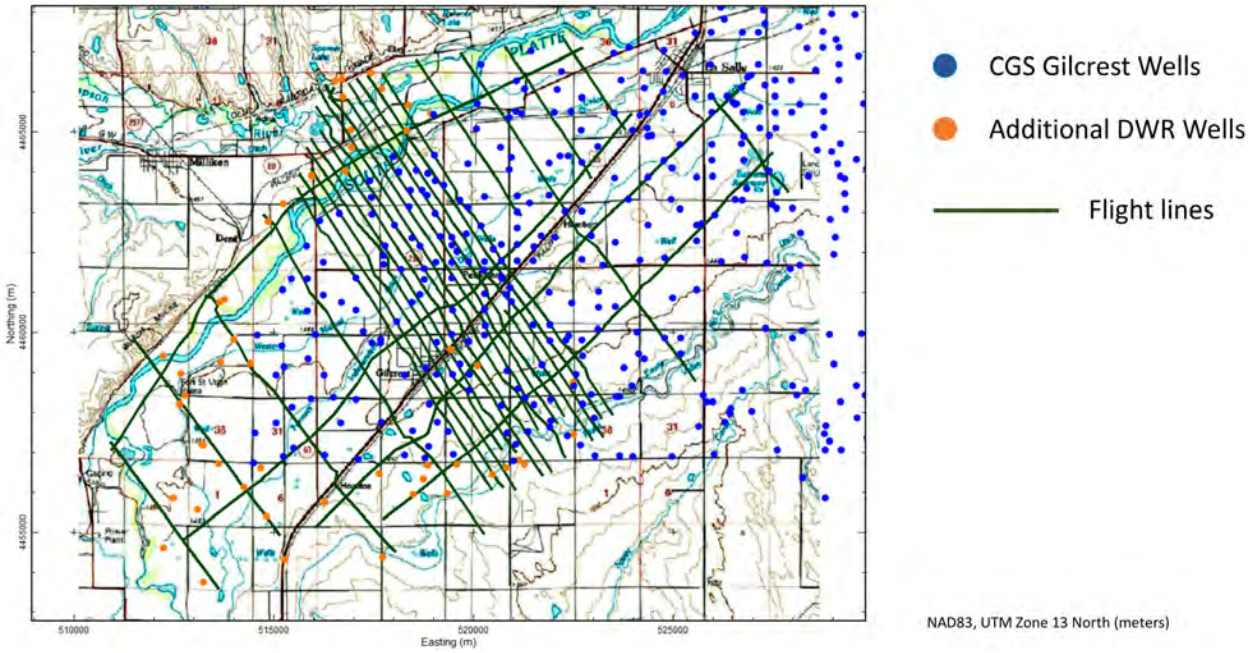

Figure 3-1. Location of the boreholes used in the Gilcrest AEM study including: 1) boreholes from Barkmann et al. (2014) as blue dots, and 2) additional boreholes form the CO-DWR (2018) database as orange dots. Flight lines are indicated as dark green lines. The base map is the 100K USGS topography map.

The borehole utilized in this study are included in Appendix_3_Deliverables/Boreholes as Geosoft Oasis montaj gdb databases and ASCII files.

3.2 Maps

Several maps were utilized in this study from Barkmann et al. (2014). These maps were delivered as ESRI ArcMap *.MDX files and were easily imported and utilized. These maps included: bedrock, surface geological maps, Quaternary deposits, transmissivity, hydraulic conductivity, depth to groundwater, saturated thickness. These maps served as a basis for the interpretation of the AEM data and were a great help in expediting the use of the information generated by the CGS. Figure 3-2 is an example of the map of the elevation of the bedrock from Barkmann et al. (2014).

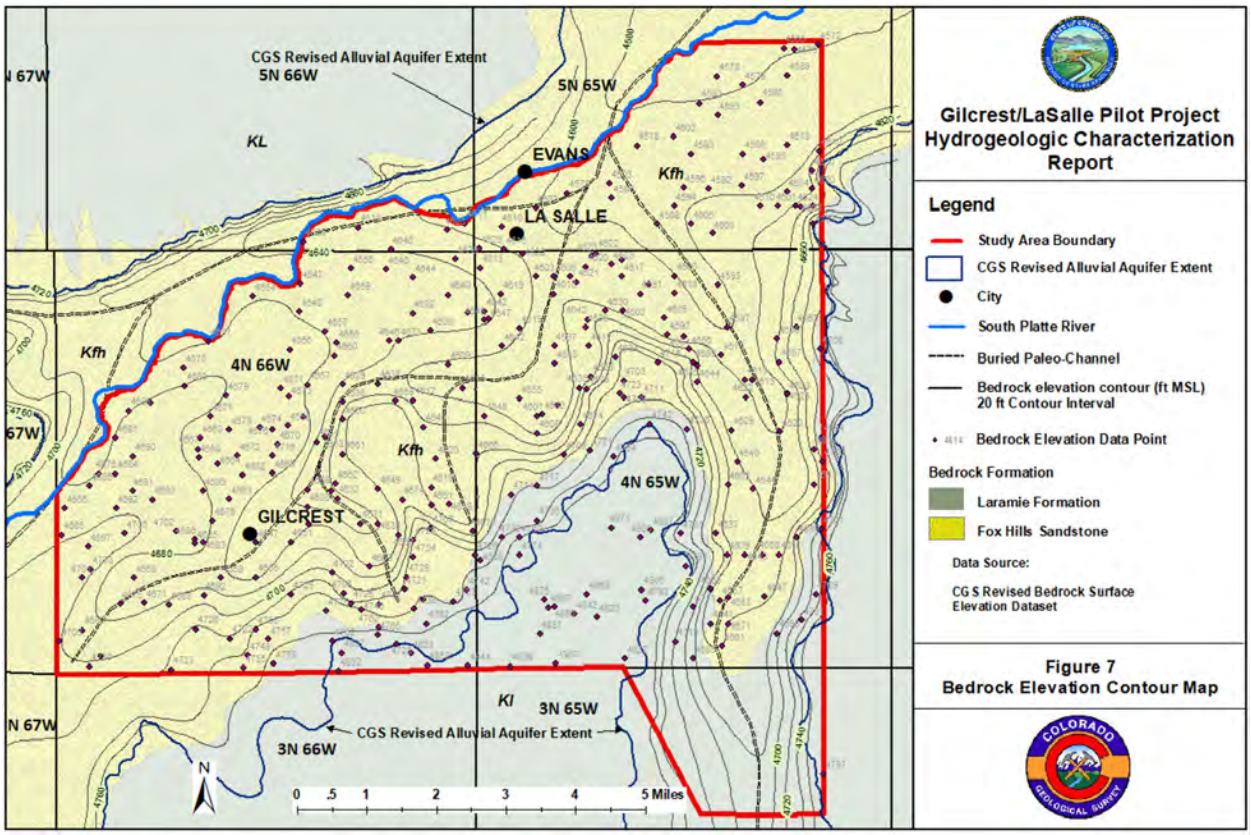

Figure 3-2. Example of the maps used from Barkmann et al (2014) showing the CGS interpretation of the bedrock elevation (modified from Barkmann et al. (2014).

3.3 Water Table

An updated water table (spring of 2017) was provided to AGF from the CO-DWR that was prepared by the CGS (Sebol and Barkmann, 2017). While this is an extremely high-quality water table, it doesn't extend over the complete AEM acquisition area (Figure 3-3). Later in section 5 an explanation of how the water table was used in the interpretation will be provided as a combination of the spring 2017 water table from Sebol and Barkmann (2017), the spring 2012 water table from Barkmann et al. (2014), data from Wellman (2015), and data from Robson et al. (2000a). Figure 3-3 is the spring 2017 elevation of the water table from Sebol and Barkmann (2017).

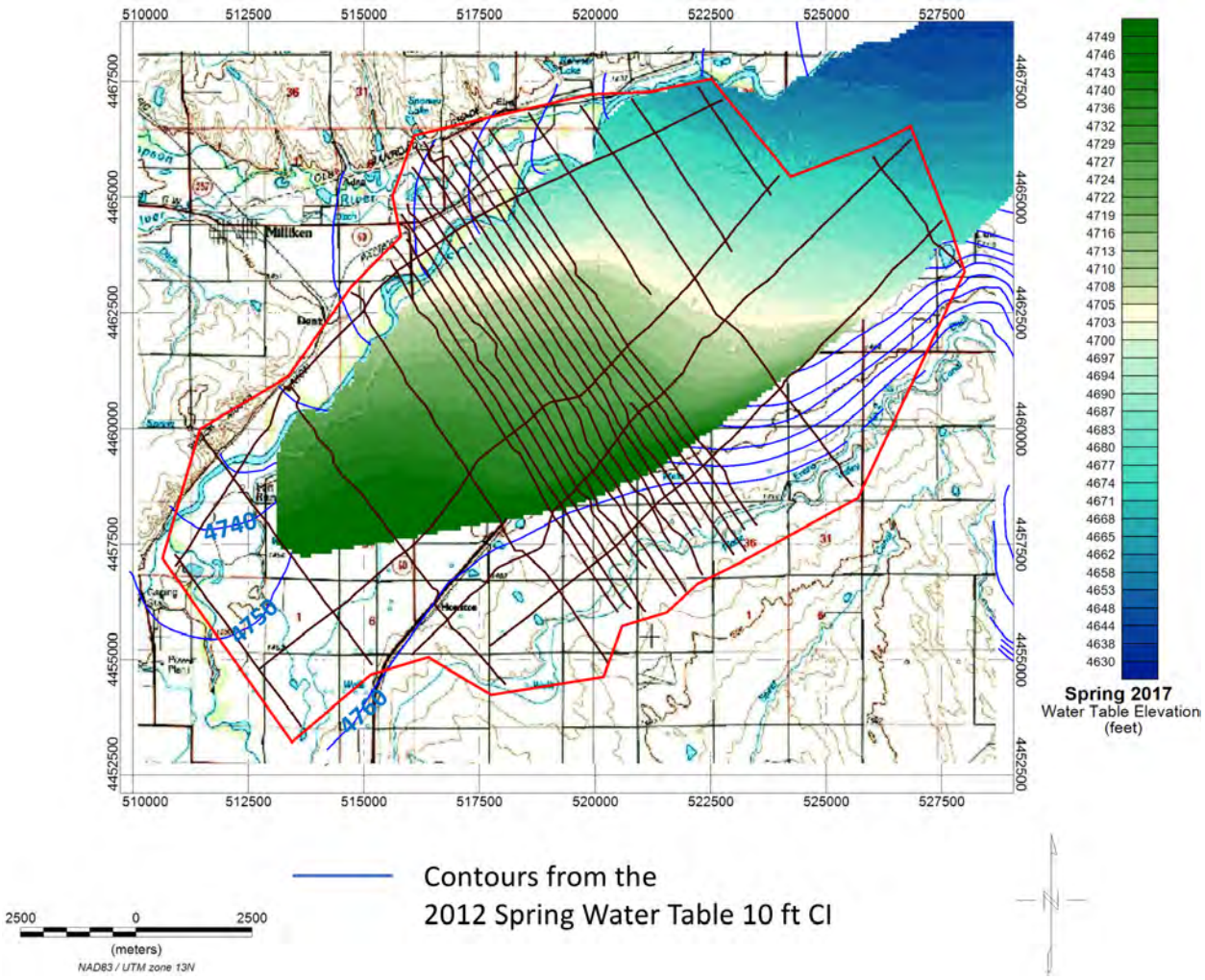

Figure 3-3. The 2017 spring water table information from Sebol and Barkmann (2017) displayed as a grid and contours "10 foot (CI) contour interval" (blue lines) from the spring 2012 water table from Barkmann et al. (2014). The AEM flight lines are shown as brown lines on the 100K USGS topography map.

4 Geophysical Methodology, Acquisition, and Processing

4.1 Geophysical Methodology

Airborne Transient Electromagnetic (TEM) or airborne Time-Domain Electromagnetic (TDEM), or generally AEM, investigations provide characterization of electrical properties of earth materials from the land surface downward using electromagnetic induction. Figure 4-1 gives a conceptual illustration of the airborne TEM method.

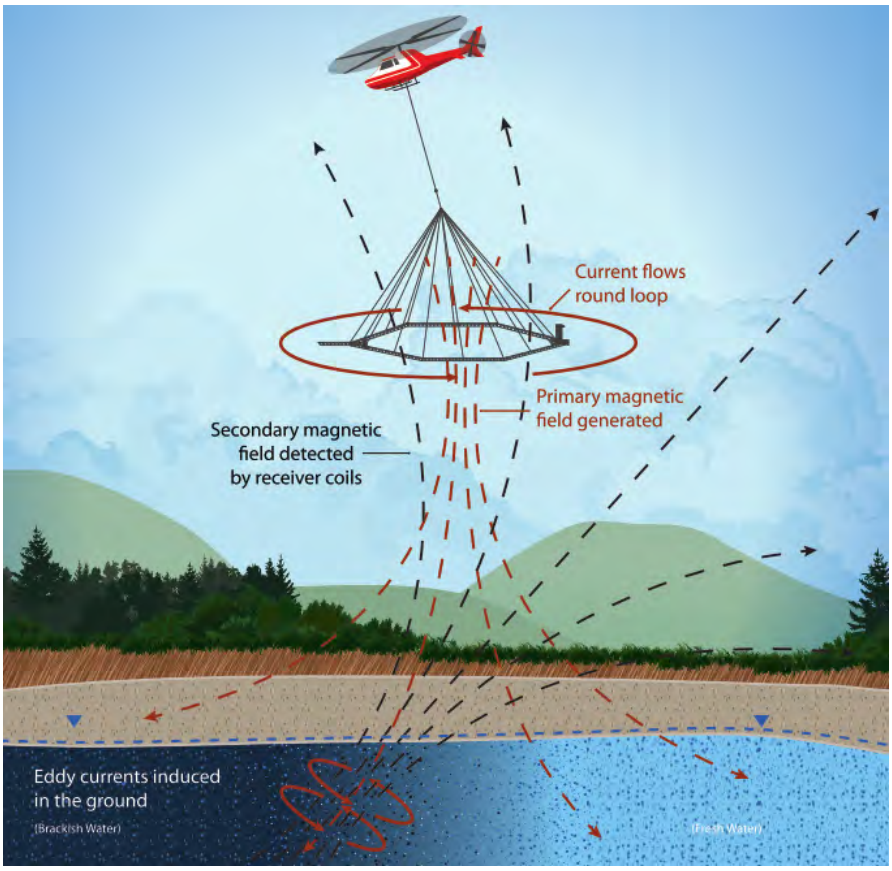

Figure 4-1. Schematic of an airborne electromagnetic survey, modified from Carney et al. (2015).

To collect TEM data, an electrical current is sent through a large loop of wire consisting of multiple turns which generates an electromagnetic (EM) field. This is called the transmitter (Tx) coil. After the EM field produced by the Tx coil is stable, it is switched off as abruptly as possible. The EM field dissipates and decays with time, traveling deeper and spreading wider into the subsurface. The rate of dissipation is dependent on the electrical properties of the subsurface (controlled by the material composition of the geology including the amount of mineralogical clay, the water content, the presence of dissolved solids, the metallic mineralization, and the percentage of void space). At the moment of turnoff, a secondary time-varying EM field, which also begins to decay, is generated within the subsurface. The decaying secondary EM field generates a current in a receiver (Rx) coil, per Ampere's Law. This current is measured at several different moments in time (each moment being within a time band called a "gate").

From the induced current, the time rate of decay of the magnetic field, B, is determined (dB/dt). When compiled in time, these measurements constitute a "sounding" at that location. Each TEM measurement produces an EM sounding at one point on the surface.

The sounding curves are numerically inverted to produce a model of subsurface resistivity as a function of depth. Inversion relates the measured geophysical data to probable physical earth properties. Figure 4-2 shows an example of a dual-moment TEM dB/dt sounding curve and the corresponding inverted electrical resistivity model.

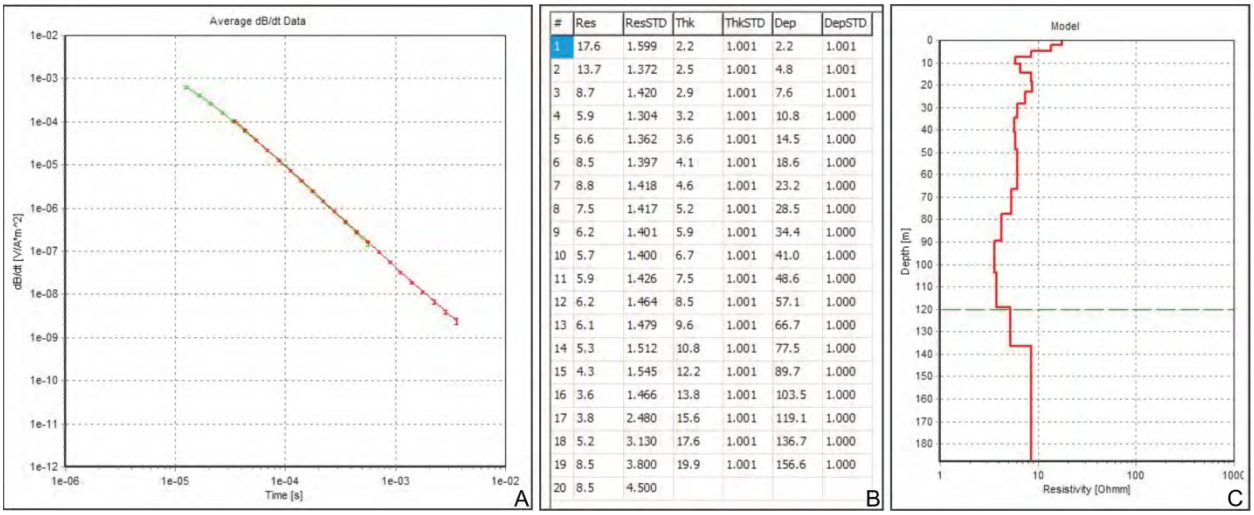

Figure 4-2. A) Example of a dB/dt sounding curve. B) Corresponding inverted model values. C) Corresponding resistivity earth model.

4.2 AEM Acquisition Timing

SkyTEM mobilized the SkyTEM304M on June 2, 2017. The system was assembled and calibrated on a prior project near Cheyenne, WY and was ferried down to the Greeley-Weld County Airport. No additional assembly or calibration was required. Production began on June 2, 2017 and continued into June 3, 2017. A total of four production flights were flown. Line-km totals from each flight are provided in Table 4-1. An "as-flown" map view of the timing and spatial orientation of the flight lines is presented in Figure 4-3. In some locations, the as-flown lines deviate from the planned lines due to infrastructure and safety as determined by the pilot. The system was then demobilized from the Greeley-Weld County Airport on June 4, 2017 after data approval.

Table 4-1. Flight line production by flight.

Date	Flight	Line-km total
2-Jun-17	60201	36.4
3-Jun-17	60301	67.7
	60302	93.7
	60303	52.1
Total		249.9

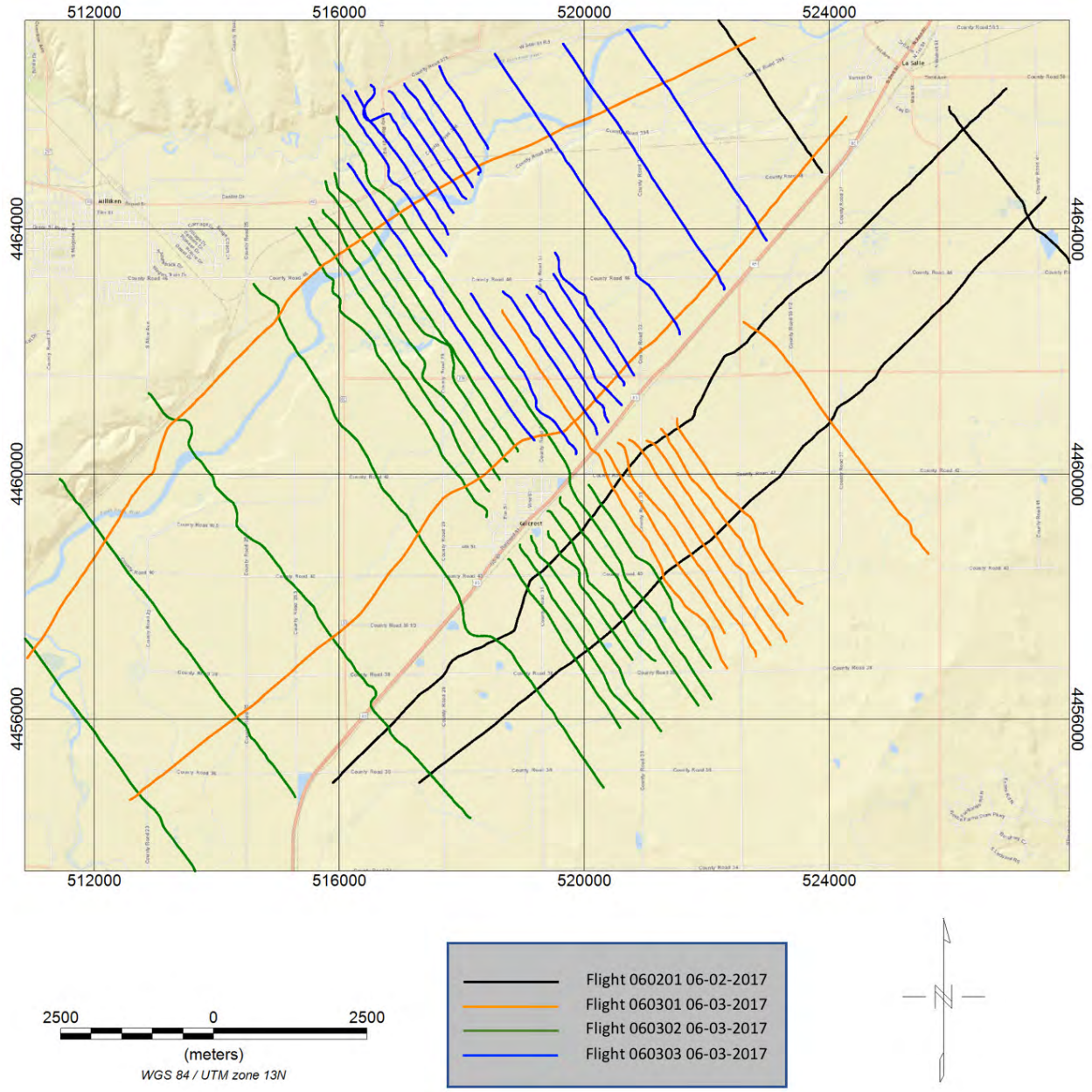

Figure 4-3. As-Flown map showing timing of the Gilcrest AEM survey data acquisition.

4.3 AEM Survey Instrumentation

AEM data were acquired using the SkyTEM304M (304M) airborne electromagnetic system (SkyTem Airborne Surveys Worldwide, 2018). The 304M is a rigid frame, dual-magnetic moment (Low and High) TEM system. The area of the 304M Tx coil is 337 m^2 and the coil contains four (4) turns of wire. A peak current of nine (9) amps is passed through one turn of wire in the Tx for Low Moment measurements and a peak current of 120 amps is passed through the four turns of wire for High Moment measurements. This results in peak Tx Low and High magnetic moments of ~3,000 Ampere-meter-squared ($A*m^2$) and ~160,000 $A*m^2$, respectively.

The SkyTEM304M system utilizes an offset Rx positioned slightly behind the Tx resulting in a 'null' position which is a location where the intensity of the primary field from the system transmitter is minimized. This is desirable as to minimize the amplitude of the primary field at the Rx to maximize the sensitivity of the Rx to the secondary fields. The SkyTEM304M multi-turn Rx coil has an effective area of 105 m^2. In addition to the Tx and Rx that constitute the TEM instrument, the SkyTEM304M is also equipped with a Total Field magnetometer (MAG) and data acquisition systems for both instruments. The SkyTEM304M also includes two each of laser altimeters, inclinometers/tilt meters, and differential global positioning system (DGPS) receivers. Positional data from the frame mounted DGPS receivers are recorded by the AEM data acquisition system. The magnetometer includes a third DGPS receiver whose positional data is recorded by the magnetometer data acquisition system. Figure 4-4 gives a simple illustration of the SkyTEM304M frame and instrument locations. The image is viewed along the +z axis looking at the horizontal x-y plane. The axes for the image are labeled with distance in meters. The magnetometer is located on a boom off the front of the frame (right side of image). The Tx coil is located around the octagonal frame and the Rx Coil is located at the back of the frame (left side of image).

The coordinate system used by the 304M defines the +x direction as the direction of flight, the +y direction is defined 90 degrees to the right and the +z direction is downward. The center of the transmitter loop, mounted to the octagonal SkyTEM frame is used as the origin in reference to instrumentation positions. Table 4-2 lists the positions of the instruments (in feet) and Table 4-3 lists the corners of the transmitter loop in feet (whereas units of meters are presented in Figure 4-4).

The DGPS and magnetometer mounted on the frame of the SkyTEM304M require the use of base stations, which are located on the ground and are positioned in an area with low cultural noise. Data from the magnetometer and DGPS base stations were downloaded each day after the end of the day's AEM flights. The DGPS and magnetometer base stations were placed at the location listed in Table 4-4. The horizontal geodetic reference used is North American Datum of 1983 (NAD83) Universal Transvers Mercator (UTM) Zone 13 North (meters). All elevations are from USGS's National Elevation Dataset (NED), referenced to the North American Vertical Datum (NAVD) of 1988; with feet as the unit of measurement.

Figure 4-5 is a photo of the SkyTEM304M in operation.

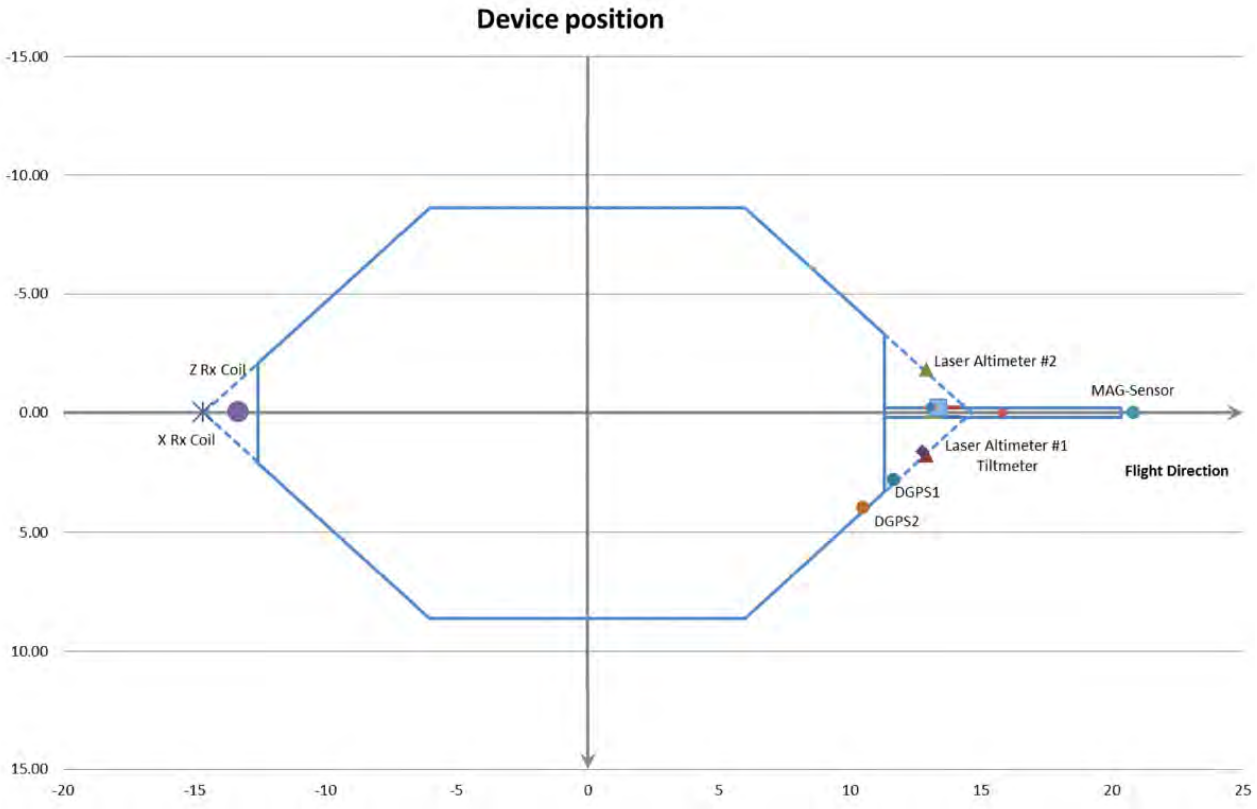

Figure 4-4. SkyTEM304M frame, including instrumentation locations and X and Y axes. Distances are in meters. Instrumentation locations listed in Table 4-2.

Figure 4-5. Photo of the SkyTEM304M system in suspension beneath the helicopter. Photo taken by John Fingerlin.

Table 4-2: Positions of instruments on the SkyTEM304M frame, using the center of the frame as the origin, in feet.

	DGPS 1	DGPS 2	Inclinometer 1	Inclinometer 2	Altimeter 1	Altimeter 2	Magnetic Sensor	Rx Coil
X	38.31	34.47	41.95	41.95	42.44	42.44	67.24	-43.46
Y	9.15	12.96	5.38	-5.38	5.87	-5.87	0	0
Z	-0.52	-0.52	-0.39	-0.39	-0.39	-0.39	-1.71	-6.56

Table 4-3: Positions of corners of the SkyTEM304M transmitter coil, using the center of the frame as the origin in feet.

Tx Corners	1	2	3	4	5	6	7	8
X	-41.46	-20.17	18.83	36.51	36.51	18.83	-20.17	-41.46
Y	-6.99	-28.18	-28.18	-10.46	10.46	28.18	28.18	6.99

Table 4-4: Locations of DGPS and magnetic field base station instruments.

Instrument	Easting (m)	Northing (m)	Zone
DGPS Base Station – Gilcrest Airport	531272	4475067	UTM 13N
Magnetometer Base Station – Gilcrest Airport	531270	4475039	UTM 13N

4.4 Test Site Calibration in Denmark

All SkyTEM systems are calibrated to a specific ground test site in Lyngby, Denmark prior to being used for production work (HydroGeophysics Group Aarhus University, 2010; HydroGeophysics Group Aarhus University, 2011; Foged et al., 2013). The calibration process involves acquiring data with the system hovering at different altitudes, from 5 m to 50 m, over the Lyngby site. Acquired data are processed and a scale factor (time and amplitude) is applied so that the inversion process produces the model that approximates the known geology at Lyngby.

4.5 System Ground and Airborne Tests

Ground tests included checking for system operation including the following sub-systems: 1) transmitter (Tx) current amplitude and stability including waveform recording of both high moment (HM) and low moment (LM); 2) receiver (Rx) functionality for both Z and X-components, 3) laser altimeter operation; 4) GPS operation; 5) tilt meter/attitude sensor operation and calibration; 6) navigation and wireless communication; 7) airborne magnetometer operation; 8) base station magnetometer stability and field strength stability; and 9) DGPS base station operation.

Airborne tests are conducted to establish and confirm the minimum primary field signal level, otherwise known as the “null” position, of both the Z and X Rx components. This is done by mechanically moving the Rx’s to locate the best null positon by multiple flights. At the time of the establishment of the nulls

the system is flown to a high level to eliminate the earth response. At that altitude, typically 1,000 meters above ground level (AGL), only the background noise of the system and the helicopter is received. That is checked against the designed system noise level and used as a calibration point. In addition to the calibrations and the nulls, the system is operated to ensure the mechanical stability of the system and that all acquisition systems are functional.

4.6 System Flight Parameters

4.6.1 Flight Height

The system height was specified at 30 meters AGL; however, due to safety and other judgments by the pilot the flight heights will deviate. The goal is to maintain a height as low as possible in the window from 25 to 50 m AGL. In the Gilcrest data set the average height was 34.10 m AGL with a minimum of 20.5 m AGL and a maximum of 95.50 m AGL. The maximum flight heights were encountered over large powerlines. Those data were removed from the dataset before inversion due to EM coupling and did not impact the final product. A map of the flight height throughout the survey area is presented in Figure 4-6.

4.6.2 Flight Speed

Speed determines the distance between ground samples. However, there is a tradeoff between the cost of the survey and the speed of the system related to the foot print of the system. In many surveys, the specified speed is 100 km/hr. The critical factor in the flight speed is to maintain a speed where the system is as level as possible. This may require that the pilot speed up in the downwind direction or slowdown in the up-wind direction. The pilot uses the readout display of the system tilt angles to help maintain this speed. A map of the flight speeds of the Gilcrest survey is presented in Figure 4-7. The average ground speed of the survey was 68.50 km/hr with a minimum ground speed of 21.5 km/hr and a maximum ground speed of 95.5 km/hr.

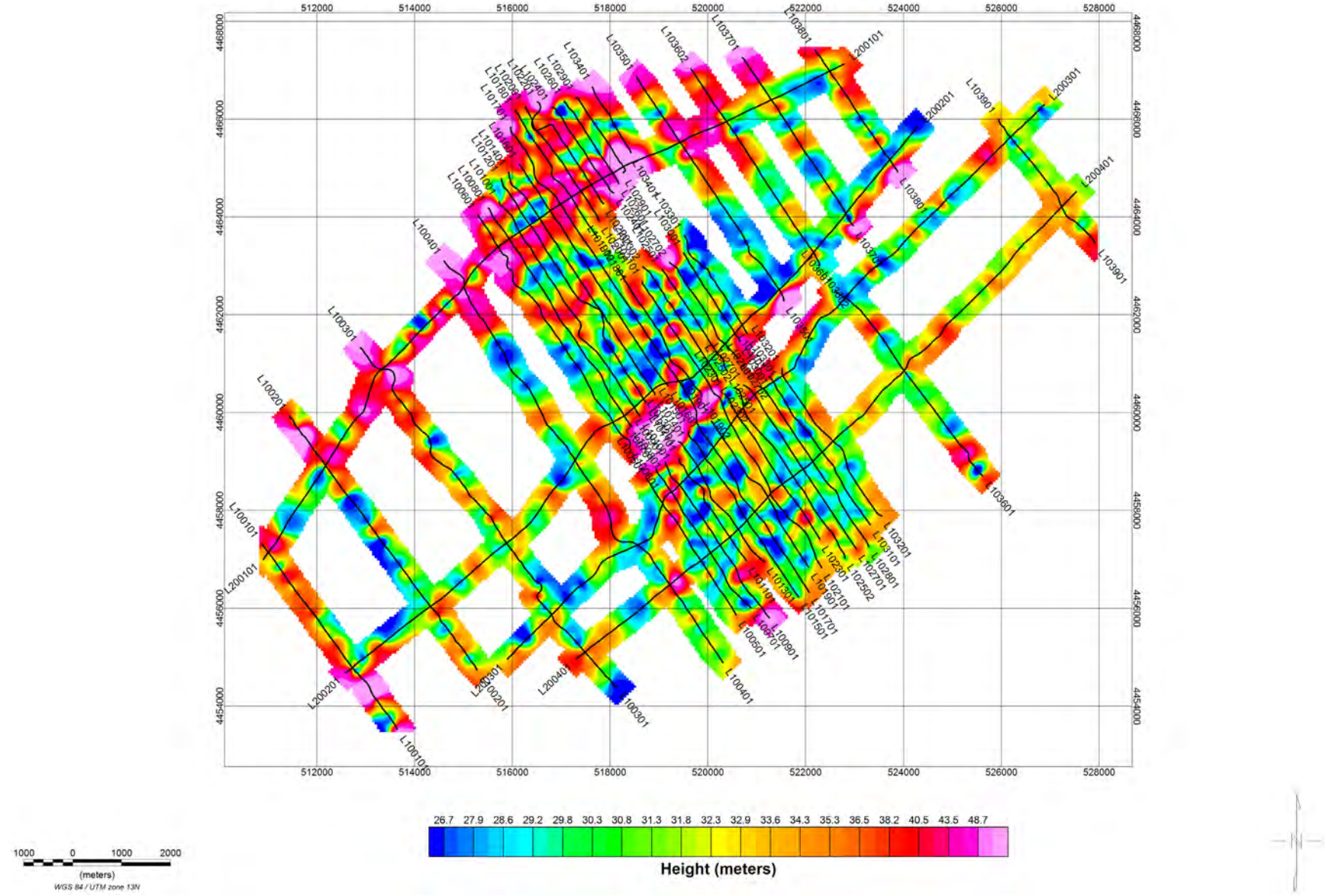

Figure 4-6. Map of the system height recorded during the Gilcrest survey, as-flown flight lines are indicated as black lines.

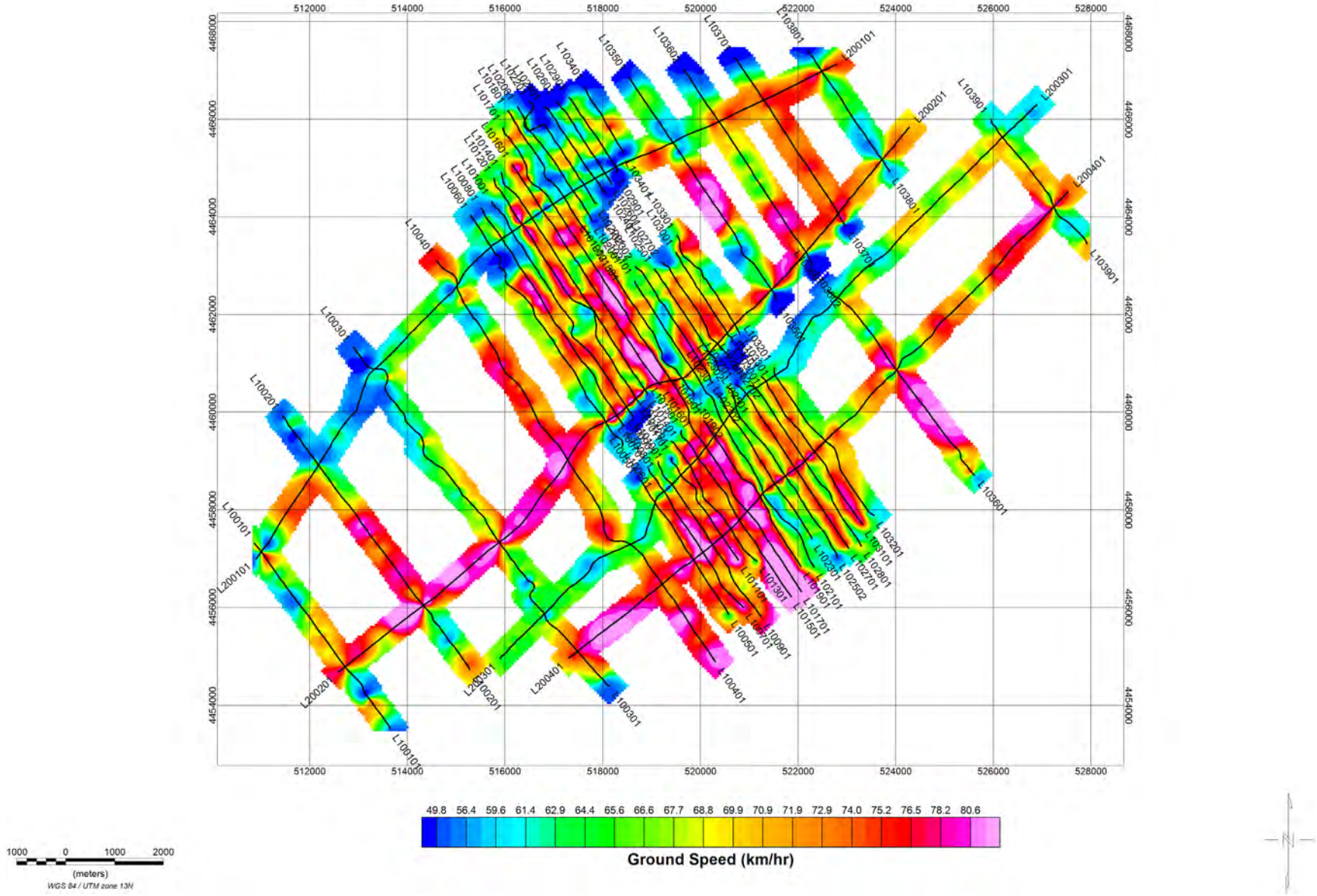

Figure 4-7. Map of the ground speed recorded during the Gilcrest survey. The as-flown flight lines are indicated as labeled black lines.

4.6.3 System Angles

System angles are critical to ensure that quality data are submitted to the inversion. The system's Tx initial current at time-off of 0.0 sec is the image of the size of the loop on the surface. If the system is tilted, that image will be less than the original size of the TX. Inversion algorithms can account for ±10 degrees of angle in calculating the effective Tx size. To this end, it is important to keep the Tx frame within ±10 degrees. The position of the Rx is also impacted by the angle of the system and any deviation from perpendicular has an impact by including off perpendicular components. As noted, algorithms can account for ±10 degrees in the Rx angle. Both the X-Angle (in the direction of flight) and the Y-Angle (perpendicular to the direction of flight) were checked for the Gilcrest survey. When the system is flown over obstacles or while turning around at the end of a line, the angles can be higher than the ±10 degrees. These flight line edges are typically cut out of the survey data set prior to inversion. Figure 4-8 and Figure 4-9 are plots of the X-angle and the Y-angle tilts, respectively. During the Gilcrest survey, both angles were within acceptable ranges. The X-angle averaged approximately -0.66 degrees with a minimum of -7.96 degrees and a maximum of 11.2 degrees. The Y-angle tilt averaged about 0.68 degrees with a minimum of -8.90 degrees and a maximum of 14.89 degrees.

4.6.4 Transmitter Current

The SkyTEM system utilizes a dual-moment system (High (HM) and Low (LM)) and two different Tx currents and waveforms. These waveforms are recorded before and after the survey to ensure that no changes have occurred during the survey. Figure 4-10 and Figure 4-11 are plots of the recorded low moment (LM) and the high moment (HM) Tx waveforms, respectively. The LM Tx source is used to highlight the very near surface geology and the HM current source is used to get more electromagnetic power at depth to characterize the deeper geologic units

The current should be stable throughout the survey, but changes in the temperature can impact the resistance of the Tx wire and circuit by either increasing or lowering the peak current output. The peak current is recorded during acquisition of each sounding and is used to adjust the Tx waveform in the inversion. For the Gilcrest survey the LM mean current was 8.73 amp with a minimum current of 8.70 amp and a maximum current of 8.77 amp. For the HM, the mean current was 113.85 amp with a minimum current of 112.33 amp and a maximum current of 115.03 amp. Both moments show stability in the current and provided no problems in the inversion.

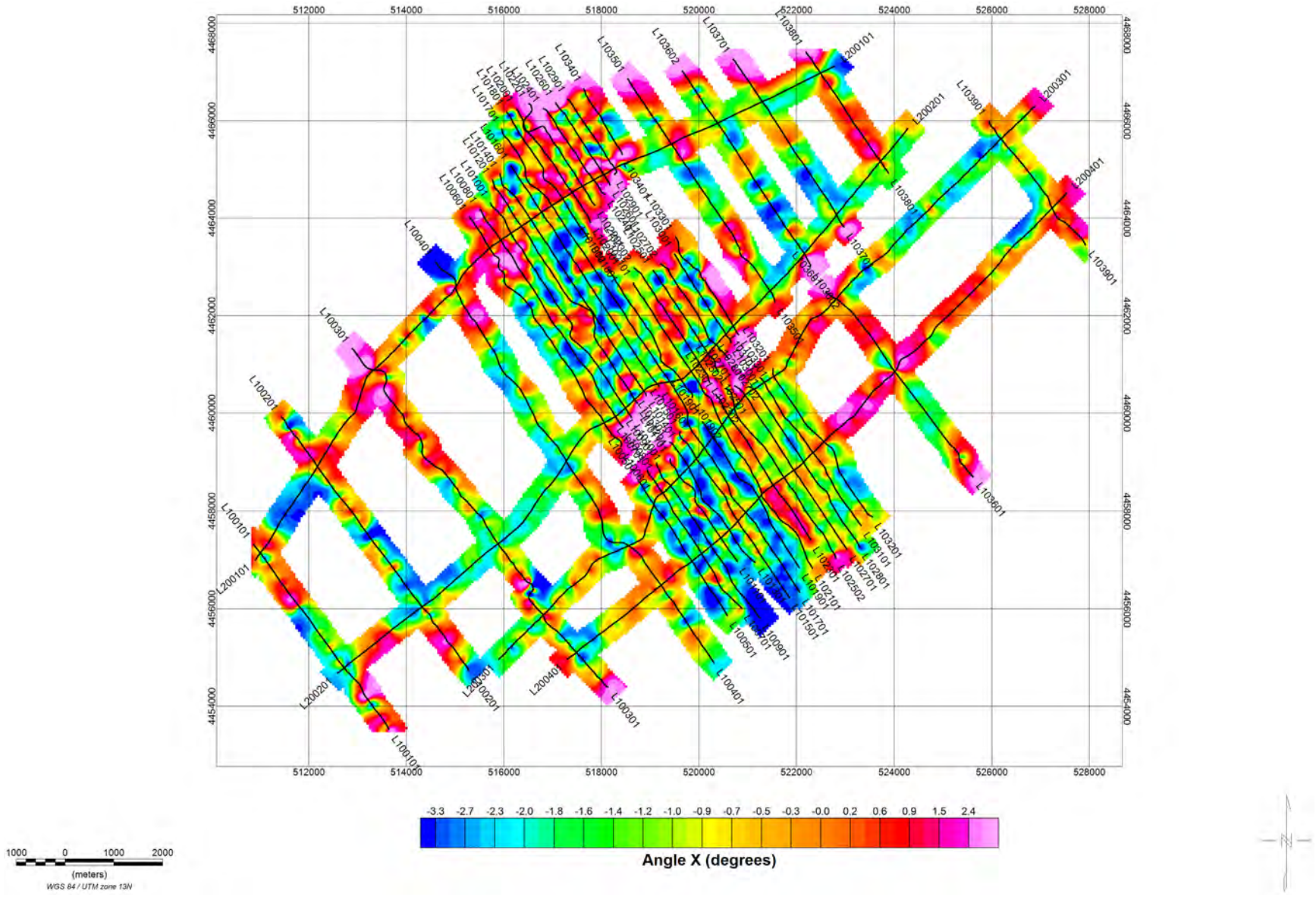

Figure 4-8. Map of the X-angle tilt recorded during the Gilcrest survey. The as-flown flight lines are indicated as black lines.

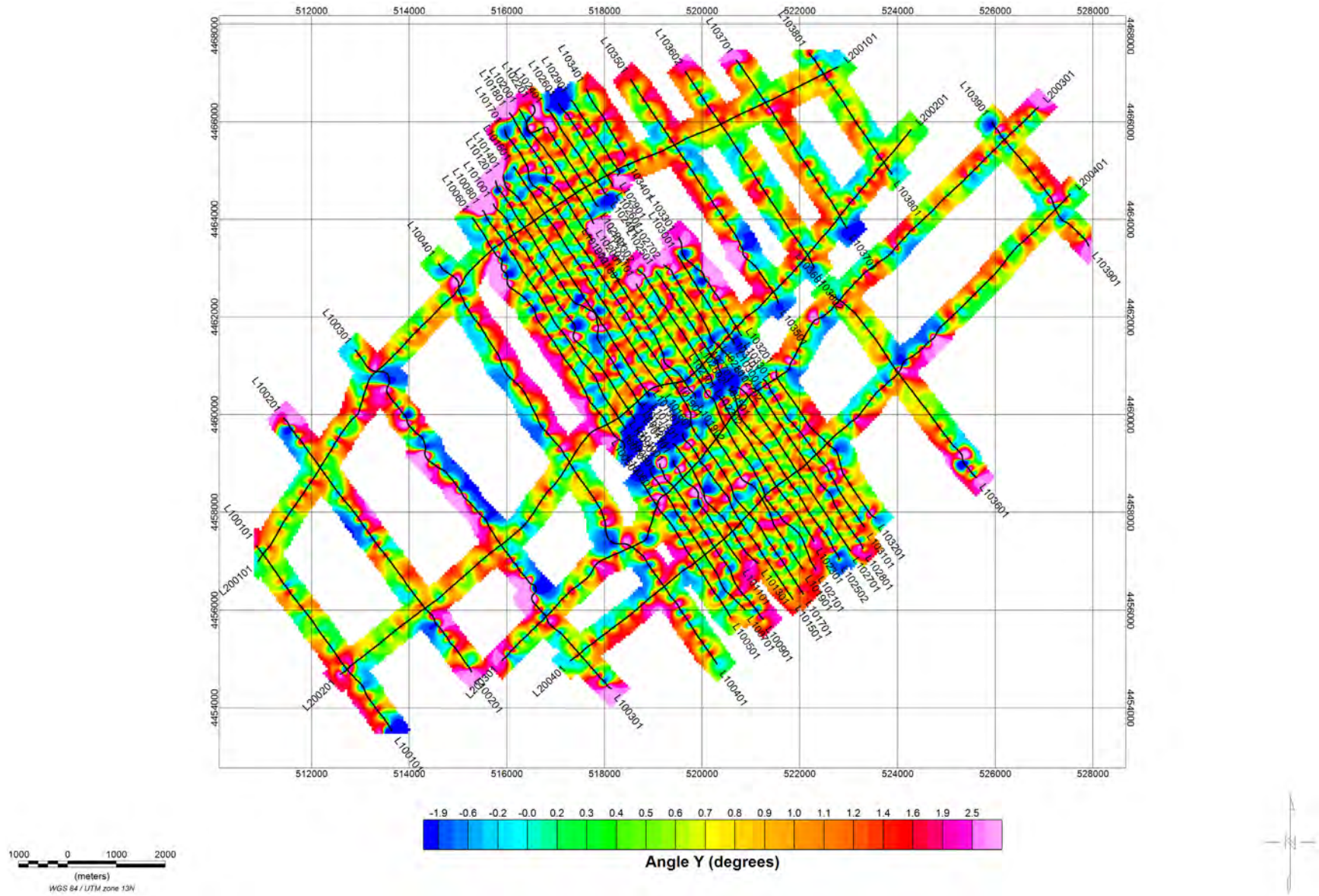

Figure 4-9. Map of the Y-angle tilt recorded during the Gilcrest survey. The as-flown flight lines are indicated as black lines.

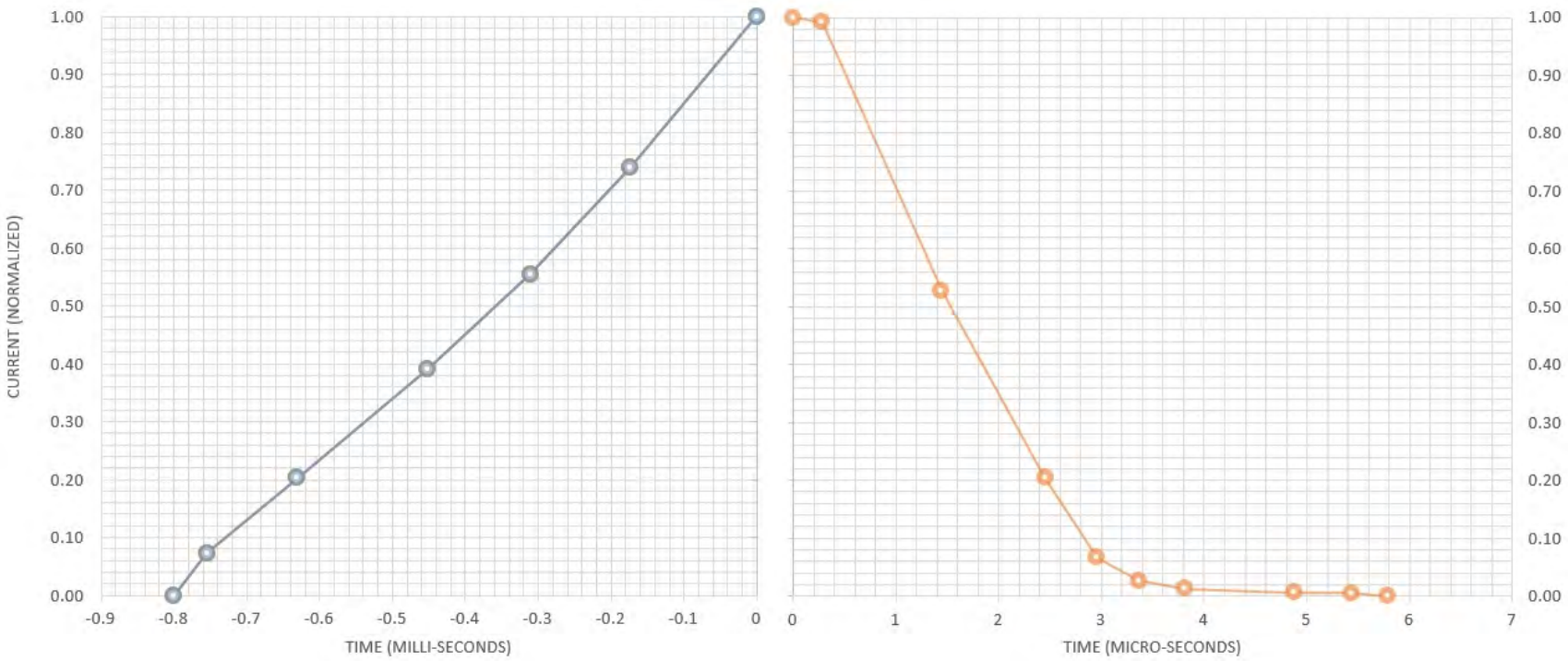

Figure 4-10. Plot of the 210 Hz LM waveform recorded during the Gilcrest survey. Current ramp up is on the left and the ramp down to turn off is on the right. Note the different x-axis scales between the left and right sides of the figure.

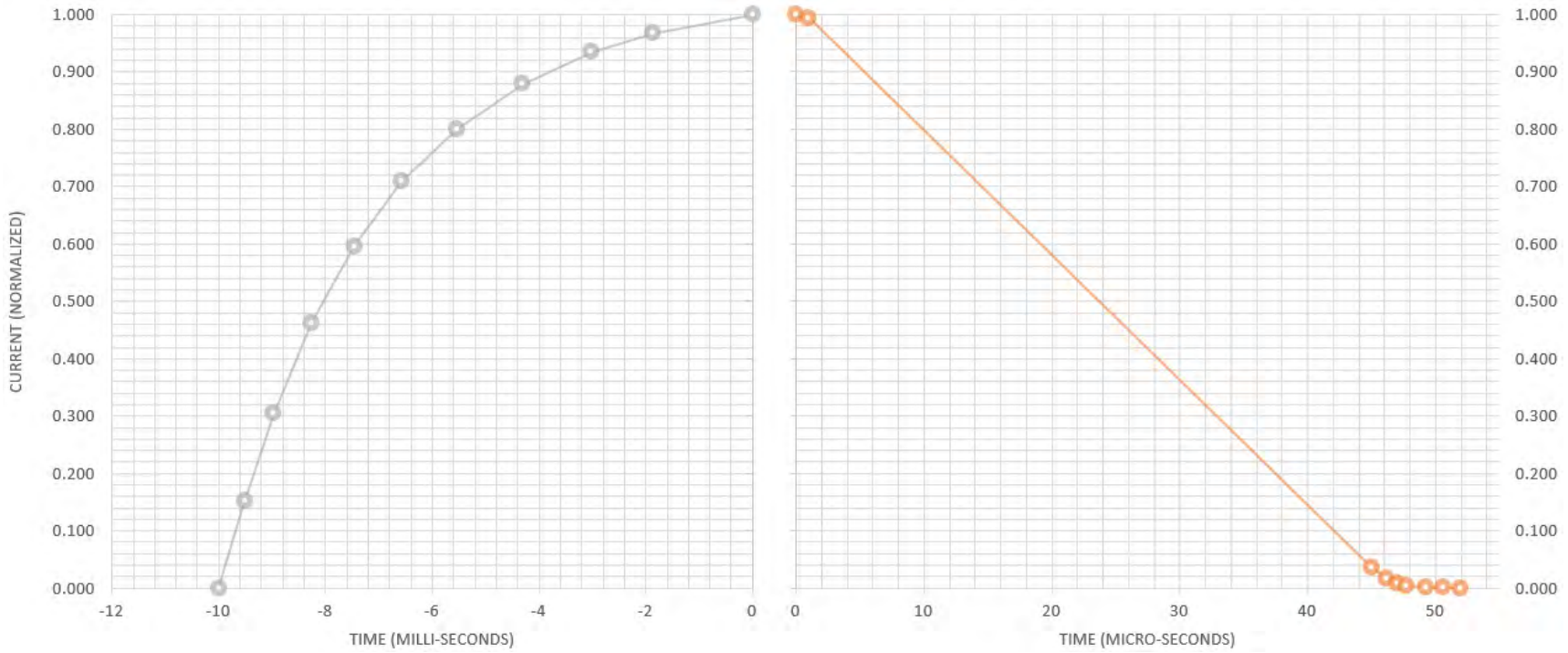

Figure 4-11. Plot of the 22.5 Hz HM waveform recorded during the Gilcrest survey. Ramp up is on the left and ramp down to turn off is on the right. Note the different x-axis scales between the left and right sides of the figure.

4.7 Power Line Noise Intensity

The SkyTEM system is configured to provide an estimate of the amplitude of the powerline noise intensity (PLNI) of the 60 Hz signals. The PLNI is produced by performing a spectral frequency content analysis on the raw received Z-component SkyTEM data. For every HM data block, a Fourier Transform (FT) is performed on the latest time gate data. The FT is evaluated at the local power line transmission frequency (60 Hz) yielding the amplitude spectral density of the local power line noise. The PLNI map is useful when investigating the impacts of powerlines on the data quality. The 60 Hz powerline signals have little impact on the Rx signal due to time-gating and proper filtering. However, the conductive wires that are used to transmit the power do cause EM coupling impacts on the data and those data need to be removed prior to inversion. The PLNI for the Gilcrest AEM survey is presented in Figure 4-12.

4.8 Magnetics

As part of the SkyTEM system a Total Field magnetometer is included in the data acquisition package. The magnetic field signal is useful for determining deep seated geological contacts and is also extremely valuable for locating intrusive bodies. Neither of those was the target of the survey within Gilcrest. However, the magnetic field is also sensitive to anthropogenic features that contain ferrous metal and is also used in the electromagnetic decoupling process. A plot of the residual magnetic signal in the area of the Gilcrest is presented in Figure 4-13. Both geological structure and cultural features can be identified within the survey area.

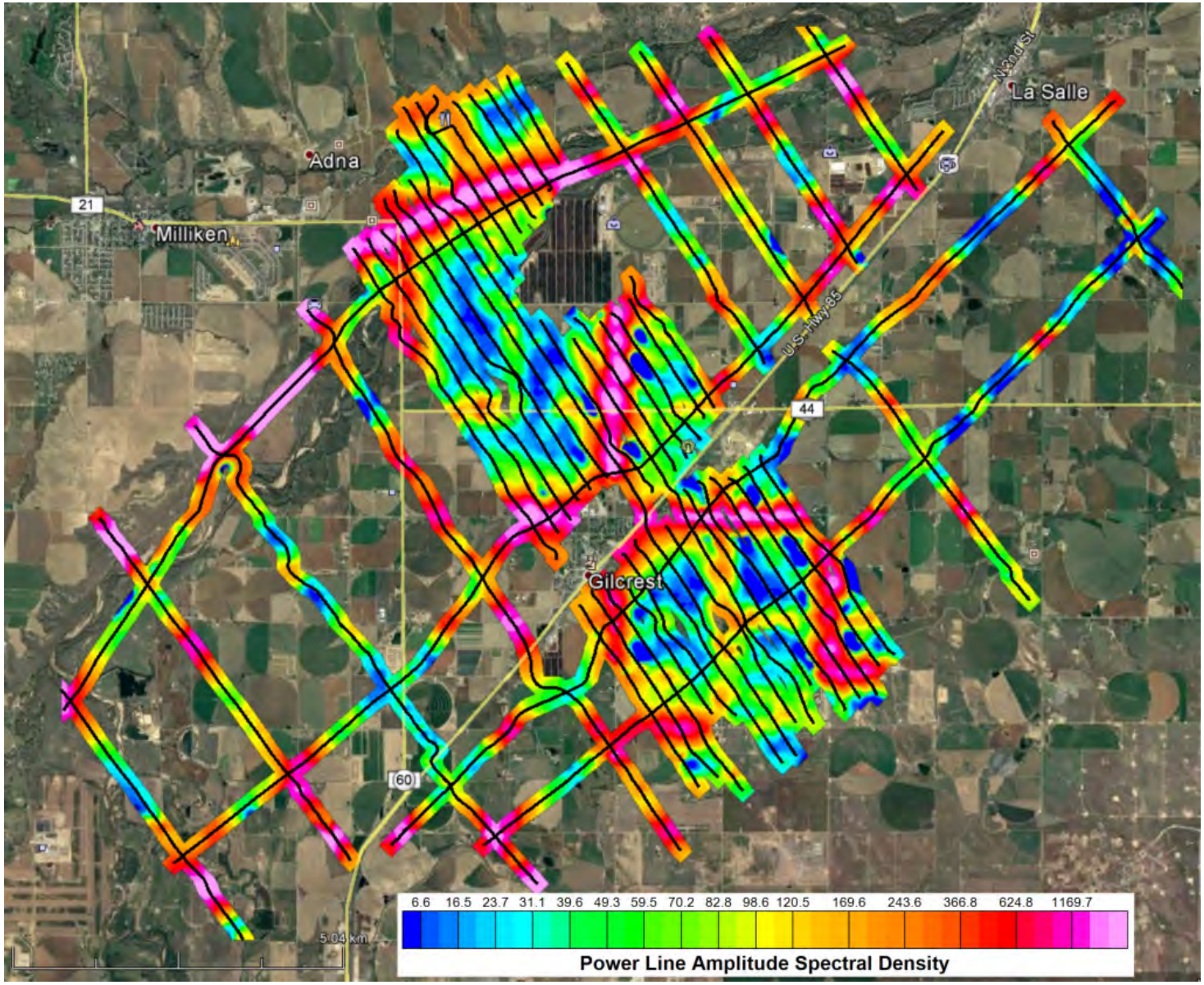

Figure 4-12. Power Line Noise Intensity (PLNI) for the Gilcrest AEM survey area. The as-flown flight lines are indicated as black lines.

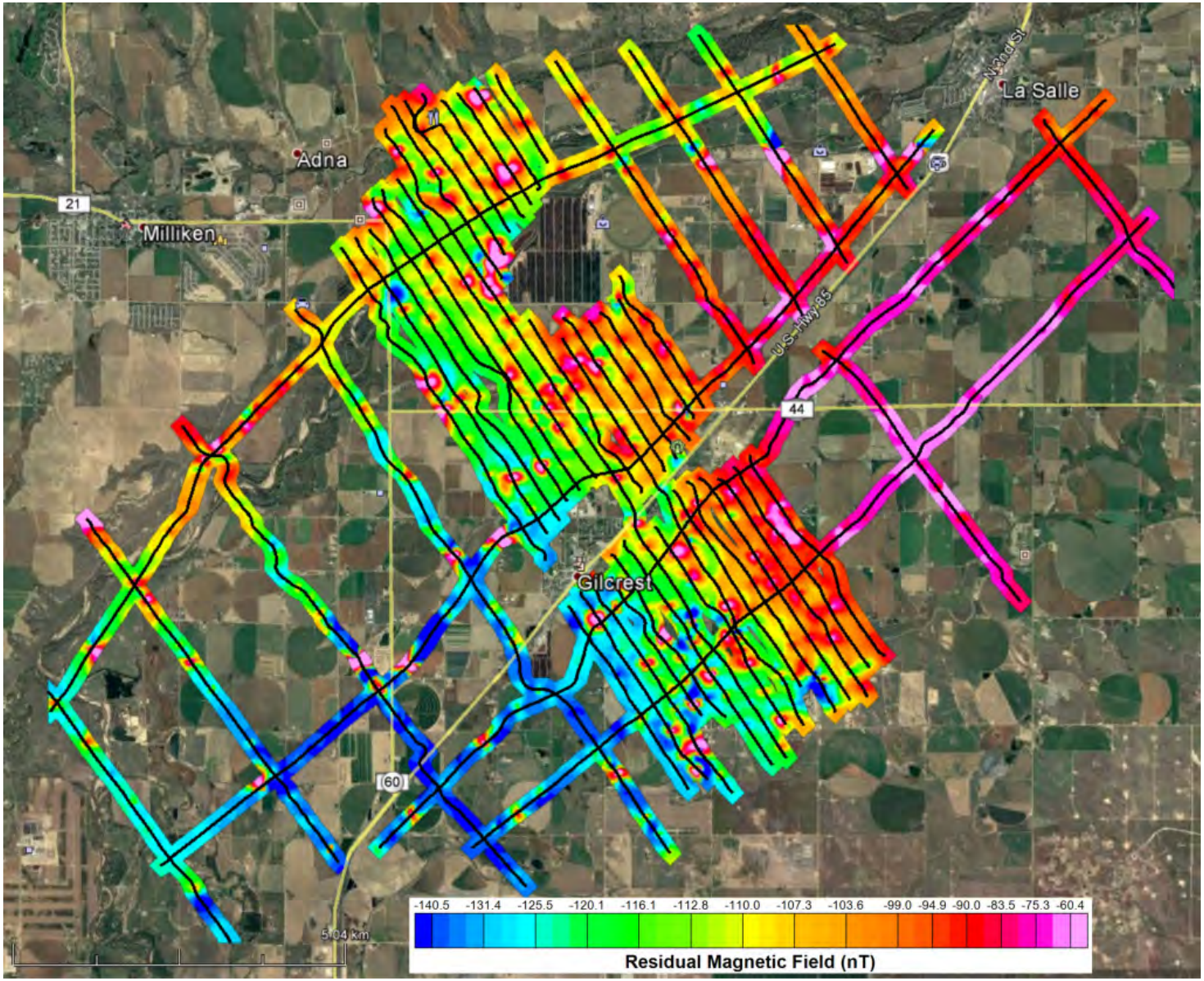

Figure 4-13. Residual magnetic total field for the Gilcrest survey area. The as-flown flight lines are indicated as black lines.

4.9 Primary Field Compensation

A standard SkyTEM data acquisition procedure involves review of acquired raw data by SkyTEM in Denmark for Primary Field Compensation (PFC) prior to continued data processing by AGF (Schamper et al., 2014). The primary field of the transmitter affects the recorded early time gates, which in the case of the LM, are helpful in resolving the near surface resistivity structure of the ground. The LM waveform is calculated and then used in the PFC correction to correct the early time gates.

4.10 Automatic Processing

The AEM data collected by the 304M were processed using Aarhus Workbench version 5.4.0.0 (at Aarhus Geosoftware (http://www.aarhusgeosoftware.dk/aarhus-workbench-ib3ao) described in HydroGeophysics Group, Aarhus University (2011).

Automatic processing algorithms provided within the Workbench program are initially applied to the AEM data. DGPS locations were filtered using a stepwise, second-order polynomial filter of nine seconds with a beat time of 0.5 seconds, based on flight acquisition parameters. The AEM data are corrected for tilt deviations from level and so filters were also applied to both tilt meter readings with a median filter of three seconds and an average filter of two seconds. The altitude data were corrected using a series of two polynomial filters. The lengths of both eighth-order polynomial filters were set to 30 seconds with shift lengths of six (6) seconds. The lower and upper thresholds were 1 and 100 meters, respectively. Trapezoidal spatial averaging filters were next applied to the AEM data. The times used to define the trapezoidal filters for the Low Moment were $1.0x10^{-5}$ sec, $1.0x10^{-4}$ sec, and $1.0x10^{-3}$ sec with widths of 8, 10, and 12 seconds. The times used to define the trapezoid for the High Moment were $1.0x10^{-4}$ sec, $1.0x10^{-3}$ sec, and $1.0x10^{-2}$ sec with widths of 10, 12, and 20 seconds. The trapezoid sounding distance was set to 2.5 seconds and the left/right setting, which requires the trapezoid to be complete on both sides, was turned on. The spike factor and minimum number of gates were both set to 25 percent for both soundings. Lastly, the locations of the averaged soundings were synchronized between the two moments.

4.11 Manual Processing and Laterally-Constrained Inversions

After the implementation of the automatic filtering, the AEM data were manually examined using a sliding two minute time window. The data were examined for possible electromagnetic coupling with surface and buried utilities and metal, as well as for late time-gate noise. Data affected by these were removed. Examples of locating areas of EM coupling with pipelines or power lines and recognizing and removing coupled AEM data in Aarhus Workbench are shown in Figure 4-14 and Figure 4-15, respectively. Examples of two inversions, one without EM coupling and the other with EM coupling, are shown in Figure 4-16. Areas were also cut out where the system height was flown greater than 200 feet above the ground surface which caused a decrease in the signal level.

The AEM data were then inverted using a Laterally-Constrained Inversion (LCI) algorithm (HydroGeophysics Group Aarhus University, 2011). The profile and depth slices were examined, and any remaining electromagnetic couplings were masked out of the data set. Vertical constraints on the

resistivity were set at 2.7 and at 1.6 for the horizontal resistivity constraints with a reference distance of 100 m (328 ft) and a fall-off power of 0.75.

After final processing, 72.0 line-miles (116.6 line-km) of data were retained for the final inversions for the Gilcrest AEM survey area. This amounts to a data retention of 46.6%. This was due to the large amount of infrastructure within the survey area.

In Figure 4-17 are flight lines with blue colors representing data retained for inversion and red lines representing data removed due to infrastructure and late time noise.

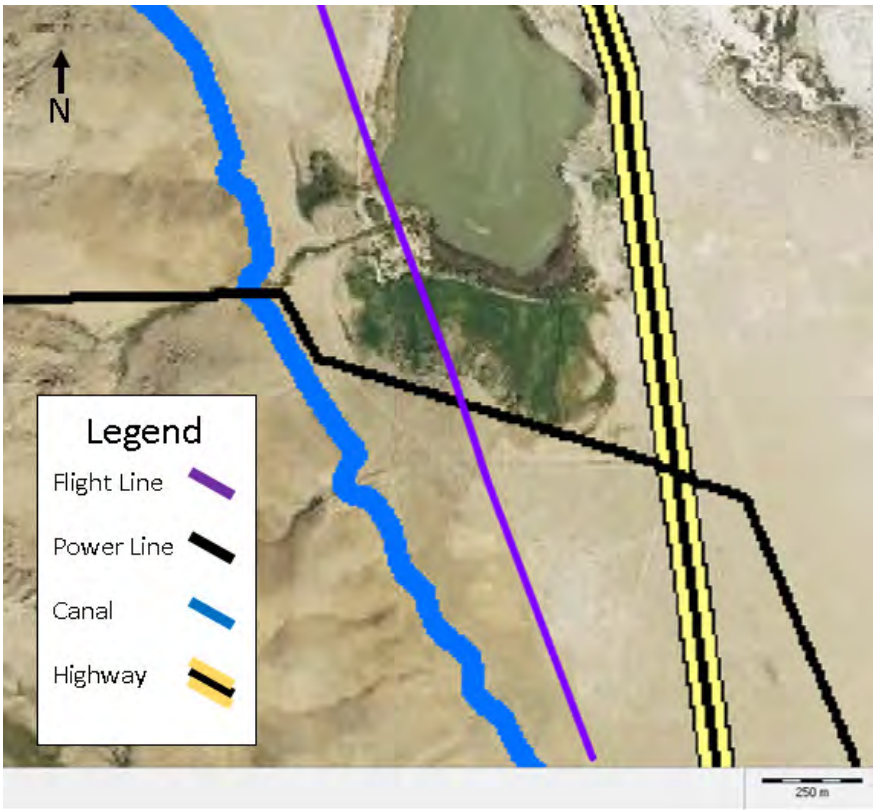

Figure 4-14. Example locations of electromagnetic coupling with pipelines or power lines.

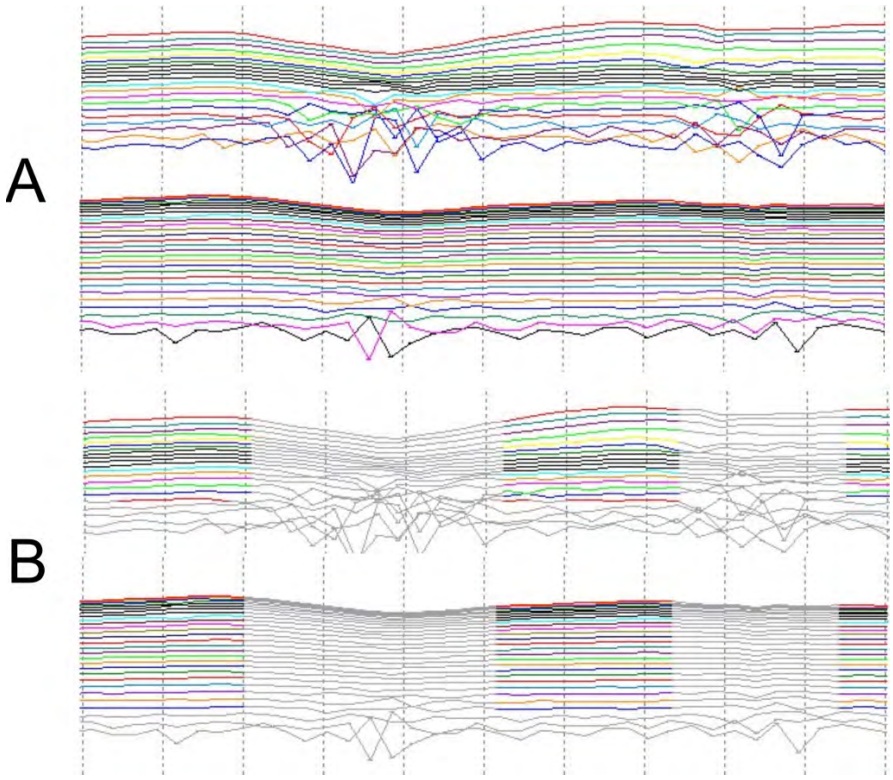

Figure 4-15. Example of AEM data affected by electromagnetic coupling in the Aarhus Workbench editor. A) Unedited data with the Low Moment on top and the High Moment on the bottom. B) Same data after editing.

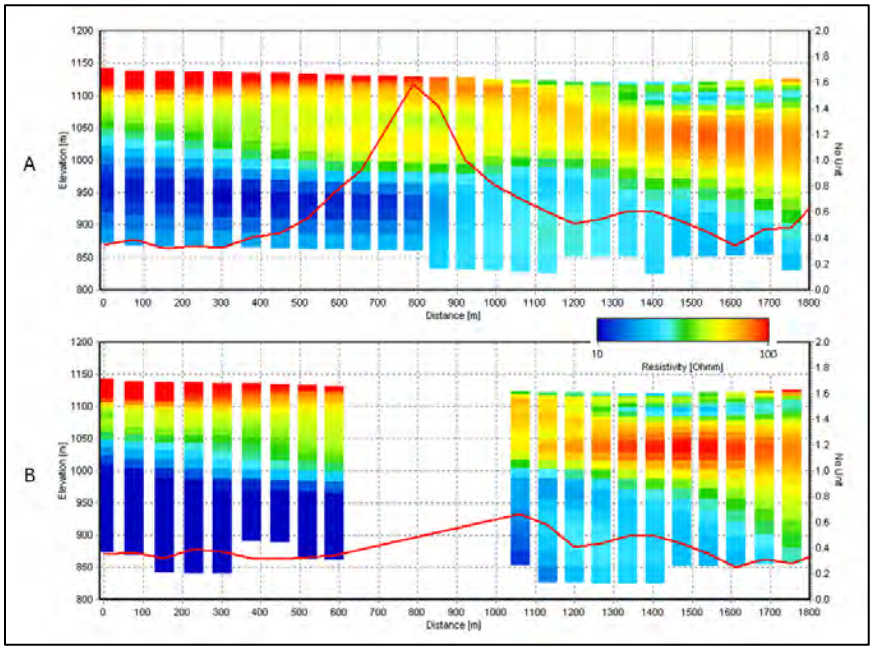

Figure 4-16. A) Example of Laterally-Constrained inversion results where AEM data affected by coupling with pipelines and power lines were not removed. B) Inversion results where AEM data affected by coupling were removed.

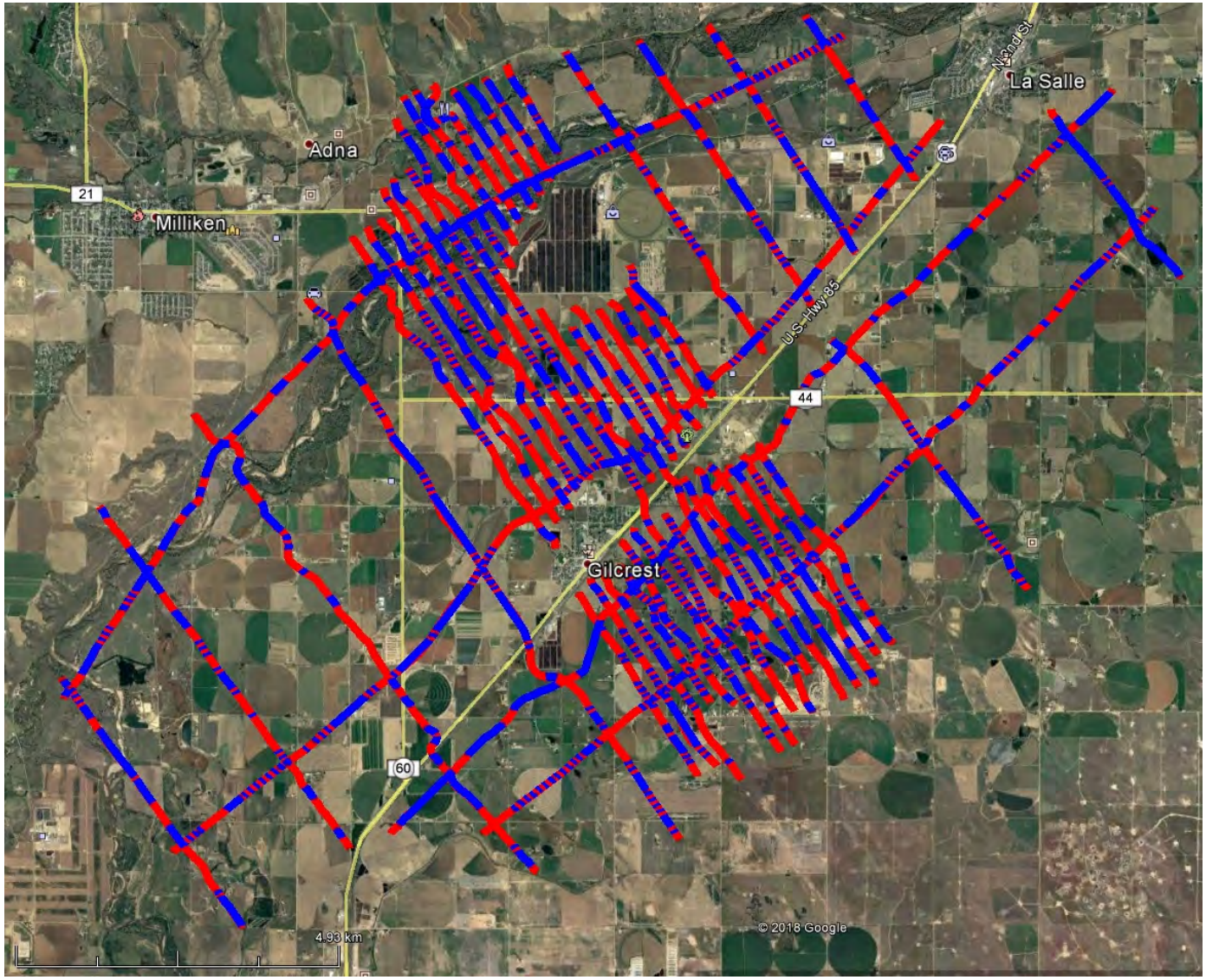

Figure 4-17. Locations of inverted data (blue lines) along the AEM flight lines (red lines) in the CCWCD survey area. Where blue lines are not present indicates decoupled (removed) data. Google Earth kmz's of the inverted data locations as well as the flight lines are included in Appendix_3_Deliverables\KMZ.

4.12 Spatially-Constrained Inversion

Following the initial decoupling and LCI analysis, Spatially-Constrained Inversions (SCI) were performed. SCIs use EM data along, and across, flight lines within user-specified distance criteria (Viezzoli et al., 2008).

The Gilcrest AEM data were inverted using SCI smooth models with 30 layers, each with a starting resistivity of 20 Ohm-m (equivalent to a 20 ohm-m halfspace). The thicknesses of the first layers of the models were about 3 ft with the thicknesses of the consecutive layers increasing by factors of 1.02 to 1.11. The depths to the bottoms of the 29th layers were set to 1,034 ft, with thicknesses up to about 72 ft. The thicknesses of the layers increase with depth (Table 4-5 and Figure 4-18) as the resolution of the technique decreases. The spatial reference distance, ***s***, for the constraints were set to 246 ft with power law fall-off of 0.75. The vertical and lateral constraints, ***ResVerSTD*** and ***ResLatStD***, were set to 2.4 and 1.4, respectively, for all layers.

One important thing to note is that these SCI inversions included an analysis of the data received while the current was still turning off using a system response deconvolution technique recently developed by Andersen et al. (2018). The result is that earlier times/higher frequencies are recorded which translates into sampling shallower depths leading to higher resolution of the very near surface.

In addition to the recovered resistivity models, the SCIs also produce data residual error values (single sounding error residuals) and Depth of Investigation (DOI) estimates. The data residuals compare the measured data with the response of the individual inverted models (Christensen et al., 2009). The DOI provides a general estimate of the depth to which the AEM data are sensitive to changes in the resistivity distribution at depth (Christiansen and Auken, 2012). Two DOI's are calculated: an "Upper", more conservative, DOI with a cumulative sensitivity of 1.2 and a "Lower", less conserative, DOI with a cumulative sensitivity of 0.6. A more detailed discussion on the DOI can be found in Asch et al. (2015).

Figure 4-19 presents a histogram of the CCWCD AEM inversion data/model residuals. A map of data residuals for the Gilcrest AEM study area is presented in Figure 4-20.

Table 4-5: Thickness and depth to bottom for each layer in the Spatially Constrained Inversion (SCI) AEM earth models. The thickness of the model layers increase with depth as the resolution of the AEM technique decreases.

Layer	Depth to Bottom (ft)	Thickness (ft)	Layer	Depth to Bottom (ft)	Thickness (ft)
1	3.3	3.3	16	232.3	46.2
2	6.9	3.6	17	280.8	48.5
3	11.0	4.1	18	331.8	50.9
4	15.5	4.5	19	385.3	53.5
5	20.5	5.0	20	441.4	56.2
6	26.1	5.6	21	499.8	58.4
7	32.3	6.2	22	560.6	60.7
8	40.0	7.8	23	623.7	63.2
9	49.7	9.7	24	688.8	65.1
10	61.8	12.1	25	755.2	66.4
11	77.0	15.1	26	822.9	67.7
12	95.9	18.9	27	891.9	69.1
13	119.6	23.7	28	962.4	70.4
14	149.1	29.6	29	1034.2	71.8
15	186.1	37.0			

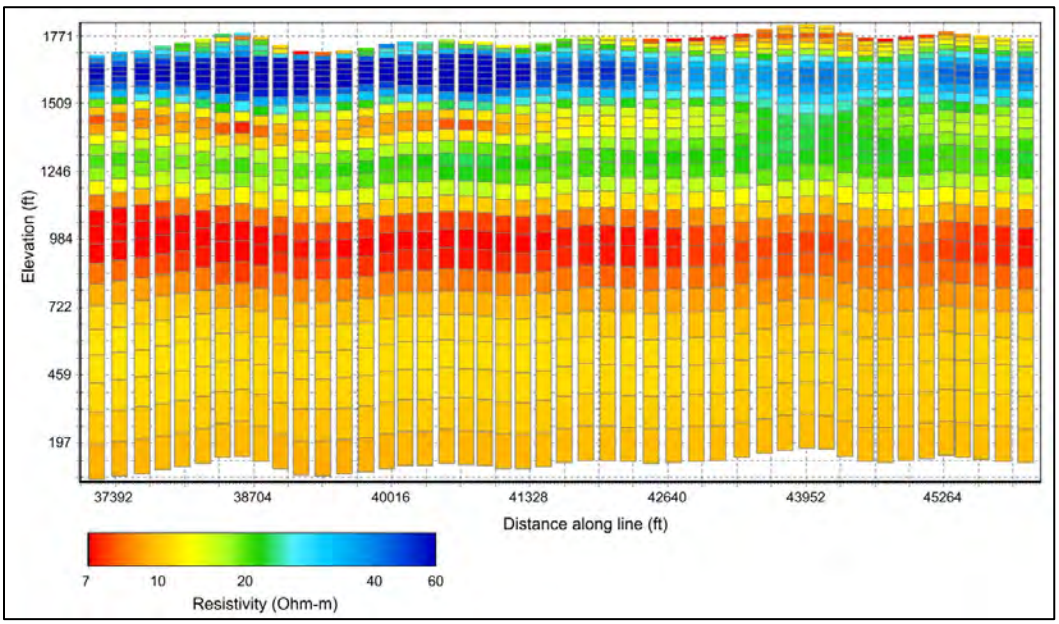

Figure 4-18. An example of an AEM profile illustrating increasing model layer thicknesses with depth.

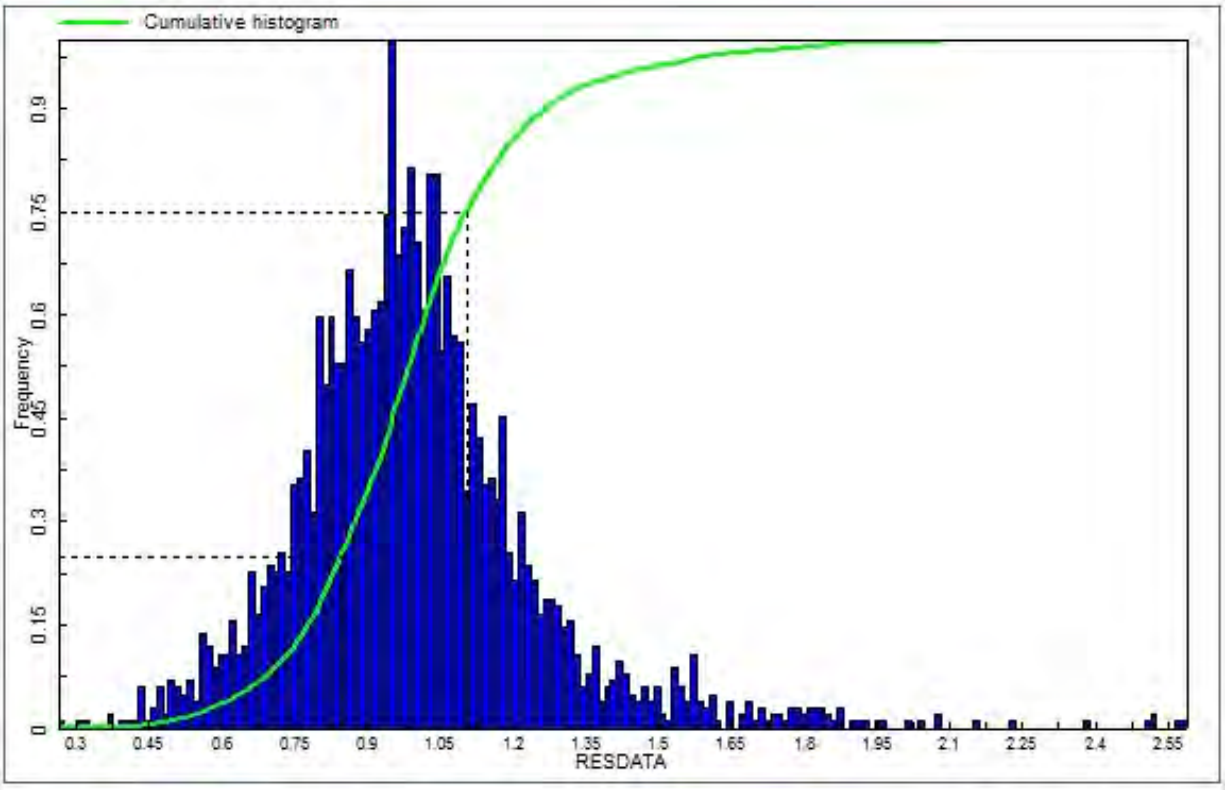

Figure 4-19. Data/model residual histogram for the CCWCD SCI inversion results.

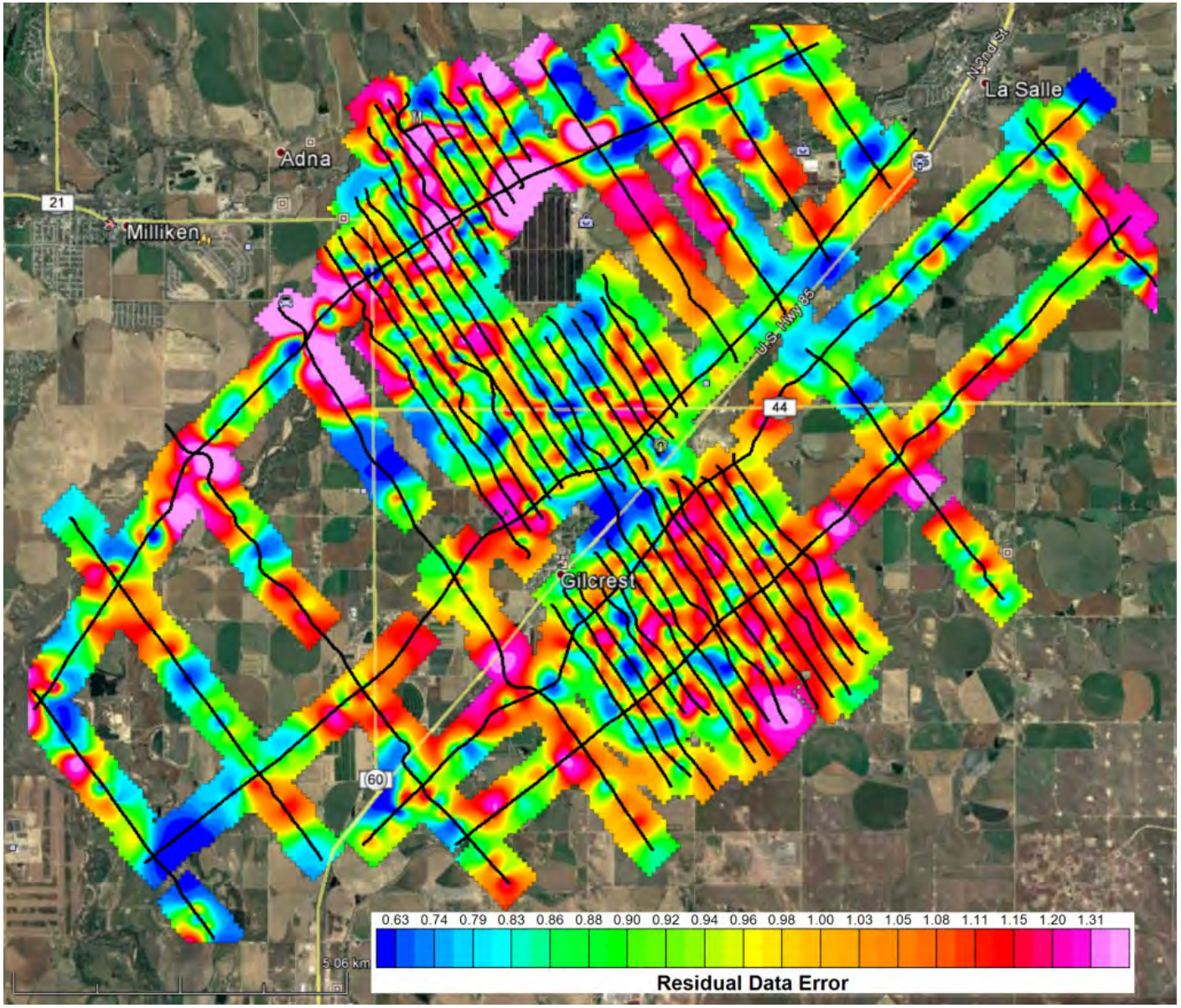

Figure 4-20. Map of data residuals (ResData) for the CCWCD SCI inversion results. The as-flown flight lines are indicated as black lines.

5 AEM Results and Interpretation

This section provides the details on the process involved in the interpretation of the CCWCD AEM data and inversion\interpretation results.

5.1 Interpretive Process

5.1.1 Merging and Splitting AEM Flight Lines

After the inversion process several short lines and line segments were combined to form continuous lines within the Gilcrest AEM survey area. These merged lines allow for improved viewing and interpretation of the AEM inversions results. Table 5-1 lists the original lines and the new combined lines. For lines that have overlapping data, the overlapping regions of the flight lines were sorted in the dominant line direction (east-west or north-south) and combined. This has no impact on the SCI as the actual X, Y, and Z locations of the survey data are used in the inversions. For display purposes, this allows for consecutive soundings in the dominant direction. Line L200101 was split into two segments L200101a and L200101b to aid in display as the lines is curved as it follows the South Platte River.

Table 5-1. Combination of flight lines within the Gilcrest AEM Survey Area.

Original Source Lines	Direction	New Line
L100501 and L100501	southeast-northwest	L201102
L100801, and L100701	southeast-northwest	L201502
L100901, and L101001	southeast-northwest	L201902
L101101, and L101201	southeast-northwest	L202302
L101301, and L101401	southeast-northwest	L202703
L101501, and L101601	southeast-northwest	L203102
L101801, L101901, and L101902	southeast-northwest	L305604
L102100, and L102101	southeast-northwest	L204102
L102201, L102301, and L102302	southeast-northwest	L306804
L102401, L102402, and L102501	southeast-northwest	L405404
L102601, L102702, and L102801	southeast-northwest	L308104
L102901, L103001, and L103101	southeast-northwest	L309003
L103201, L103301, and L103401	southeast-northwest	L309903
L103601, and L103602	southeast-northwest	L207203

5.1.2 Construction of the Project Digital Elevation Model

To ensure that the elevation used in the project is constant for all the data sources (i.e. boreholes and AEM data) a Digital Elevation Model (DEM) was constructed for the Gilcrest AEM survey area. The data were downloaded from the National Elevation Dataset (NED) located at the National Map Website (U.S. Geological Survey, 2016) at a resolution of 1 arc-second or approximately 100 ft. The geographic coordinates are in North American Datum of 1983 (NAD83), UTM Zone 13 North (meters), and the elevation values are referenced to the North American Vertical Datum of 1988 (NAVD 88) (feet). The 100 ft grid cell size was used throughout the project and resulting products. Figure 5-1 is a map of the DEM of the Gilcrest AEM survey area showing a vertical relief of 267.1 ft with a minimum elevation of 4,660.94 ft and a maximum elevation of 4,928.04 ft. This DEM was used to reference all elevations within the Gilcrest survey area. LiDAR data was not used in this project due to the 20-120 meter spacing of the stations. The NED DEM is at 30 meters and was determined to be adequate for the AEM survey. The ArcView Binary Raster Grid (*.flt) and can be found in Appendix 3 Deliverables\Grids\ESRI.

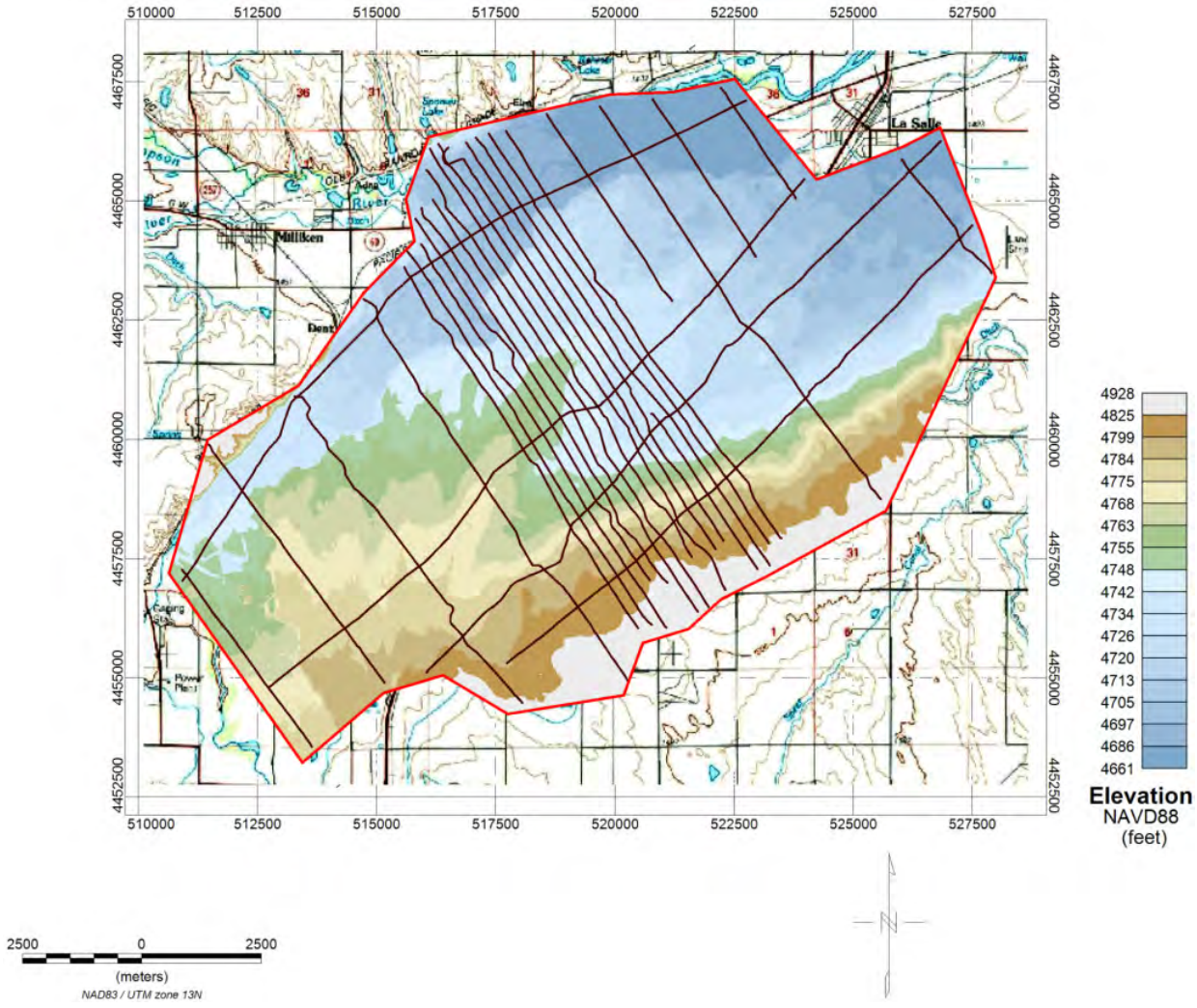

Figure 5-1. Digital elevation model (DEM) of the Gilcrest AEM survey area. Flight lines indicated by brown lines. Survey area indicated by red line. Base map is the 100K USGS topography map.

5.1.3 Interpretation of the 2D Profiles

After final AEM database preparations, characterization of the subsurface was performed in cross-section format using Encom PA (Datamine Discover, 2017). During interpretation, the horizontal and vertical scales of the profiles were adjusted to facilitate viewing. The color scale of the resistivity data was also adjusted to illuminate subtle differences in the resistivity structure within the inverted AEM resistivity data relative to the area being interpreted. The first step in the interpretation process is digitizing the contacts between the geological units including: the Quaternary (***Q***); Cretaceous Laramie Formation (***Kl***); Cretaceous Fox Hills Sandstone (***Kfh***); and Cretaceous Pierre Shale (***Kp***). The interpretive process benefited from the use of Colorado Division of Water Resources (CO-DWR) well logs (CO-DWR, 2018), which provided lithologic and well production information. The interpretations were simultaneously checked against the information in Barkmann et al. (2014), Dechesne et al. (2011), Robson et al. (2000a), and Hurr et al. (1972).

The interpretation began with picking the ***Q***, ***Kfh***, and ***Kl*** contacts. The process was iterative around the eroded segments of the ***Kl***. Finally, the ***Kp*** was picked. The ***Kp*** has a much lower resistivity than the ***Kfh*** and can be separated from the ***Kfh*** in most locations. In the areas of the resistive ***Q***, sitting on top of the resistive ***Kfh***, the interpretation was much more challenging, and the use of boreholes was necessary to estimate the ***Q***/***Kfh*** contact.

Figure 5-2 is an example of Line L200201 that is located just north of Gilcrest down the axis of the valley. The resistivity data is plotted along the line with areas that were deleted due to EM coupling indicated as gaps in the resistivity plots. The boreholes are plotted within 200 meters of the flight line and are colored by lithology. The bedrock is the ***Kfh*** in this region and is indicated by a solid black line. The contact of the ***Kfh*** and the ***Kp*** is indicated by a dashed black line. Within the ***Q*** area above the bedrock, there is an obvious electrically conductive or low electrically resistive zone that is approximately 25 feet below the surface. Several boreholes indicated the presence of a sand and silt and a silt and clay at that level. There are areas of electrically resistive material below and above the electrically conductive zone. These electrically resistive areas indicate coarser grained materials of sand, sand and gravel, and gravel that make up the Quaternary alluvium (***Qal***).

Figure 5-3 is an example of Line L306804 that is located just east of Gilcrest and is perpendicular to the axis of the valley. The resistivity data is plotted along the line with areas that were deleted due to EM coupling indicated as gaps in the resistivity plots. The boreholes are projected and plotted on the profile if they are within 200 meters of the flight line and are colored by lithology. The bedrock is a combination of ***Kfh*** and ***Kl*** and is indicated by a solid black line. The contact of the ***Kl*** and the ***Kfh*** and the ***Kfh*** and the ***Kp*** is indicated by dashed black lines. Within the ***Q*** area above the bedrock there is an obvious electrically conductive zone that is approximately 25 feet below the surface and extends from the south into the valley. Several boreholes indicated the presence of silt and clay at that level. There are areas of electrically resistive material below and above the electrically conductive zone. These electrically resistive areas indicate coarser grained materials of sand, sand and gravel, and gravel that make up the Quaternary alluvium (***Qal***). Moving toward the South Platte River, the electrically conductive layer is absent.

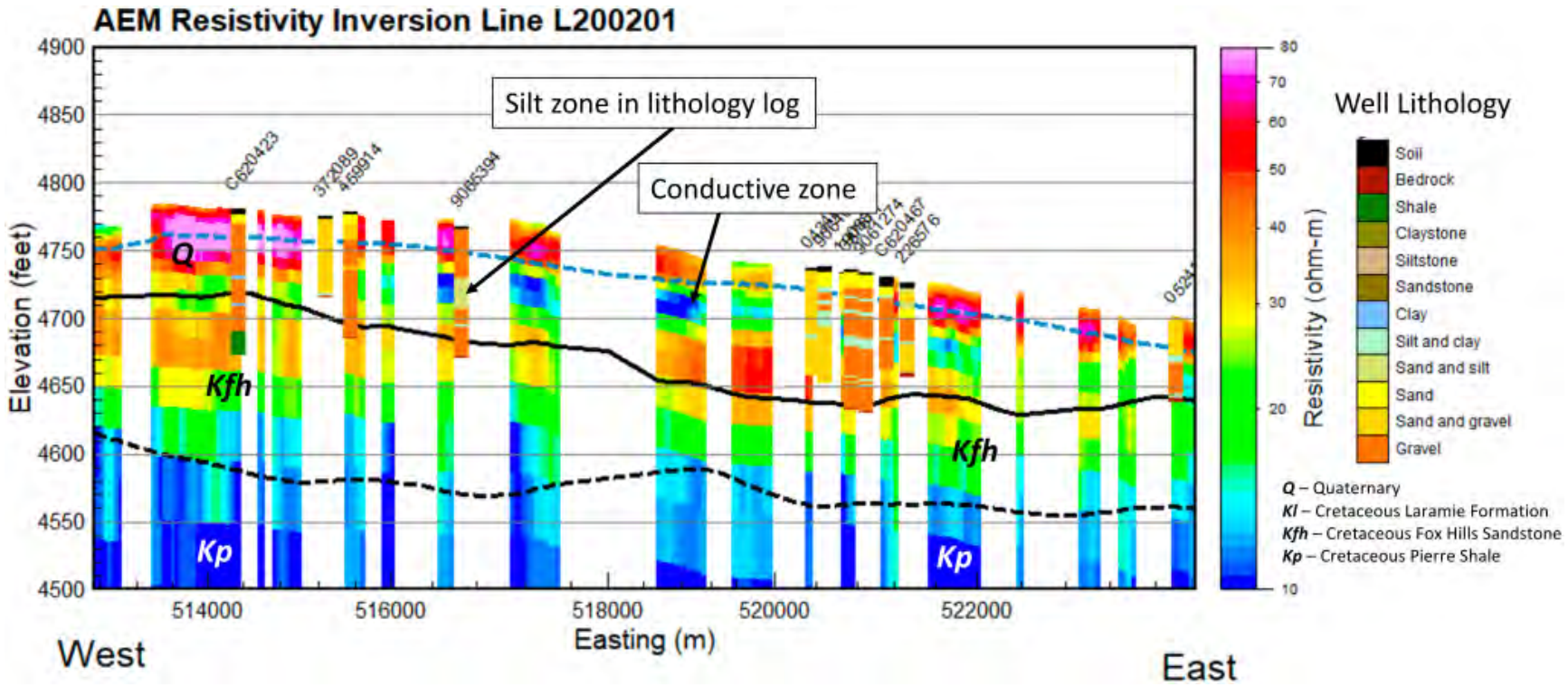

Figure 5-2. Line L200201 showing the inverted AEM resistivity profile. Boreholes are projected within 200 meters of the flight line. The dashed blue line is the water table, the solid black line is the Quaternary (*Q*) and Cretaceous Fox Hills Sandstone (*Kfh*), and the dashed black line is the *Kfh* and Pierre Shale (*Kp*) contact. Projection is NAD83 UTM Zone 13 North (meters), NAVD88 (feet).

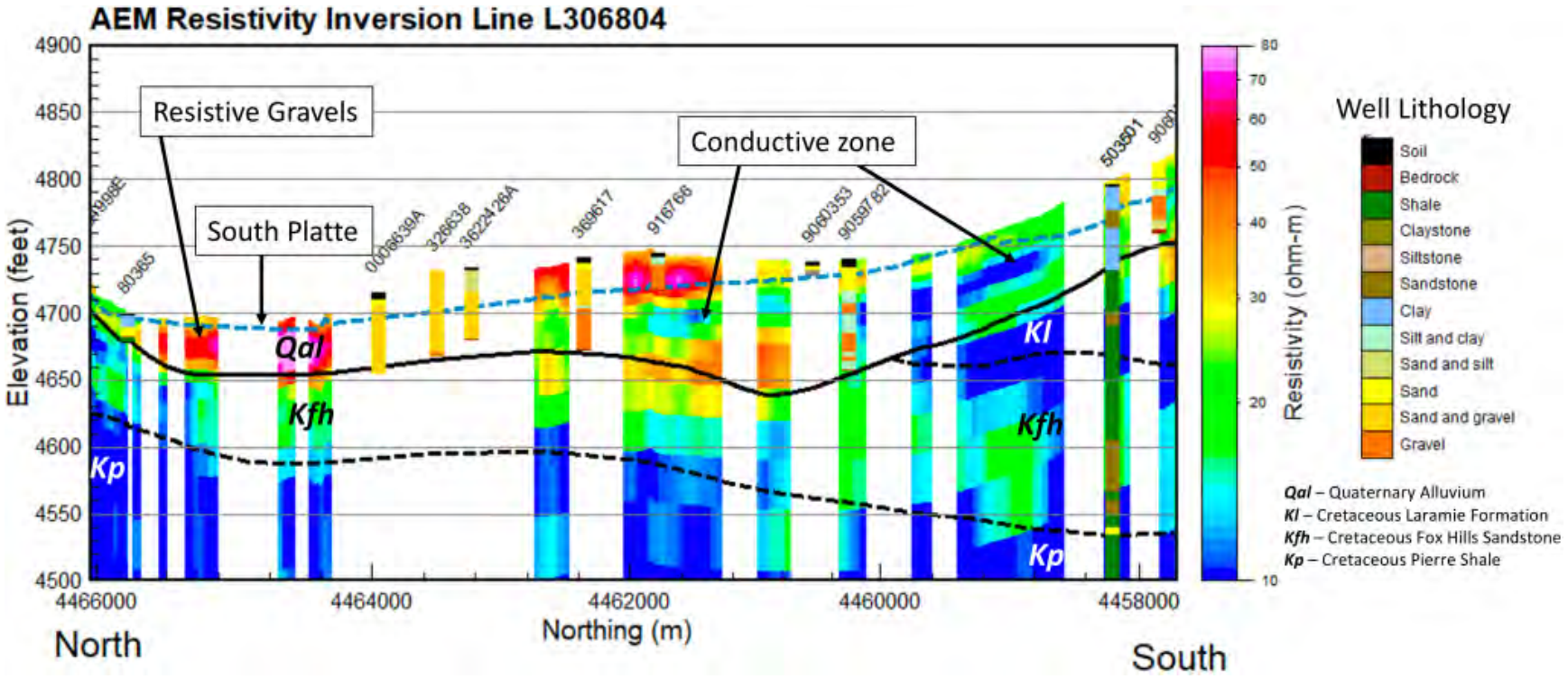

Figure 5-3. Line L306804 showing the inverted AEM resistivity profile. Boreholes are projected on the profile if within 200 meters of the flight line. The dashed blue line is the water table, the solid black line is the Quaternary (*Q*) and Cretaceous Fox Hills Sandstone (*Kfh*) contact, and the dashed black lines are the Cretaceous Laramie Formation (*Kl*) and *Kfh* contact as well as the *Kfh* and Pierre Shale (*Kp*) contact. Projection is NAD83 UTM Zone 13 North (meters), NAVD88 (feet).

Figure 5-4 is an example of Line L200101a that is located along the South Platte River. The resistivity data is plotted along the line with areas that were deleted due to EM coupling indicated as gaps in the resistivity plots. The boreholes are plotted within 200 meters of the flight line and are colored by lithology. The bedrock is the ***Kfh*** in this area and is indicated by a solid black line. The contact of the ***Kfh*** and the ***Kp*** is indicated by dashed black lines. Within the ***Qal*** area above the bedrock, there are electrically resistive sand and gravel and gravel that make up the Quaternary alluvium (***Qal***). There is also an indication of an electrically conductive unit within the ***Kfh***. The contact of the ***Kfh*** and the ***Kp*** is indicated as a change to electrically conductive or low electrically resistive materials within the ***Kp***.

5.1.4 Creating Interpretative Surface Grids

Within the Gilcrest AEM survey area, surface grids of geologic formations were produced for the ***Kl***, ***Kfh***, and the ***Kp***. To create these grids, the elevations of the AEM-interpreted tops of the formations were imported to a Geosoft Oasis montaj (OM) database (Geosoft, 2018). The interpreted elevation data were then gridded for each formation independently using the OM minimum curvature gridding (MCG) algorithm. Selected CO-DWR borehole were used to augment the AEM data.

For the ***Kl*** surface, 140 AEM picks were used in the grid with a cell size of 200 meters and the "cells to extend beyond" set to three. All other parameters were either left as the default or blank. A 5x5 cell smoothing filter was then used on the grid. The resulting grid was then clipped to the Gilcrest AEM survey area. Figure 5-5 presents a map of the elevation of the top of the ***Kl*** for the Gilcrest AEM survey area. The ***Kl*** does exist on the far western end of the survey at the edge of the AEM flight lines (Barkmann et al., 2014). However, there was insufficient data coverage to clearly pick the ***Kl*** on the western side of the South Platte River. For the ***Kfh*** surface, 883 AEM picks were used with a cell size of 200 meters and the "cells to extend beyond" set to three. A 3x3 cell smoothing filter was then used on the grid. All other parameters were either left as the default or blank. The grid was then clipped to the Gilcrest AEM survey area. Figure 5-6 is a map of the elevation of the top of the ***Kfh.*** For the top of the Cretaceous Pierre Shale (***Kp***), 347 AEM picks were used in the grid with a cell size of 200 meters and the "cells to extend beyond" set to three. A 7x7 cell smoothing filter was then used on the grid. All other parameters were either left as the default or blank. The grid was then clipped to the Gilcrest AEM survey area. A map of the elevation of the top of the ***Kp*** for the Gilcrest AEM survey area is presented in Figure 5-7. The bedrock surface for the area is a composite of the ***Kl*** and the ***Kfh***. Those surfaces were combined to provide a 200 meter grid of the bedrock in the Gilcrest AEM investigation area. A map of the elevation of the bedrock is presented in Figure 5-8. Interpretative surface grids of the Gilcrest AEM flight area can be found Appendix 3-Deliverables\Grids.

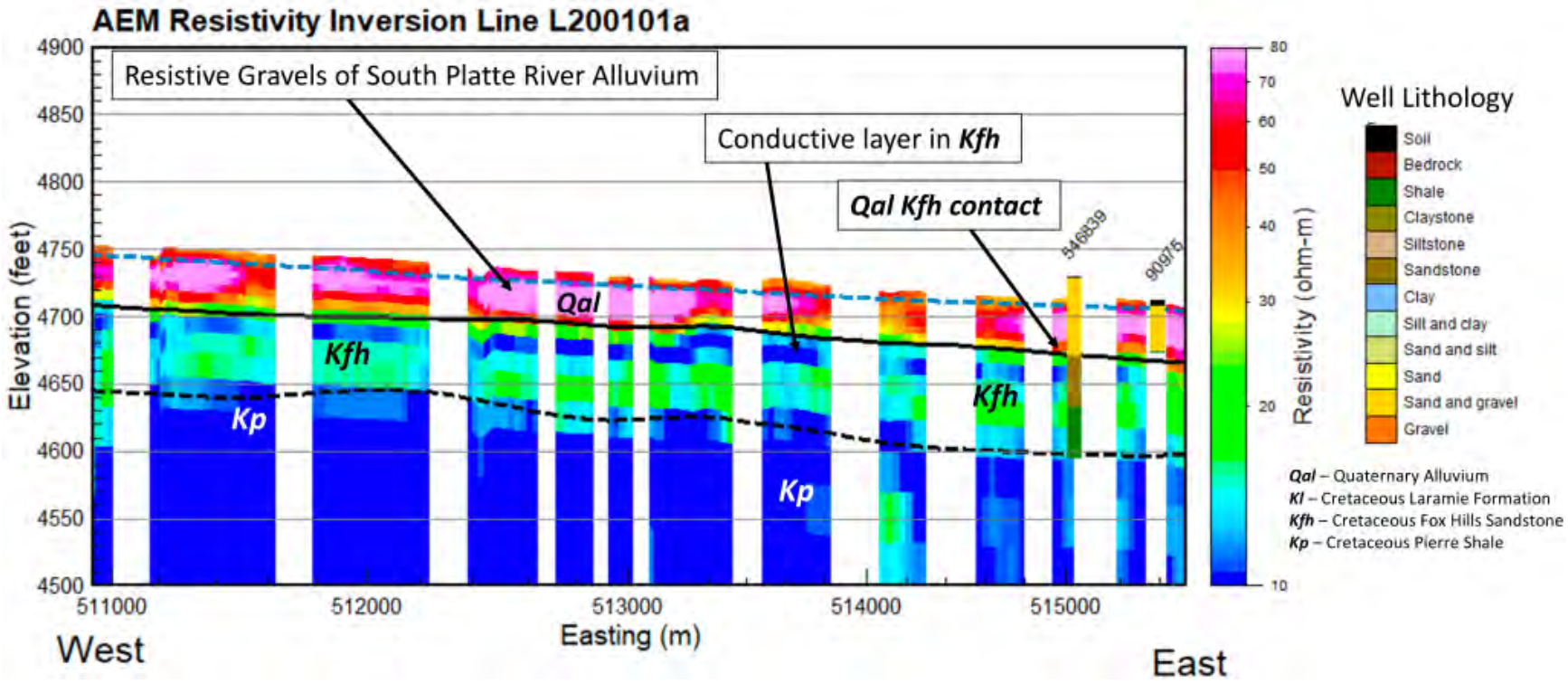

Figure 5-4. Line L200101 showing the inverted AEM resistivity profile. Boreholes are projected on the profile if within 200 meters of the flight line. The dashed blue line is the water table, the solid black line is the Quaternary (Q) and Cretaceous Fox Hills Sandstone (*Kfh*) contact, and the dashed black line is the *Kfh* and Cretaceous Pierre Shale (*Kp*) contact. Projection is NAD83 UTM Zone 13 North (meters), NAVD88 (feet).

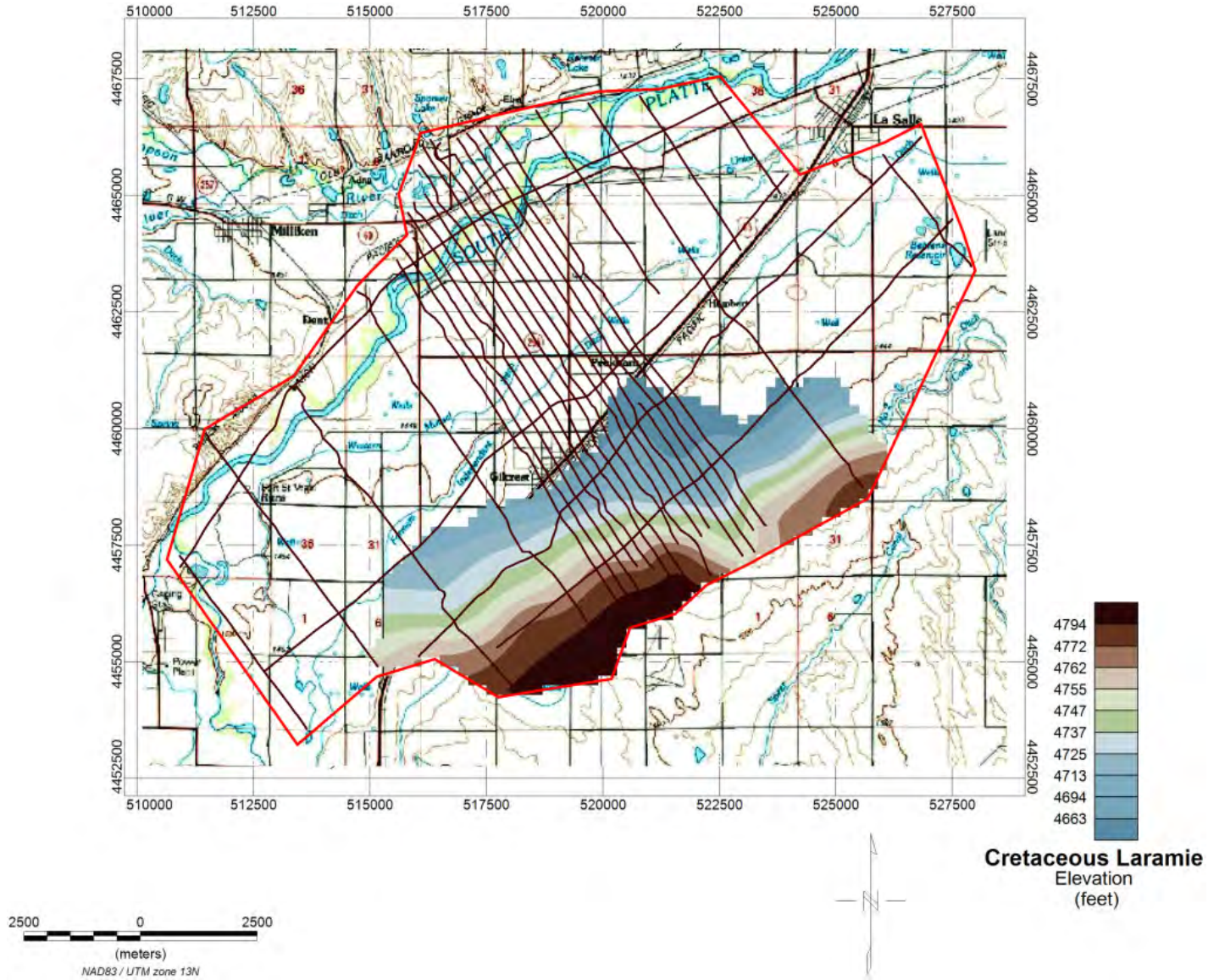

Figure 5-5. Map of the elevation of the Cretaceous Laramie Formation (*Kl*) within the Gilcrest AEM survey area. Flight lines indicated by brown lines. Survey area indicated by red line. Base map is the 100K USGS topography map.

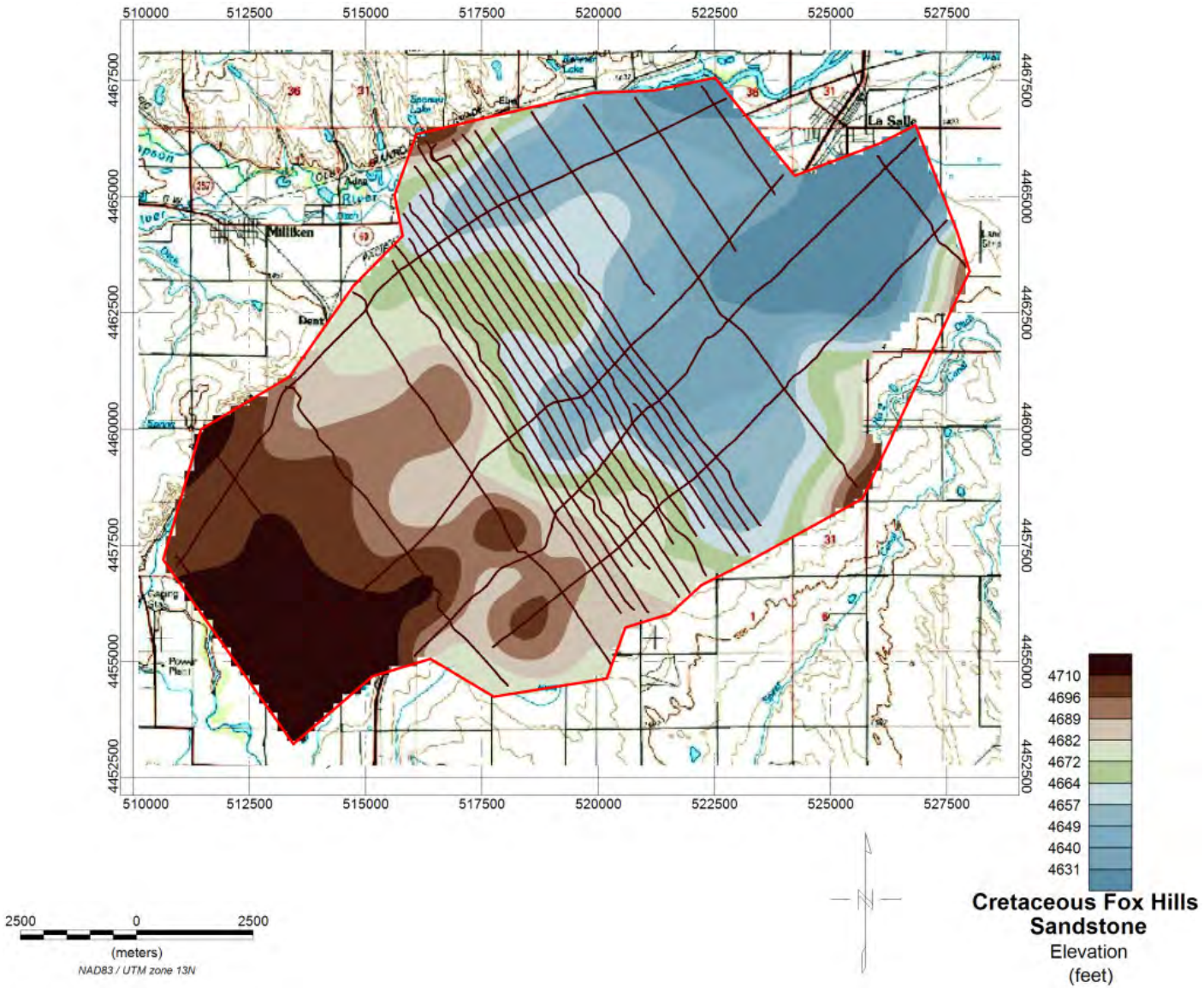

Figure 5-6. Map of the elevation of the Cretaceous Fox Hills Sandstone (*Kfh*) within the Gilcrest AEM survey area. Flight lines indicated by brown lines. Survey area indicated by red line. Base map is the 100K USGS topography map.

Figure 5-7. Map of the elevation of the Cretaceous Pierre Shale (*Kp*) within the Gilcrest AEM survey area. Flight lines indicated by brown lines. Survey area indicated by red line. Base map is the 100K USGS topography map.

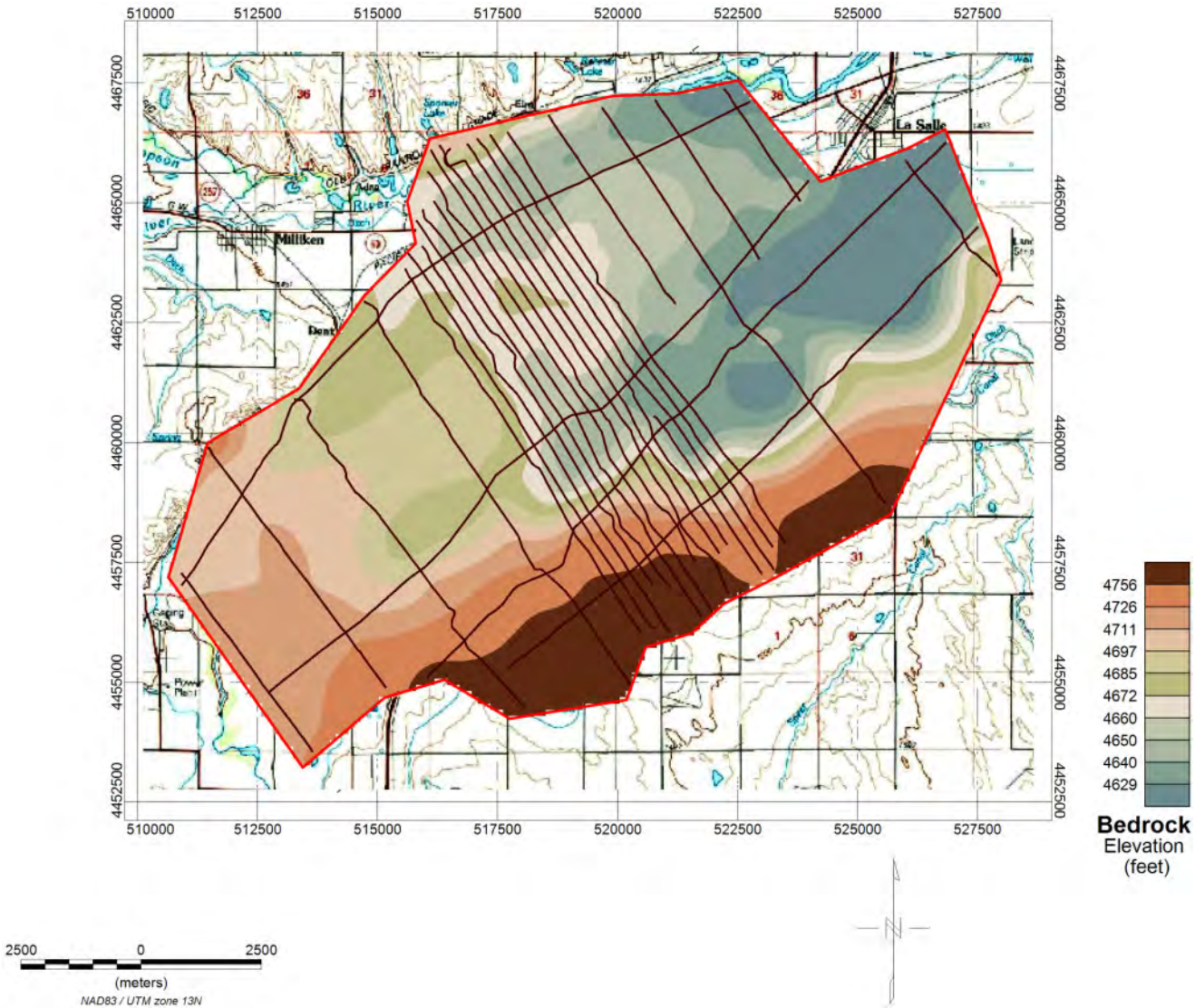

Figure 5-8. Map of the elevation of the bedrock composed of the Cretaceous Laramie Formation (*Kl*) and the Cretaceous Fox Hills Sandstone (*Kfh*) within the Gilcrest AEM survey area. Flight lines indicated by brown lines. Survey area indicated by red line. Base map is the 100K USGS topography map.

5.1.5 The Resistivity-Lithology Relationship and Interpretation of the Quaternary Deposits

Following construction of the geological surfaces, the ***Q*** deposits were isolated within the AEM data. Figure 5-9 is a ***Q*** thickness map for the Gilcrest AEM survey areas. To assist in the approximation of the saturated materials along the surveyed AEM flight lines, a water table was developed for the Gilcrest AEM survey area. This water table was built on several data sources to provide coverage over the complete area. A water table (spring of 2017) was provided to AGF from the CO-DWR that was prepared by the CGS (Sebol and Barkmann, 2017). While this is an extremely high-quality water table, it doesn't extend over the complete AEM acquisition area. Thus, this water table was merged at the extent of the AEM survey with the spring 2012 water table from Barkmann et al. (2014), data from Wellman (2015) and data from Robson et al. (2000a). The final water table used in the project has a cell size of 200 meters and is clipped to the AEM survey area (Figure 5-10). Using both the developed bedrock elevation surface and the water table elevation surface, an estimate of the saturated thickness of the ***Q*** can be calculated (Figure 5-11). Arc and Geosoft format girds of the interpretive water table surface can be found in Appendix 3-Deliverable\Grids.

The materials in the Quaternary (***Q***) were separated by four major resistivity thresholds that encompassed the lithology ranges as defined by Barkmann et al. (2014): Silt and Clay, Sand and Silt, Sand and Gravel, and Gravel. These ranges include: less than 16 ohm-m, representing Silt and Clay; 16-23 ohm-m, representing Sand and Silt; 23-40 ohm-m, representing Sand and Gravel; and 40 ohm-m or greater, representing Gravel. These breaks were identified by inspection of the AEM and the lithology from the boreholes. These values are not that different from other areas within the area of the Platte river system (AGF, 2017; Carney et al., 2015). Results of these interpretations can be found in Appendix 1 (2D profiles) and in Appendix 2 (3D images). The color scheme presented in Figure 5-12, which is based on Barkmann et al. (2014) will be used when discussing interpreted lithologies. This process could be enhanced with the addition of calibrated high quality geophysical logs coupled to high quality lithology logs.

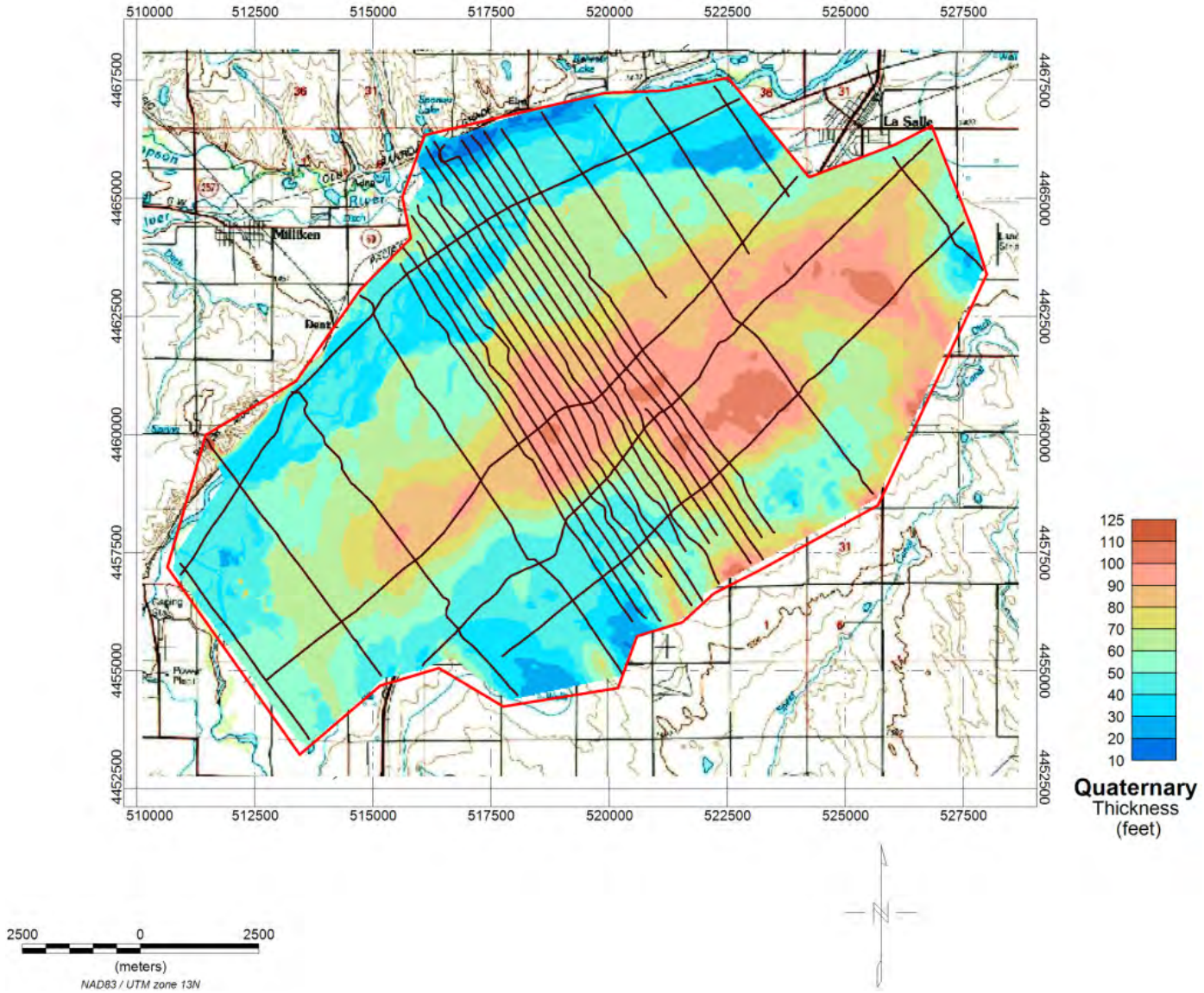

Figure 5-9. Map of the Quaternary (*Q*) thickness of the Gilcrest AEM survey area. Flight lines indicated by brown lines. Survey area indicated by red line. Base map is the 100K USGS topography map.

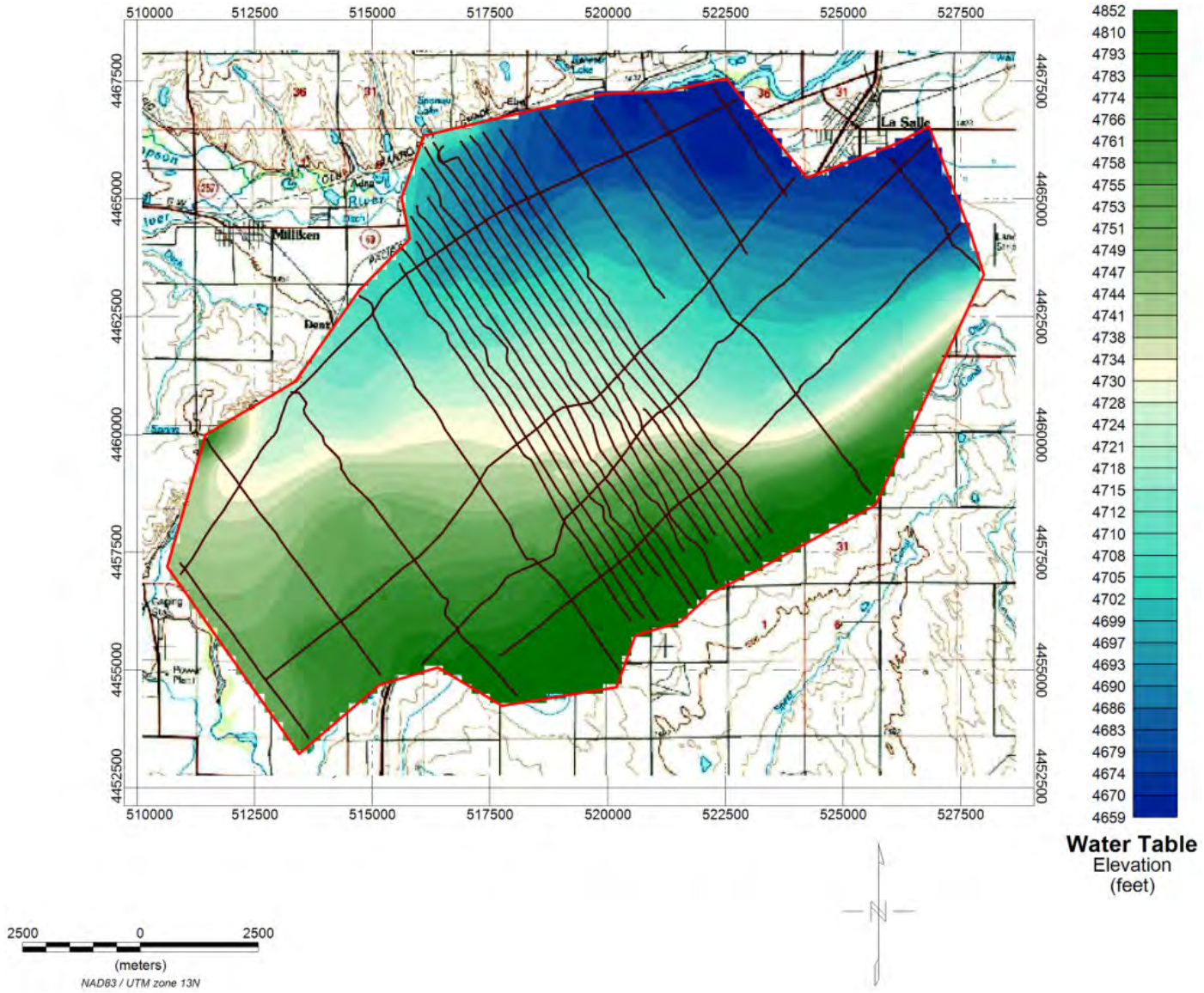

Figure 5-10. Map of the Water table constructed by AGF for the Gilcrest AEM survey area. Flight lines indicated by brown lines. Survey area indicated by red line. Base map is the 100K USGS topography map.

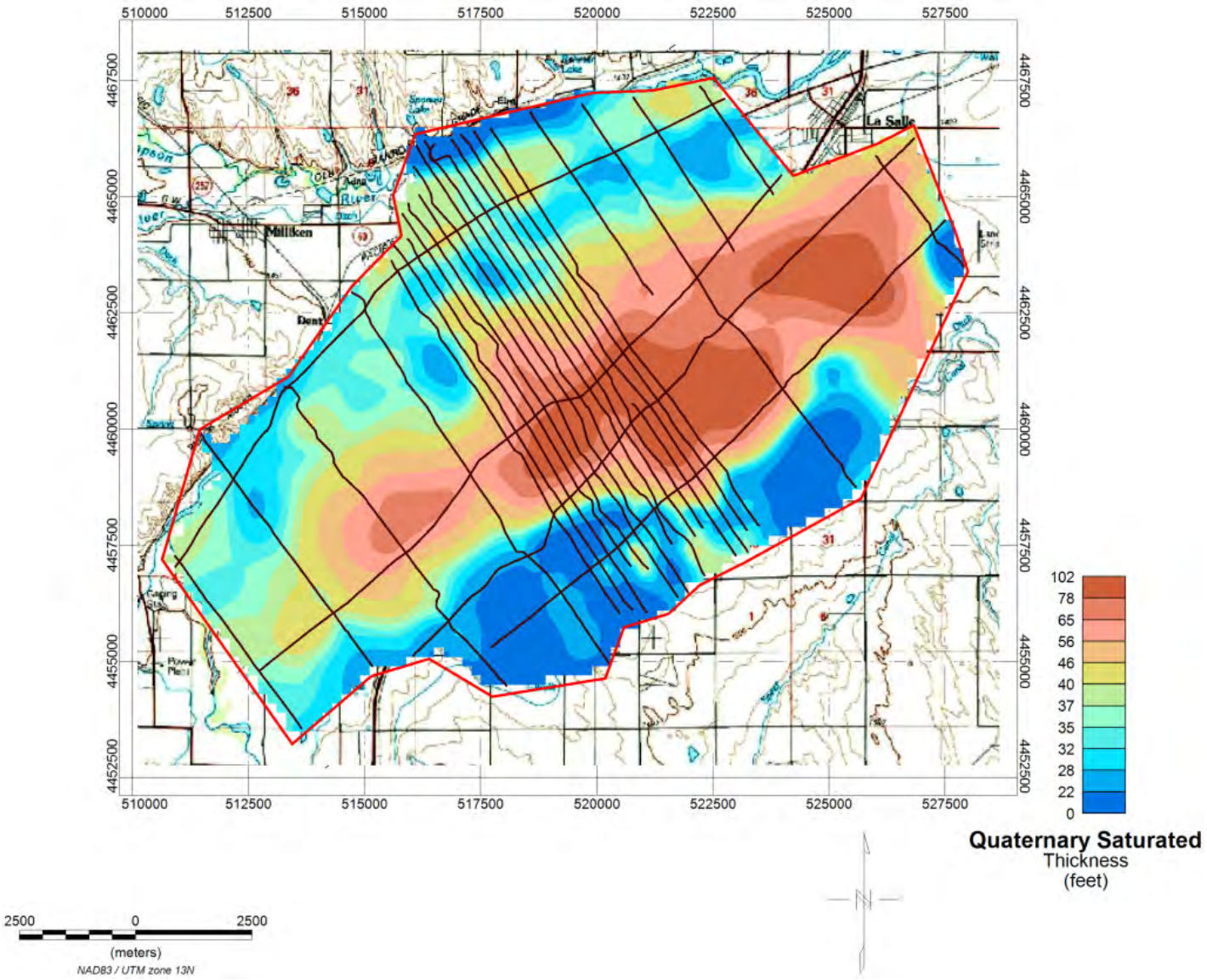

Figure 5-11. Map of the saturated thickness of the Quaternary (*Q*) in the Gilcrest AEM survey area. Flight lines indicated by brown lines. Survey area indicated by red line. Base map is the 100K USGS topography map.

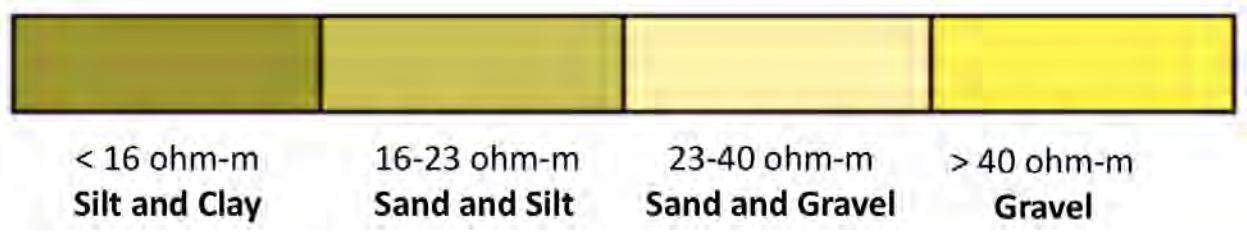

Figure 5-12. Major resistivity thresholds for interpreted lithology classes.

5.1.6 Create 3D Interpretative Voxel Grids

A series of voxel grids were completed for the Gilcrest AEM survey area. The voxel grids were made using a 200 meter grid cell size and the model layer thickness (Table 4-5 in the previous section). A minimum curvature method was used within Datamine Discover PA (Datamine Discover, 2017). All layers were referenced to their depth from the surface and then projected on the area DEM. After the grid was calculated, the grid was split at the bedrock, ***Kl***, ***Kfh***, and ***Kp*** contacts using the elevation grids discussed above in Section 5.1.4. These resulting voxel grids can be used to explore the distribution of the aquifer materials within the area in 3D. Specifically, these grids can allow for visual inspection of the volume of materials above the bedrock as well as surface materials. A 3D exploded diagram of the solid-layers within the voxel including the ***Q***, ***Kl***, ***Kfh***, and ***Kp*** is presented in Figure 5-13. The ***Q*** can also be separated by the thresholds developed above for the four lithology classes. Figure 5-14 is a 3D exploded diagram of the lithology classes within the ***Q*** materials. The voxel grids can be found in *Appendix 3-Deliverables\Voxel*.

Thickness grids were also calculated for the lithology classes. Figure 5-15, Figure 5-16, Figure 5-17, and Figure 5-18 present the thicknesses of the Silt and Clay, Sand and Silt, Sand and Gravel, and the Gravel sediment zones within the ***Q***, respectively. When these grids are displayed, the materials that are below and above the thresholds are transparent only showing the thicknesses of the materials within the specified thresholds of the lithology classes.

Also of interest in the area of the Gilcrest AEM survey area is the ***Kfh*** which is typically used as a domestic water source. As explained above, the ***Kfh*** was divided out of the voxel. Within the ***Kfh,*** there are zones of greater resistive material that relate to the presence of sandstone-dominant units within the unit. The more electrically conductive, or lower resistivity materials, relate to the shale-dominant. Using a cutoff of greater than 18 ohm-m, a thickness of resistive ***Kfh*** was generated (Figure 5-19).

Estimates of the recharge potential of an area can be made by looking at the surface layers (Table 4-5) of the voxel grids which represents the average resistivity of that depth interval. This can be important in sighting new recharge ponds and other managed aquifer recharge (MAR) projects. The first six layers (Table 4-5) of the voxel model for the Gilcrest AEM survey area are presented in Figure 5-20 (0-3 ft), Figure 5-21 (3-7 ft), Figure 5-22 (7-11 ft), Figure 5-23 (11-16 ft), Figure 5-24 (16-21 ft), and Figure 5-25 (21-26 ft). The silt and clay layer becomes more prevalent as the depth increases; particularly beyond 16 and 21 feet. The grids can be found in *Appendix 3-Deliverables\Grids*.

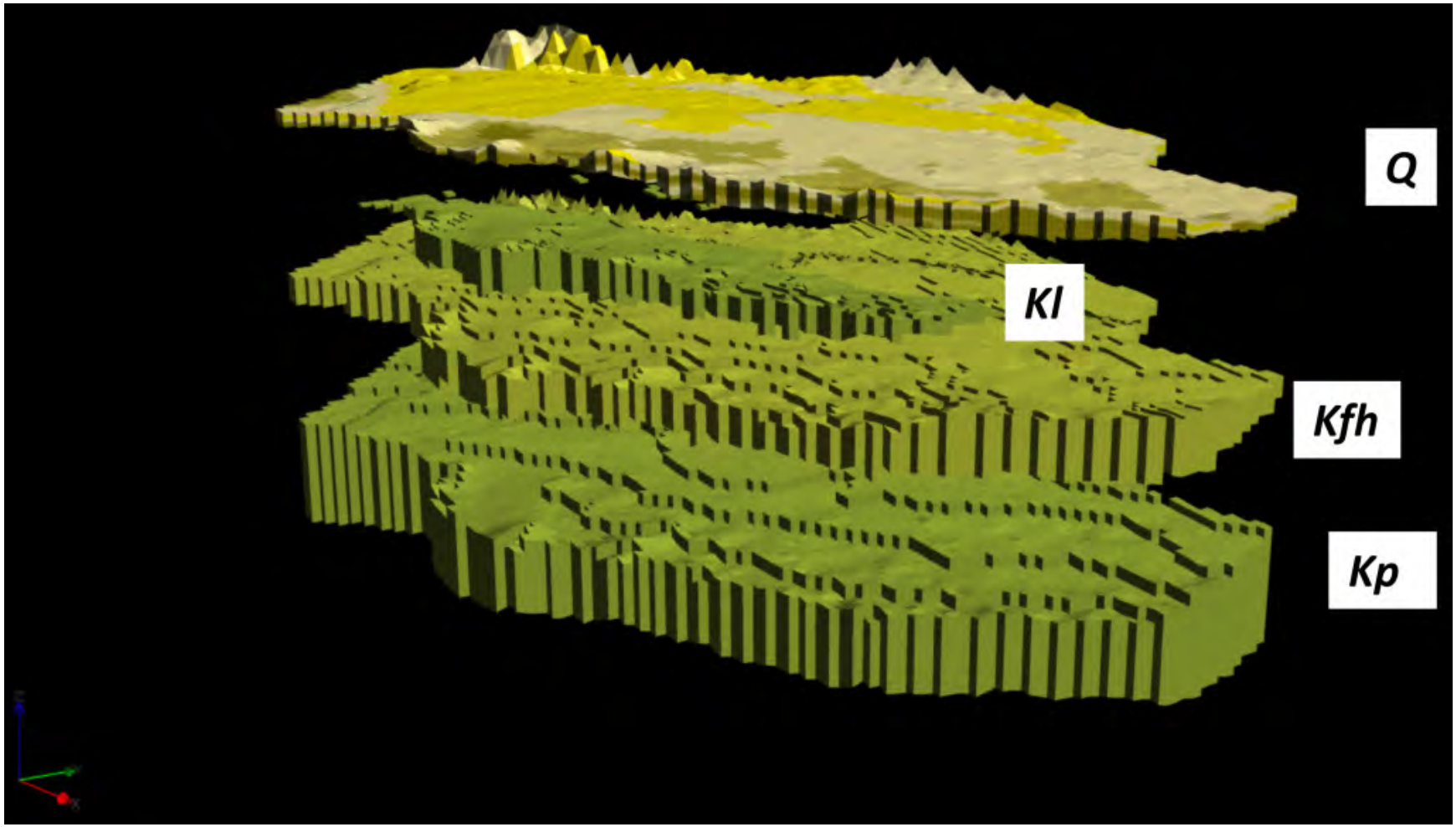

Figure 5-13. 3D exploded diagram of the geological solid-layers within the voxel including the Quaternary (*Q*), Cretaceous Laramie Formation (*Kl*), Cretaceous Fox Hills Sandstone (*Kfh*), and Cretaceous Pierre Shale (*Kp*). View from east to the west.

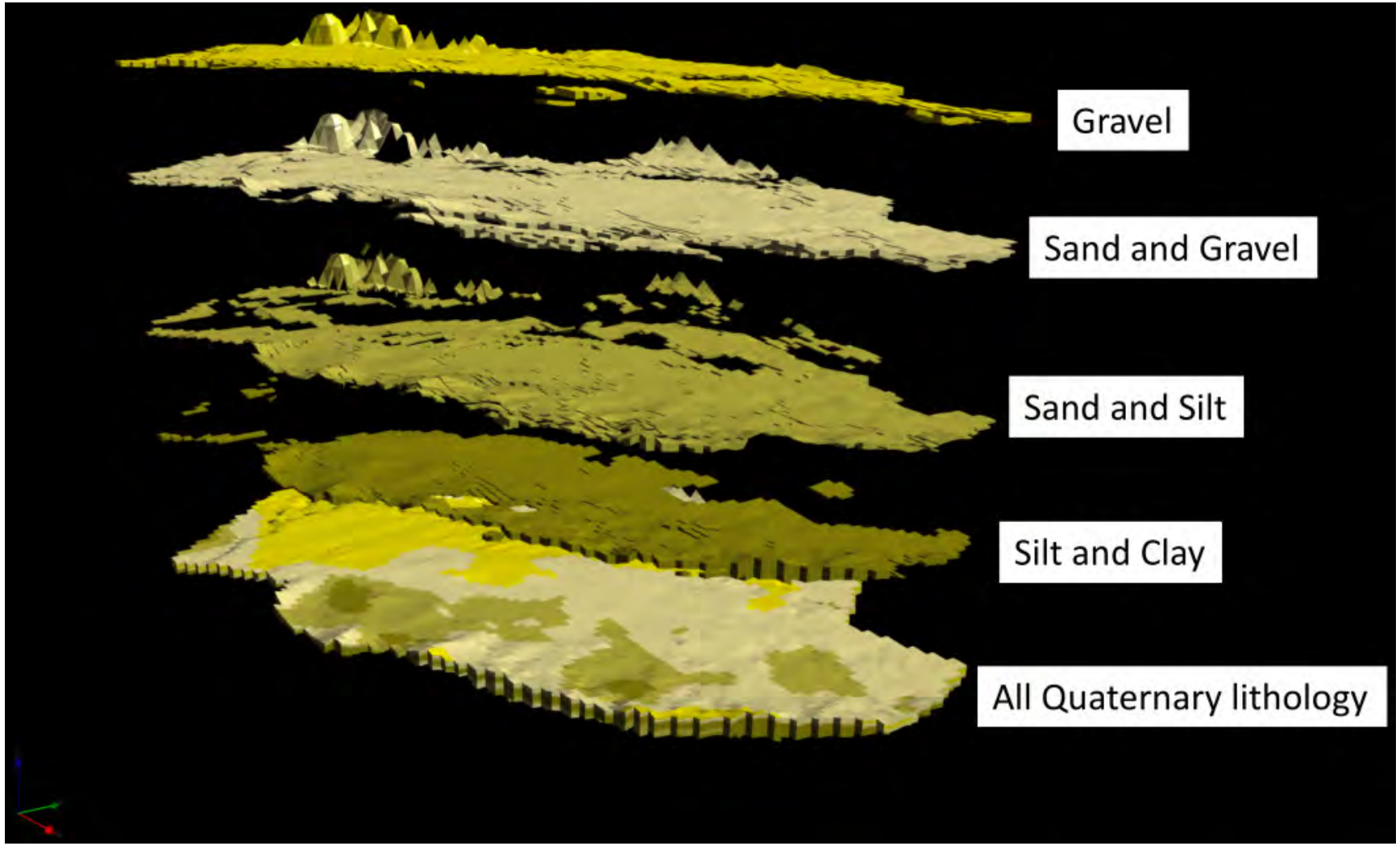

Figure 5-14. 3D exploded diagram of the Quaternary (*Q*) by the lithology classes of Silt and Clay, Sand and Silt, Sand and Gravel, and Gravel. View from east to the west.

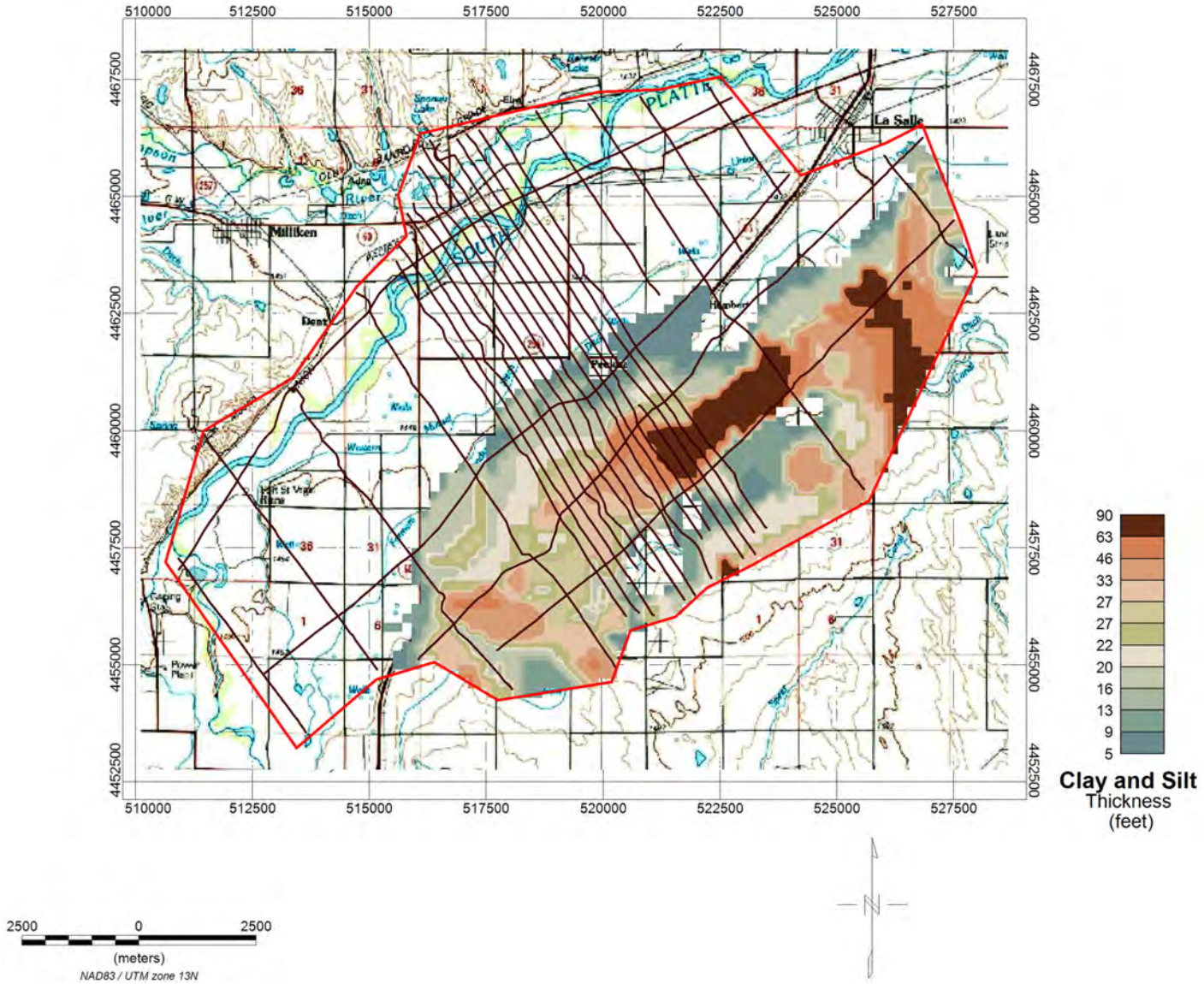

Figure 5-15. Map of the thickness of the Silt and Clay within the Quaternary over the Gilcrest AEM survey area. Flight lines indicated by brown lines. Survey area indicated by red line. Base map is the 100K USGS topography map.

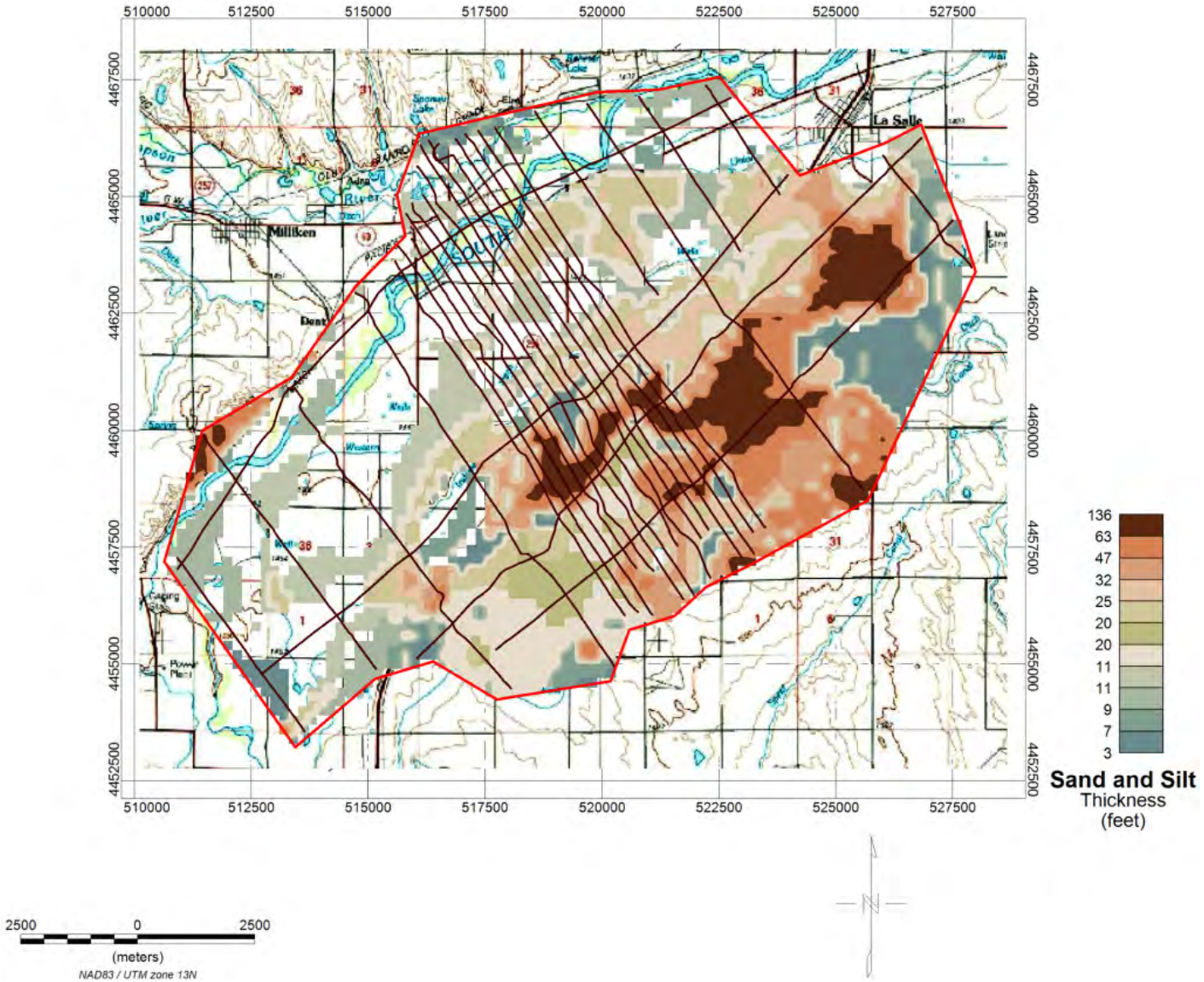

Figure 5-16. Map of the thickness of the Sand and Silt within the Quaternary over the Gilcrest AEM survey area. Flight lines indicated by brown lines. Survey area indicated by red line. Base map is the 100K USGS topography map.

Figure 5-17. Map of the thickness of the Sand and Gravel within the Quaternary over the Gilcrest AEM survey area. Flight lines indicated by brown lines. Survey area indicated by red line. Base map is the 100K USGS topography map.

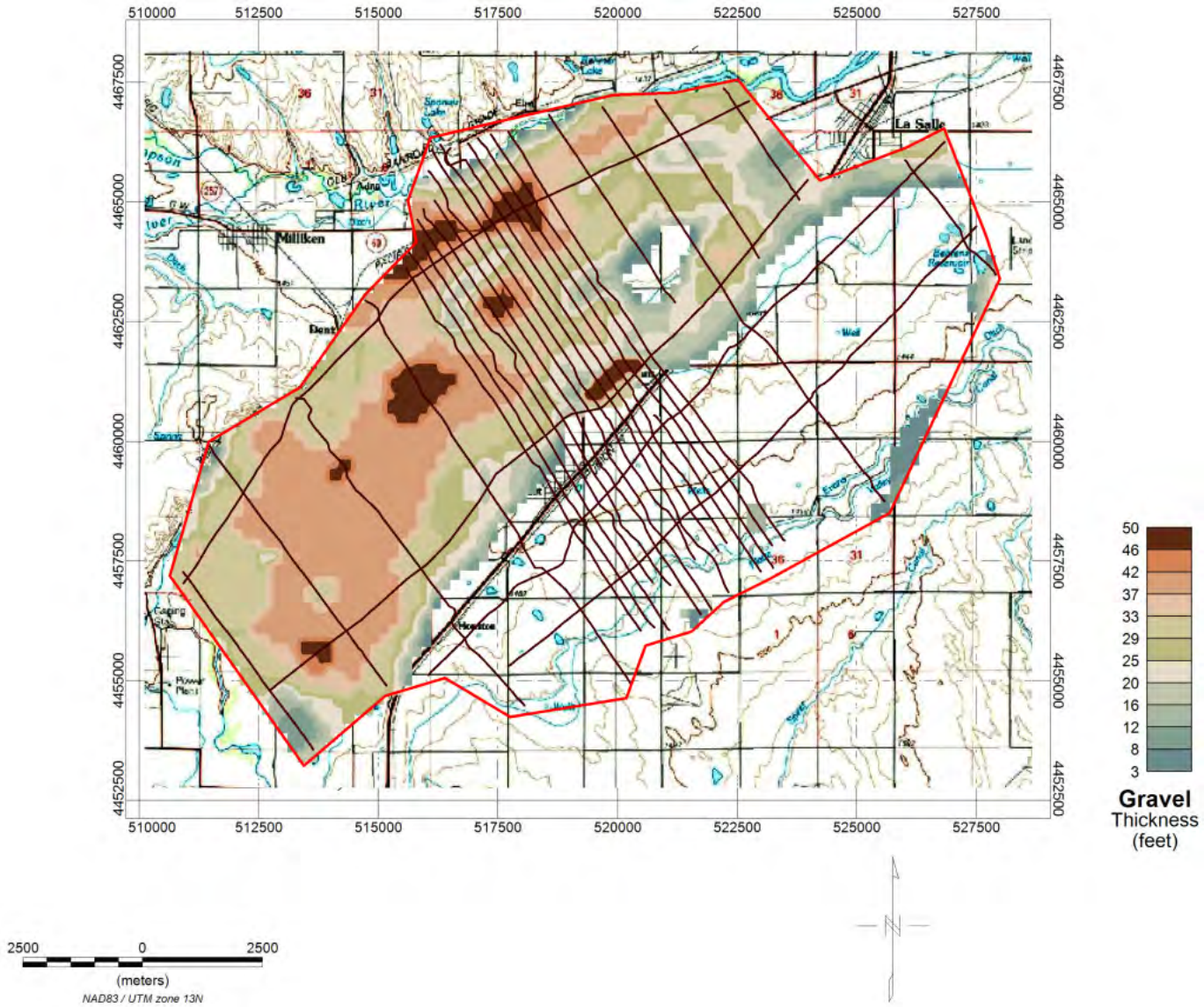

Figure 5-18. Map of the thickness of the Gravel within the Quaternary over the Gilcrest AEM survey area. Flight lines indicated by brown lines. Survey area indicated by red line. Base map is the 100K USGS topography map.

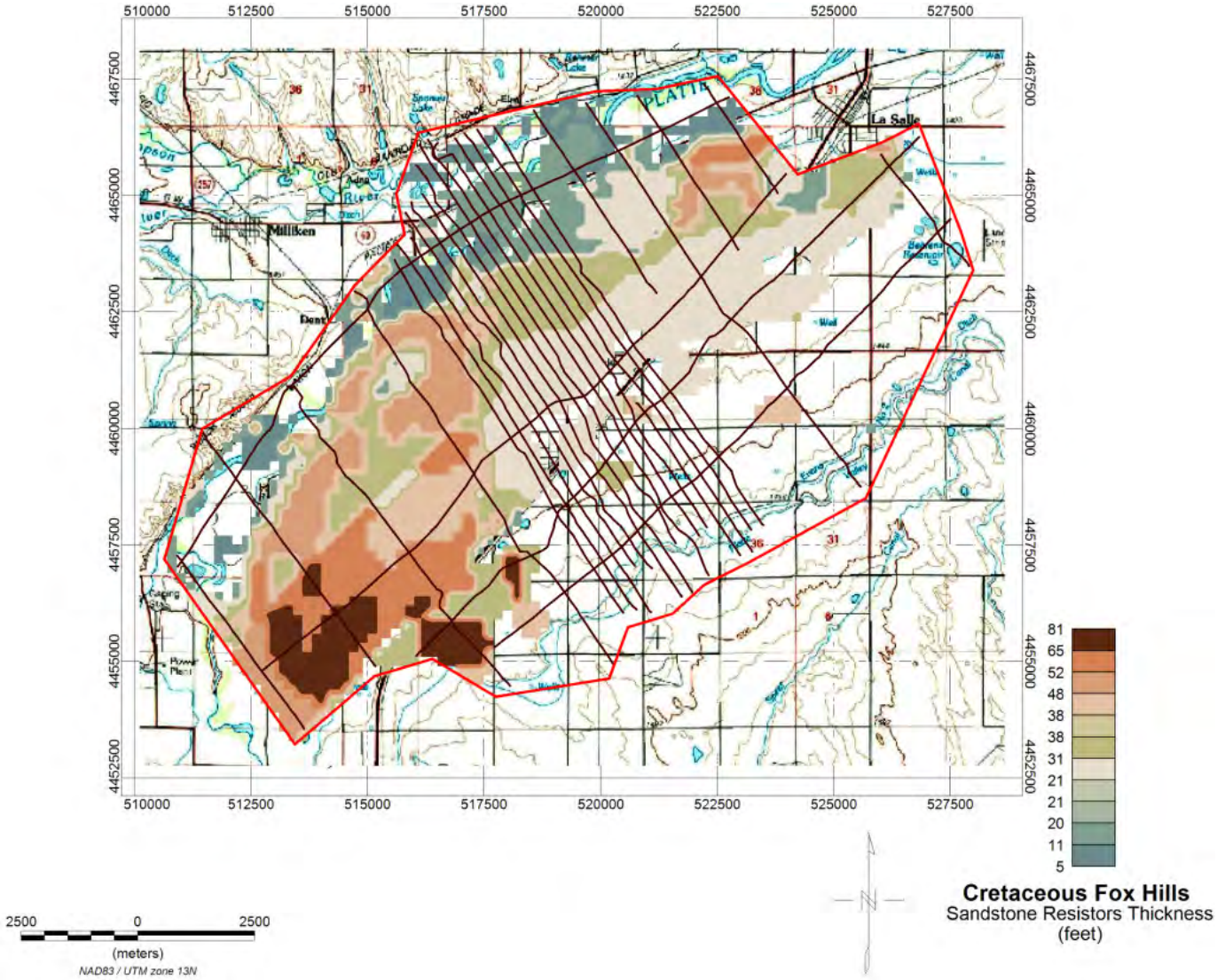

Figure 5-19. Map of the thickness of the resistive Cretaceous Fox Hills Sandstone (*Kfh*) using a cutoff of greater than 18 ohm-m. This represents the locations of the sandstone within the Gravel within the *Kfh* over the Gilcrest AEM Survey Area. Flight lines indicated by brown lines. Survey area indicated by red line. Base map is the 100K USGS topography map.

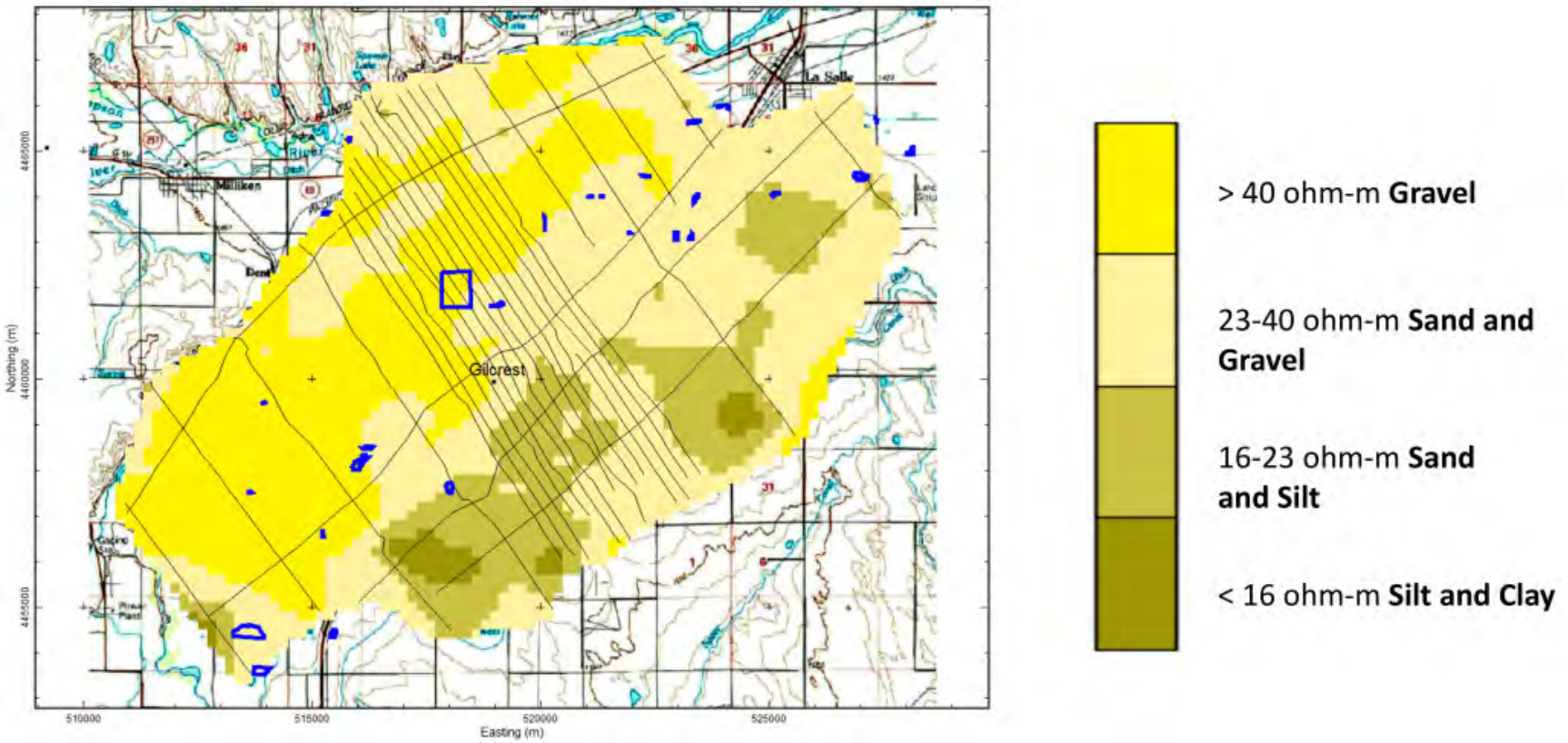

Figure 5-20. Map of the interpreted lithologies for the layer from 0 to ~3 feet in depth for the Gilcrest AEM survey area. Blue areas indicate current CCWCD recharge projects. Flight lines indicated by black lines. Base map is the 100K USGS topography map. Projection is NAD83 UTM Zone 13 North (meters).

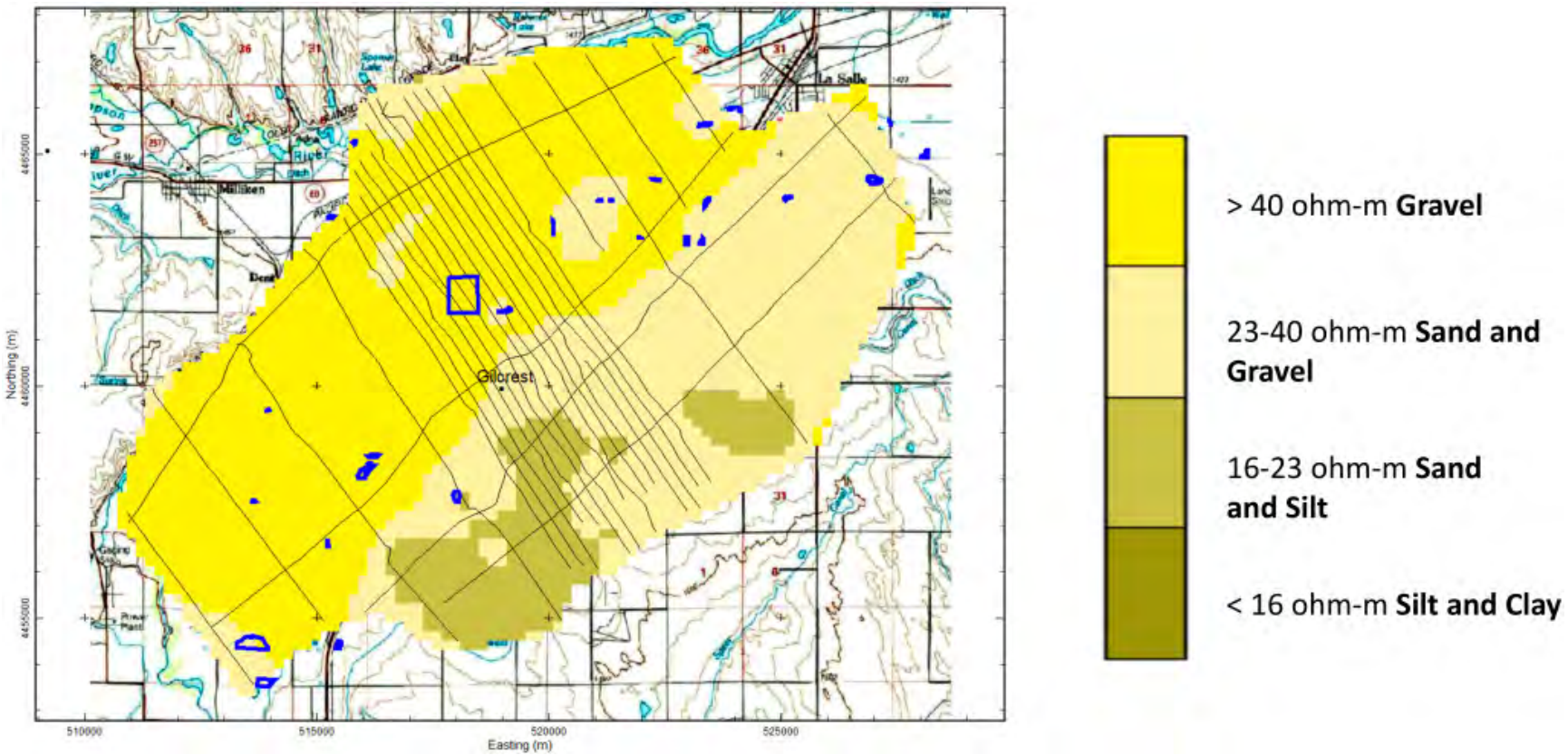

Figure 5-21. Map of the interpreted lithologies for the layer from ~3 to ~7 feet in depth for the Gilcrest AEM survey area. Blue areas indicate current CCWCD recharge projects. Flight lines indicated by black lines. Base map is the 100K USGS topography map. Projection is NAD83 UTM Zone 13 North (meters).

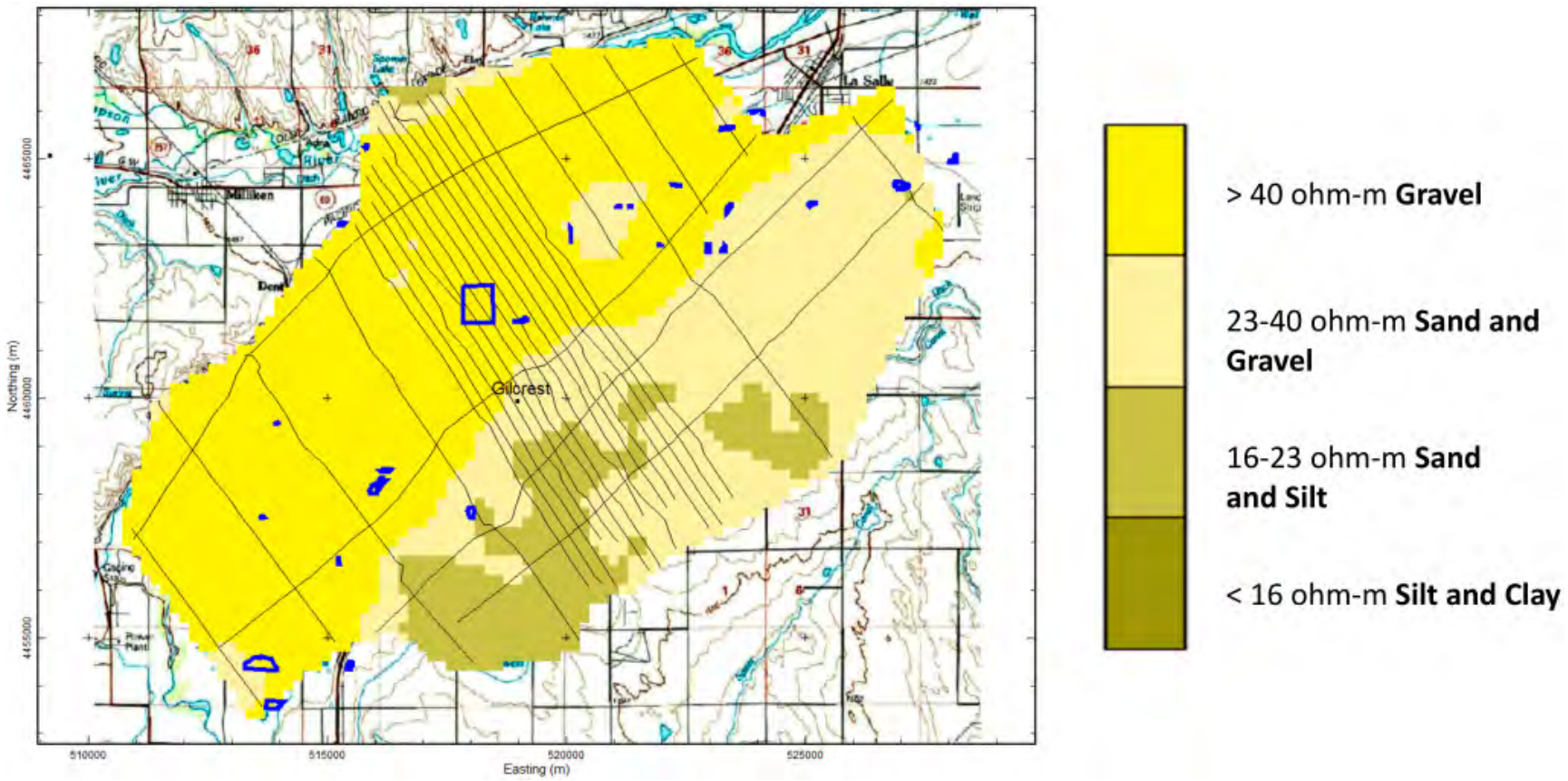

Figure 5-22. Map of the interpreted lithologies for the layer from ~7 to ~11 feet in depth for the Gilcrest AEM survey area. Blue areas indicate current CCWCD recharge projects. Flight lines indicated by black lines. Base map is the 100K USGS topography map. Projection is NAD83 UTM Zone 13 North (meters)

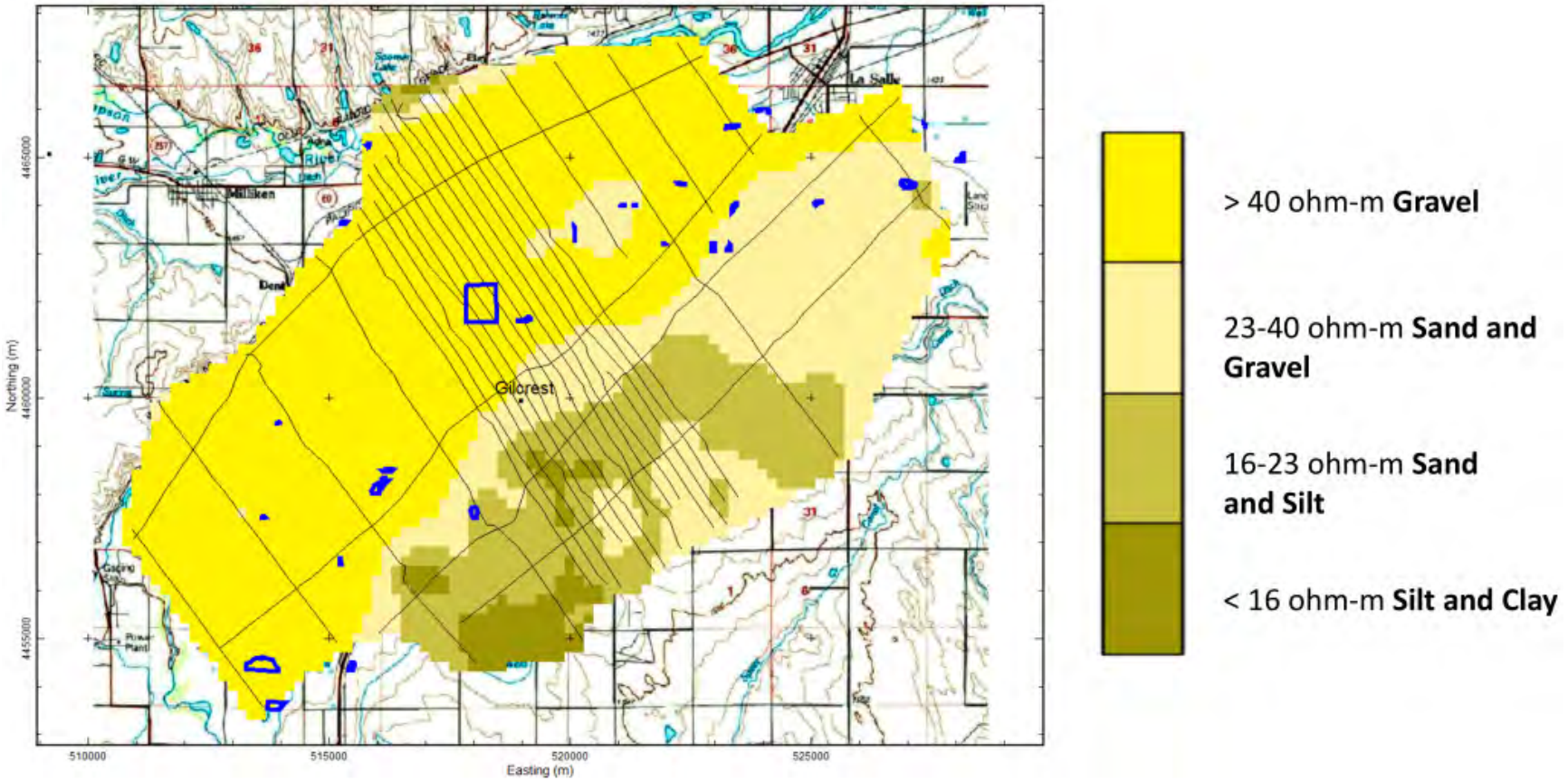

Figure 5-23. Map of the interpreted lithologies for the layer from ~11 to ~16 feet in depth for the Gilcrest AEM survey area. Blue areas indicate current CCWCD recharge projects. Flight lines indicated by black lines. Base map is the 100K USGS topography map. Projection is NAD83 UTM Zone 13 North (meters).

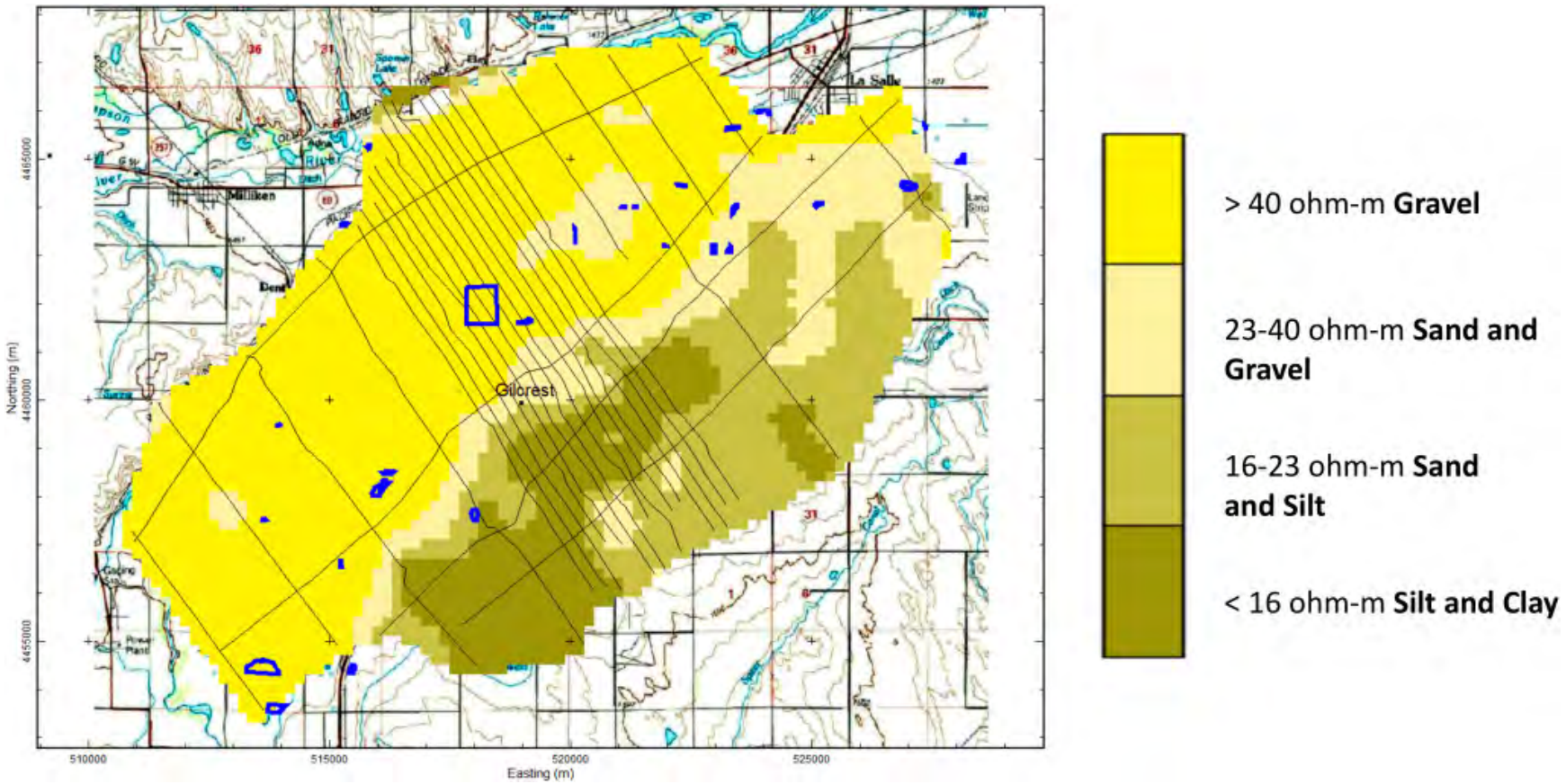

Figure 5-24. Map of the interpreted lithologies for the layer from ~16 to ~21 feet in depth for the Gilcrest AEM survey area. Blue areas indicate current CCWCD recharge projects. Flight lines indicated by black lines. Base map is the 100K USGS topography map. Projection is NAD83 UTM Zone 13 North (meter).

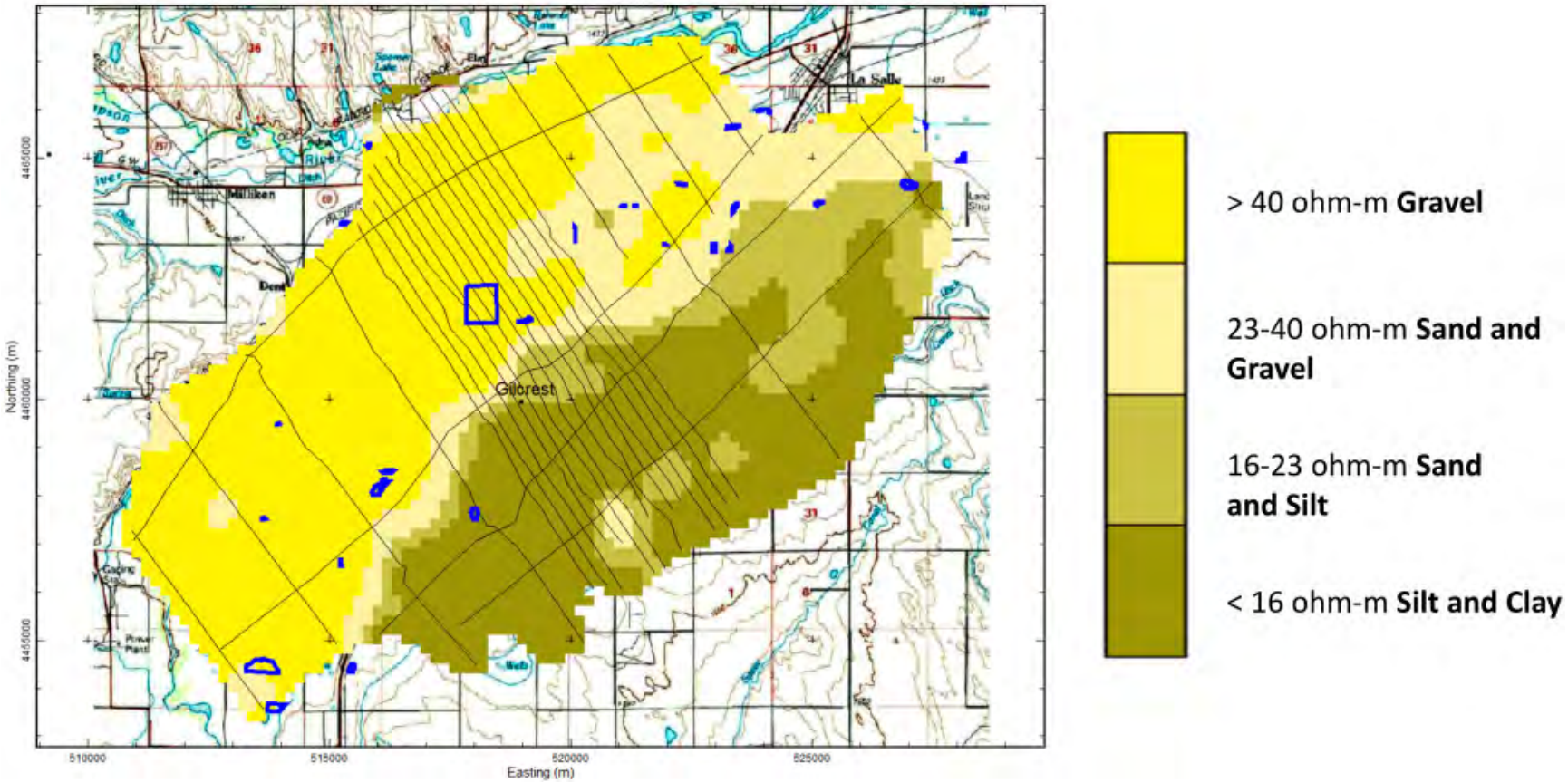

Figure 5-25. Map of the interpreted lithologies for the layer from ~21 to ~26 feet in depth for the Gilcrest AEM survey area. Blue areas indicate current CCWCD recharge projects. Flight lines indicated by black lines. Base map is the 100K USGS topography map. Projection is NAD83 UTM Zone 13 North (meter).

5.2 Hydrogeological Framework of the Gilcrest AEM Survey Area

The AEM reveals variability in the Quaternary (***Q***) deposits across the Gilcrest AEM survey area. These ***Q*** deposits lie unconformably upon the ***Kfh*** and ***Kl*** bedrock. The ***Q*** makes up the aquifer materials consisting of sand and gravel alluvial deposits overlying the Cretaceous bedrock units. Figure 5-26 displays in 3D the overall distribution of ***Q***, ***Kl***, ***Kfh*** and ***Kp*** materials (as described in the previous section) across the Gilcrest survey area. The subsurface distribution of ***Q*** materials can be generally characterized into two distinct areas: 1) silt and clay combined with sand and silt areas, and 2) sand and gravel areas combined with gravel areas. These areas are a mixture of deposits as summarized in Section 2.1. The thickness of the sand and gravel combined with the gravel lithology classes shows the strong impact of alluvial deposits (Figure 5-27). The ***Q*** deposits contain an extensive deposit of fine grained material composed of silt and clay southeast of the South Platte River which is a hydrogeologic boundary condition in that area (Figure 5-28).

5.2.1 The Quaternary Aquifer

The Quaternary aquifer of the Gilcrest survey area is predominantly composed of ***Q*** unconsolidated aquifer materials classified as packages of gravel, sand and gravel, sand and silt, and non-aquifer materials made up of silt and clay (Figure 5-29). These materials are sitting on the ***Kl*** and ***Kfh*** which composes the bedrock for the area. The map showing the elevation of the bedrock can be found in Figure 5-30. This new AEM and borehole derived bedrock elevation map can be compared to the bedrock elevation determined by boreholes alone from Barkmann et al. (2014). A map of the difference between the CGS bedrock map and interpreted AEM-derived bedrock is presented in Figure 5-31. Most of the area shows small to subtle differences with the exception of a couple of areas that show a difference of ~79 foot. At the very edges of the grid care needs to be taken as the AEM was constrained to the area of data coverage. The thickness of the ***Q*** materials within the Gilcrest survey area range from ~10 to ~125 feet thick (Figure 5-32.) The thickness of the ***Q*** materials increases in thickness from the sides of the South Platte Valley toward the paleochannel in the center of the survey area. Note that the paleochannel parallels the South Platte River for most of its length within the survey area and then appears to make a bend to the east near the survey boundary on the east side (there is limited data from the AEM flights to confirm this bend). However, this is very close to the area of the paleochannel as mapped by the CGS (Barkmann et al., 2014). The ***Q*** alluvial system can be very heterogeneous in places with a changing mix of all lithology classes as seen in Profile L200201 which extends from west to east through the survey area (Figure 5-33). Most of the Gilcrest AEM survey area contains sand and gravel aquifer materials that act as a groundwater supply conduit which is hydrologically connected to the surface water system. Accompanying the aquifer materials are areas of non-aquifer materials.

The non-aquifer (silt and clay) materials are typically located proximally to the near-surface, within 20-40 feet of the land surface, as near-continuous layers of silt and clay along the south side of the survey area (Figure 5-34). This layer can locally act as an aquiclude or semi confining to confining unit and prevent recharge to the lower aquifer, or serve as a locally confining unit. Wells in the area can be affected by these confining and semi-confining conditions.

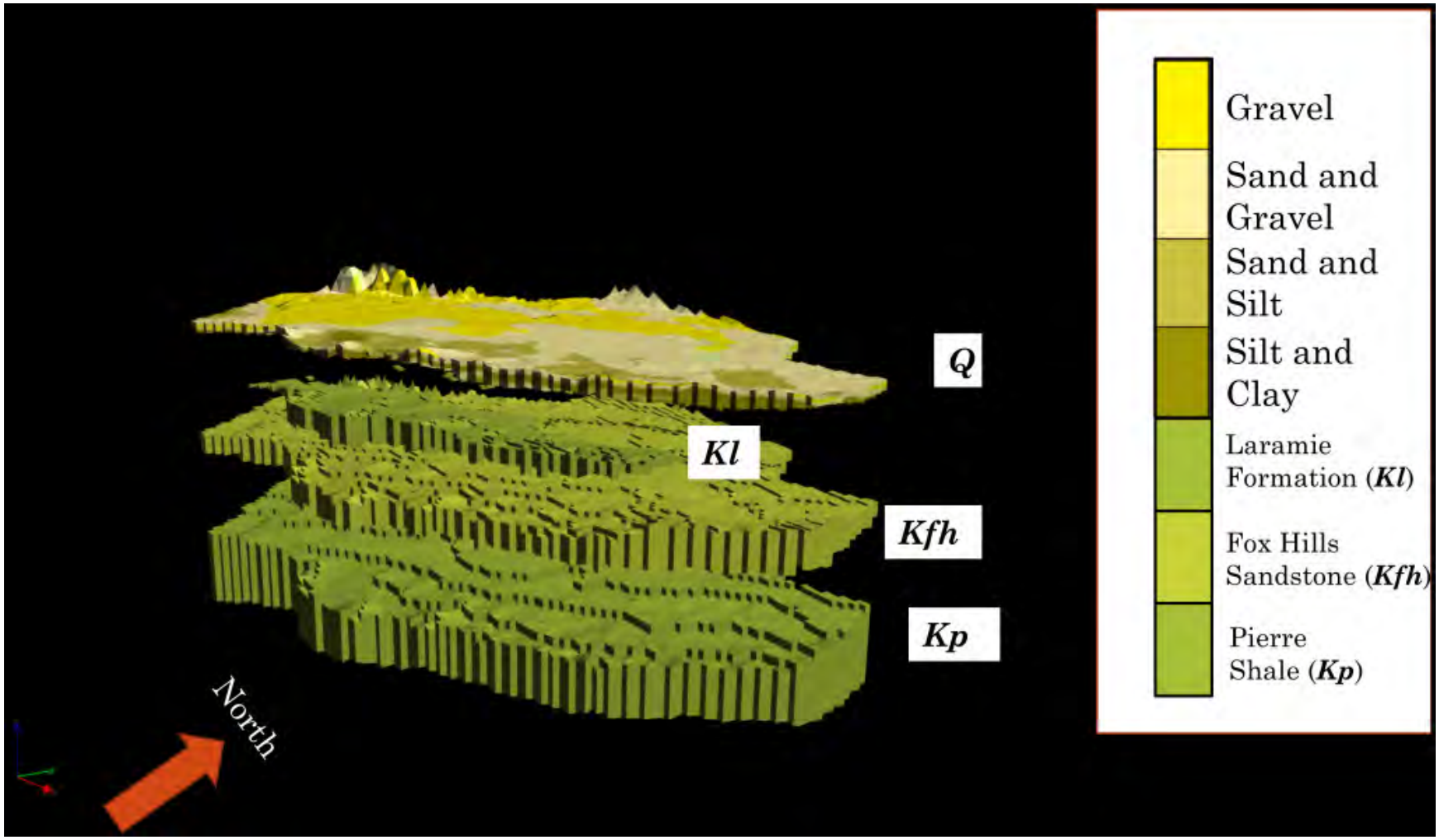

Figure 5-26. 3D exploded images of the overall distribution of Quaternary (*Q*), Cretaceous Laramie Formation (*Kl*), Cretaceous Fox Hills Sandstone (*Kfh*) and Cretaceous Pierre Shale (*Kp*) layers within the Gilcrest survey area.

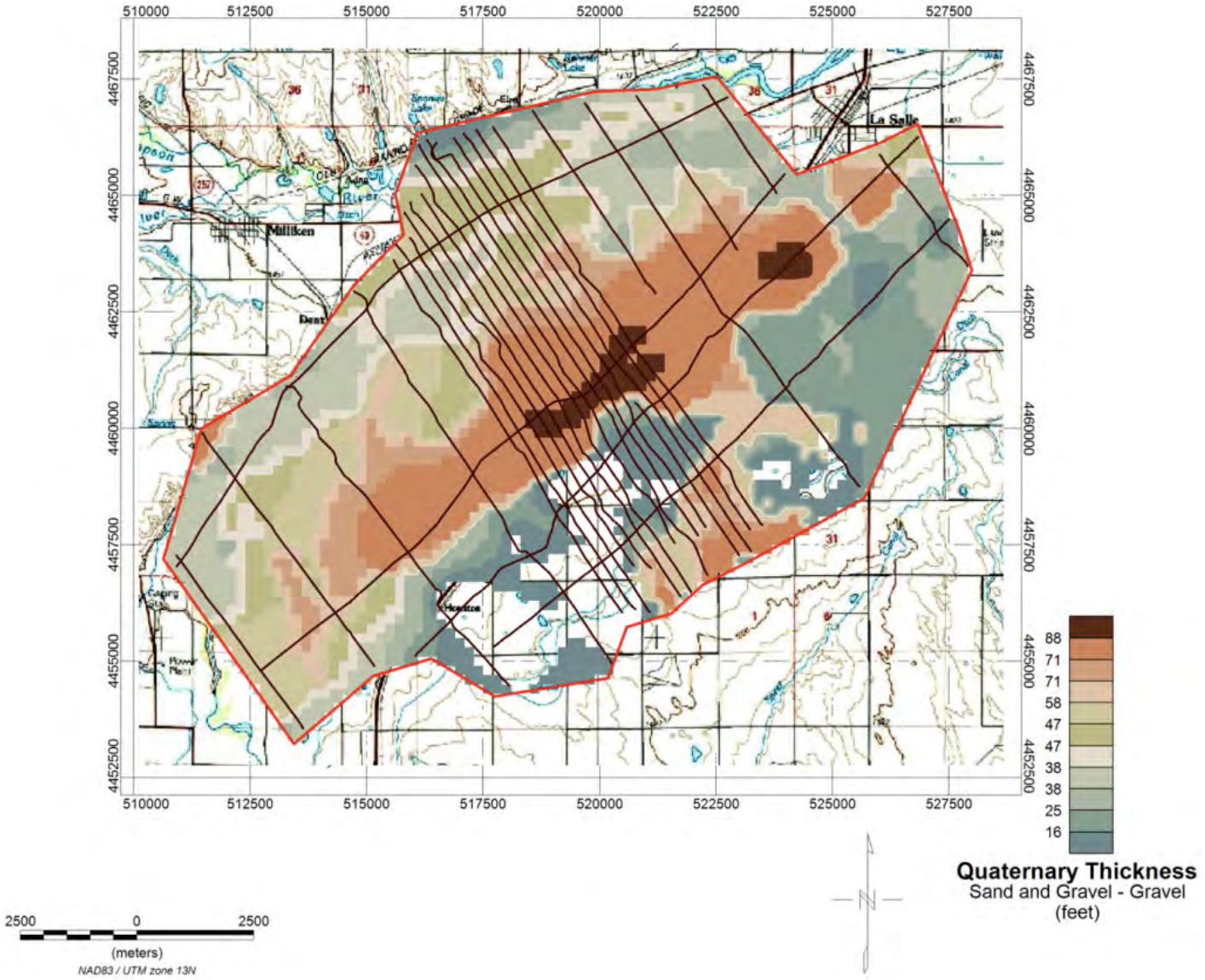

Figure 5-27. Map of the Quaternary (*Q*) sand and gravel combined with the gravel lithology classes in the Gilcrest survey area. Flight lines are indicated by brown lines. Red line indicates AEM survey area. Base map is the 100K USGS topography map.

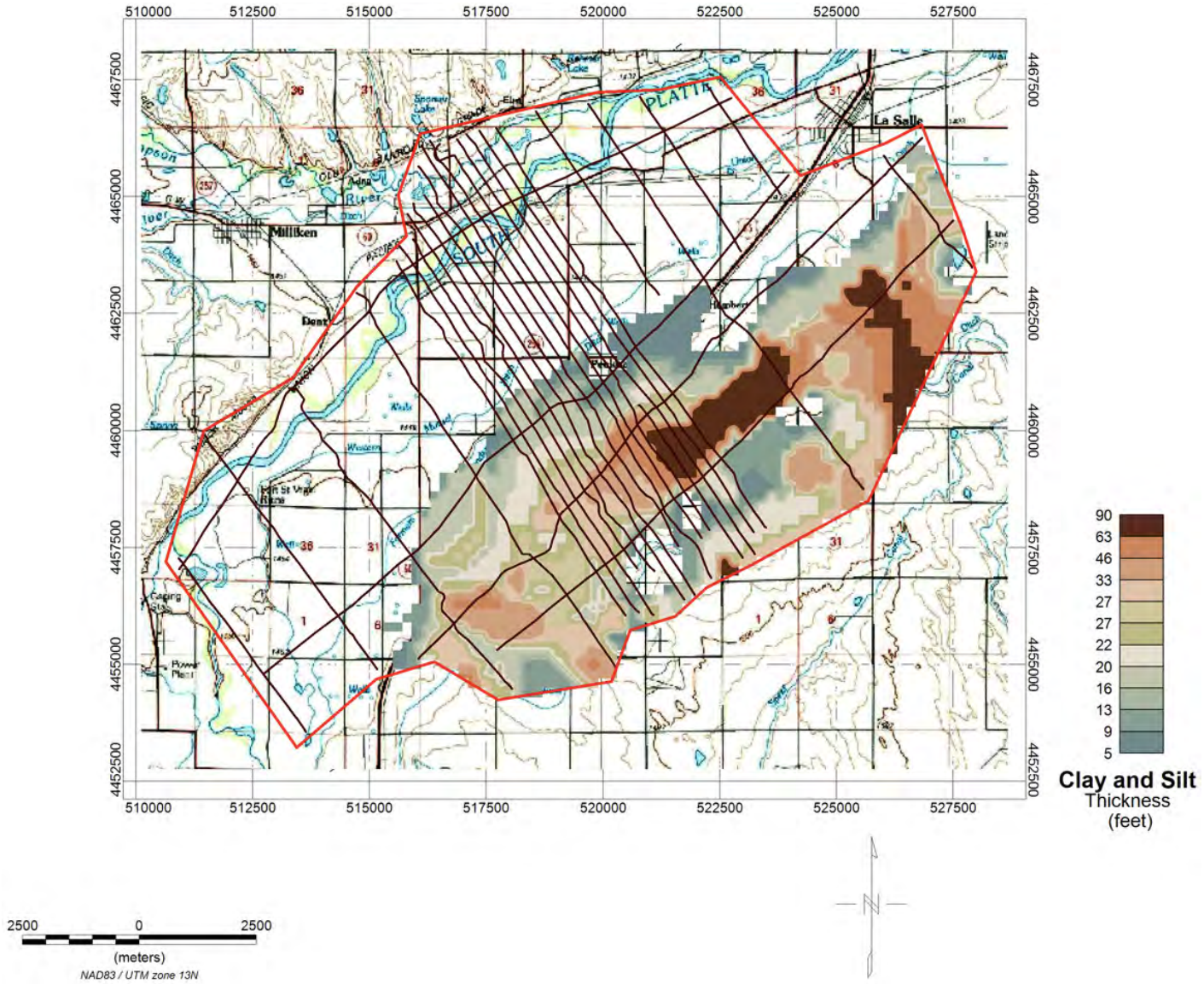

Figure 5-28. Map of Quaternary silt and clay lithology class thickness in the Gilcrest survey area. Flight lines are indicated by brown lines. Red line indicates AEM survey area. Base map is the 100K USGS topography map.

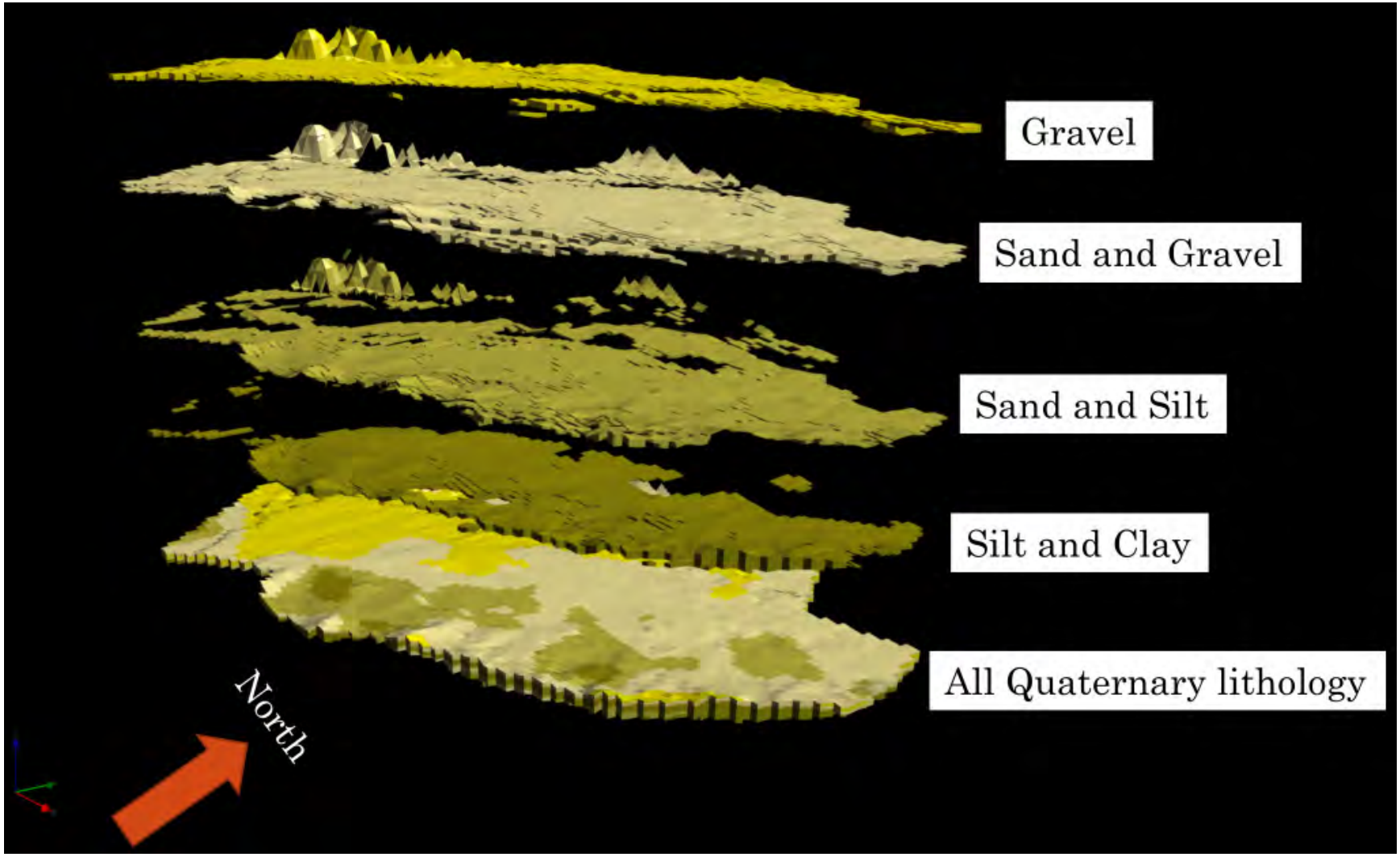

Figure 5-29. 3D exploded images of the complete package of Quaternary (*Q*) unconsolidated aquifer materials, and gravel, sand and gravel, sand and silt, and non-aquifer materials made up of silt and clay in the Gilcrest survey area.

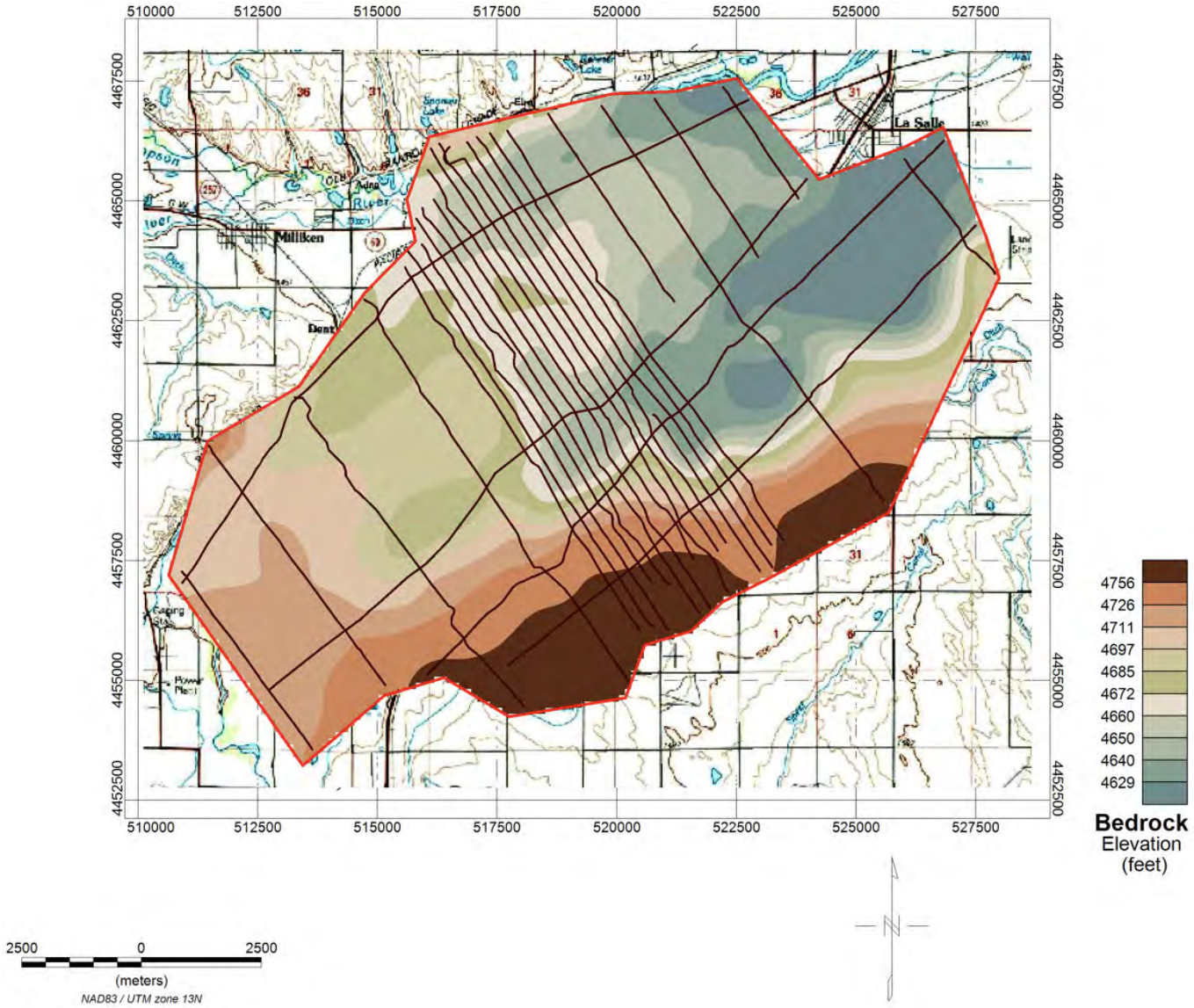

Figure 5-30. Map of the bedrock elevation of the Gilcrest survey area. Flight lines are indicated by brown lines. Red line indicates AEM survey area. Base map is the 100K USGS topography map.

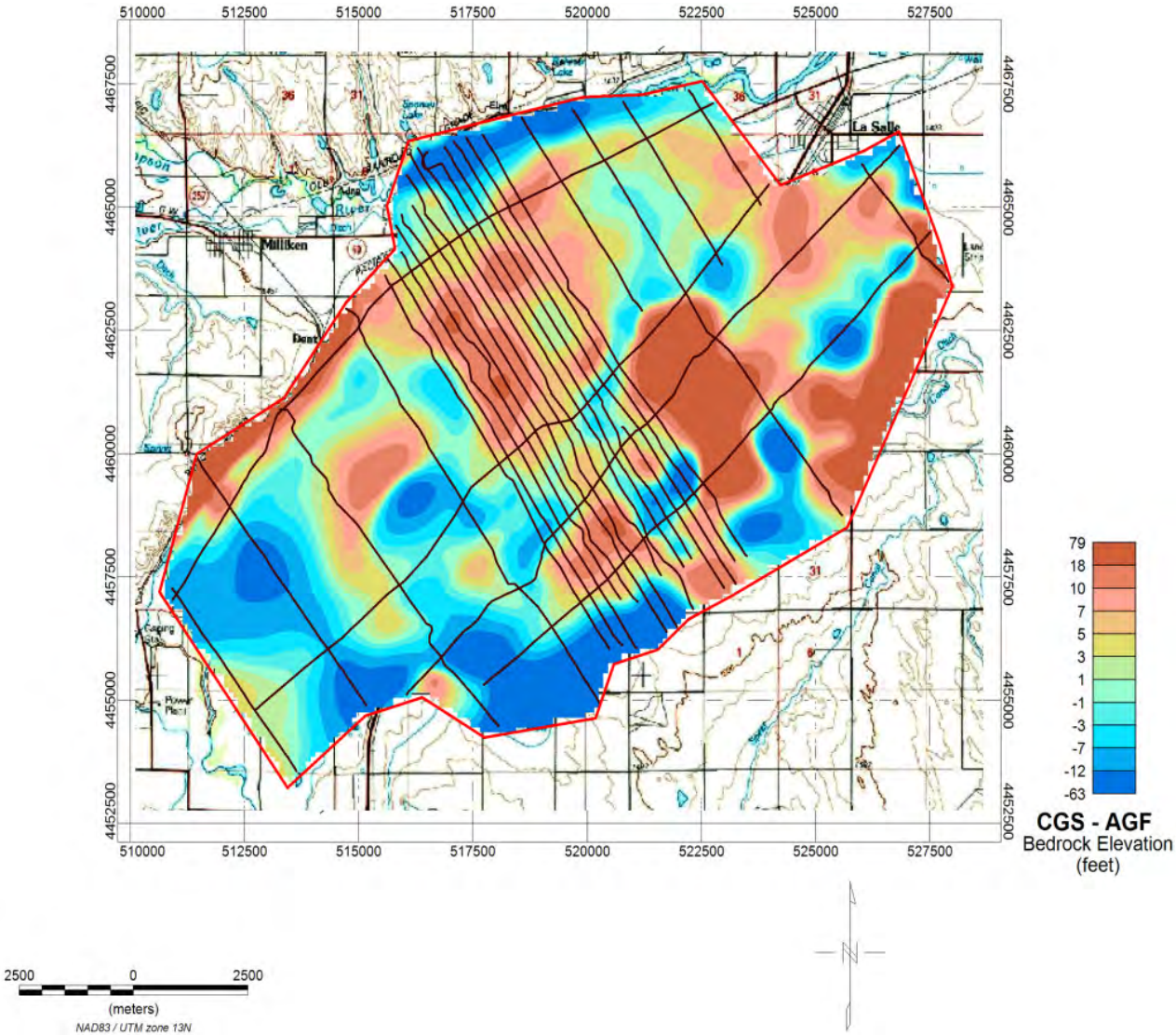

Figure 5-31. Map of the difference between the interpreted AEM and borehole derived bedrock and the Colorado Geological Survey bedrock (Barkmann, et al., 2014). Flight lines are indicated by brown lines. Red line indicates AEM survey area. Base map is the 100K USGS topography map.

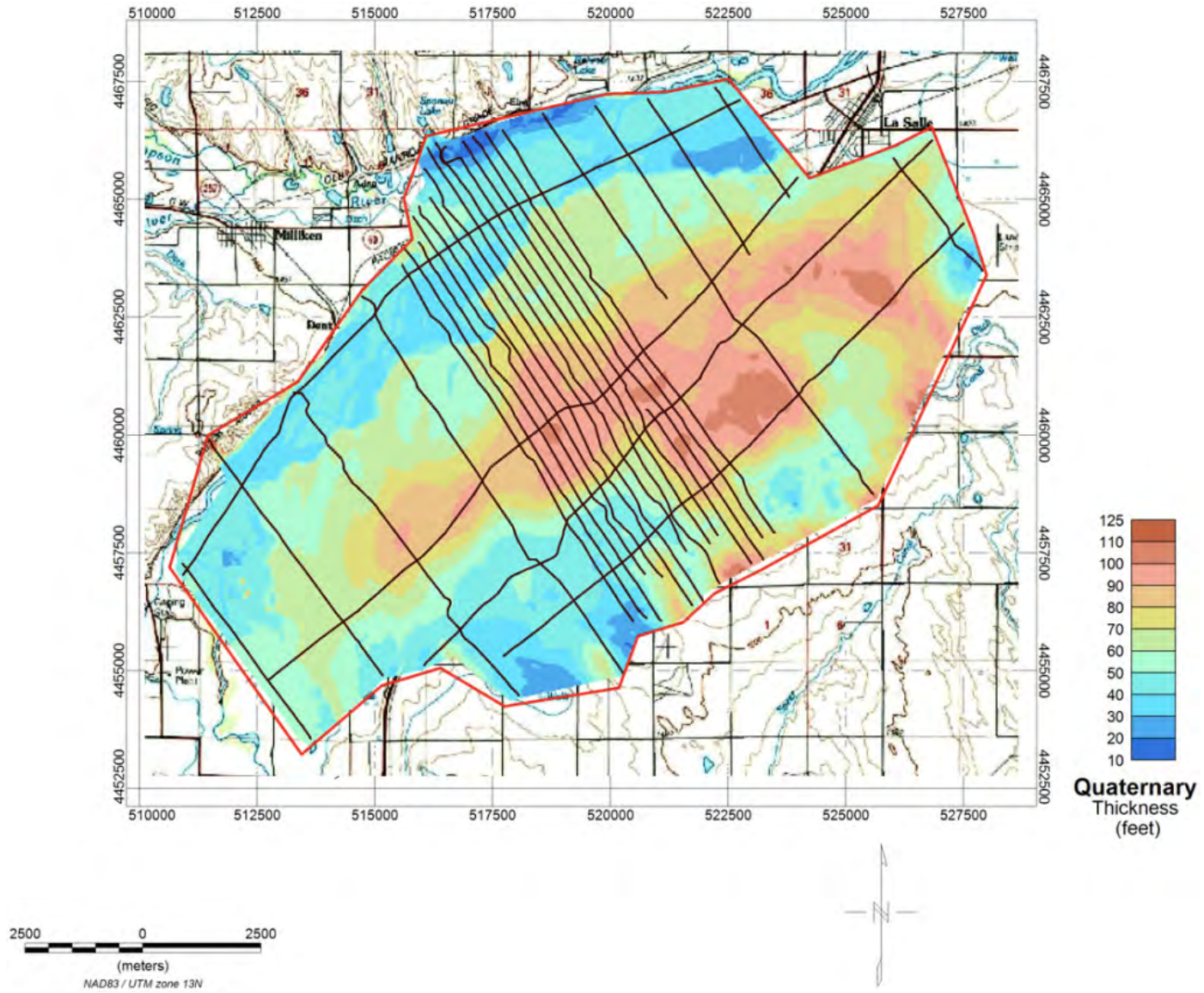

Figure 5-32. Map of Quaternary thickness within the Gilcrest survey area. Flight lines are indicated by brown lines. Red line indicates AEM survey area. Base map is the 100K USGS topography map.

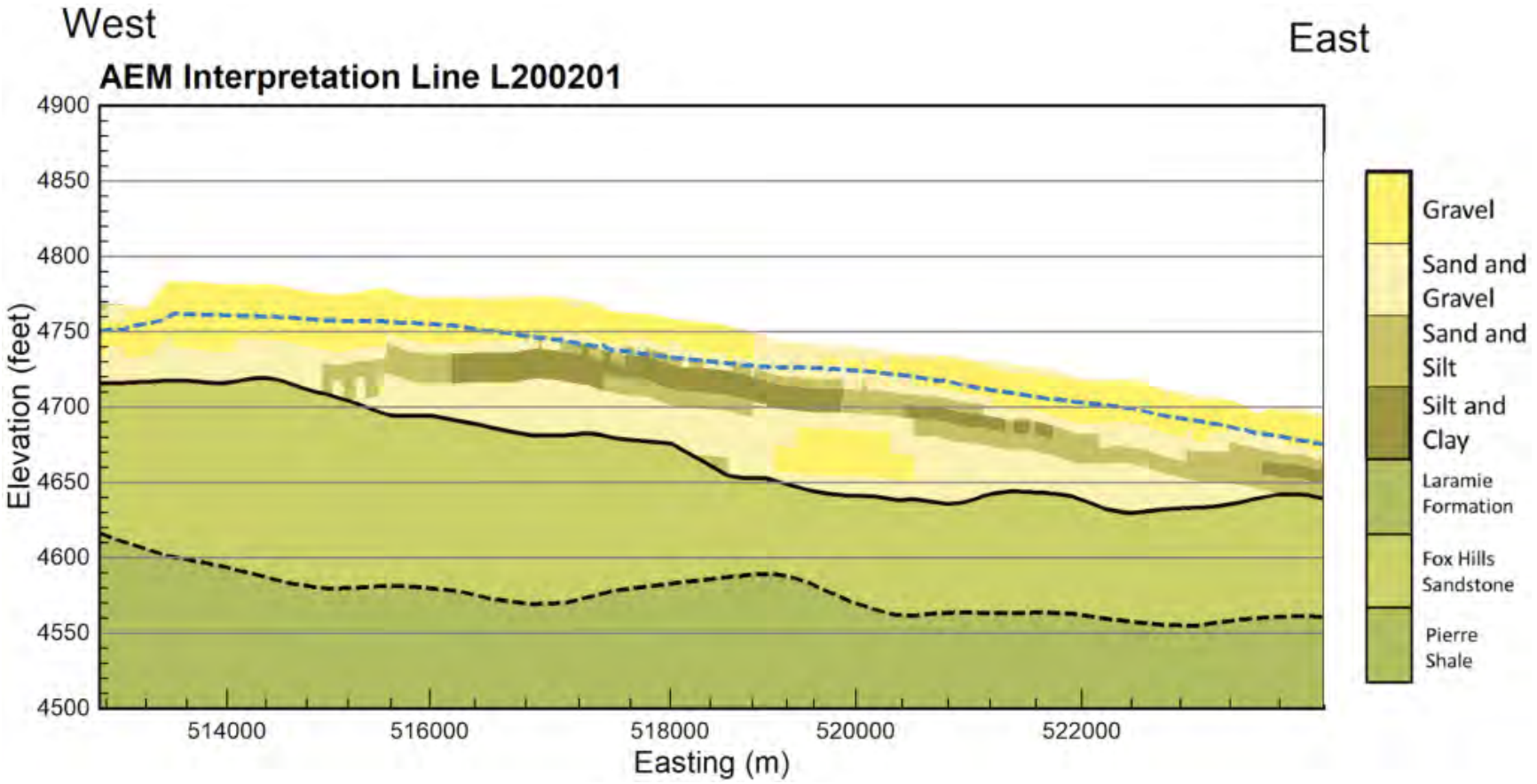

Figure 5-33. Profile L200201 showing the heterogeneity of the Quaternary unconsolidated materials within the Gilcrest AEM survey area. The dashed blue line is the water table, the solid black line is the bedrock and the dashed black line is the contact of the Cretaceous Fox Hills Sandstone and the Cretaceous Pierre Shale. NAD83 UTM Zone 13 North (meters), NAVD88 (feet).

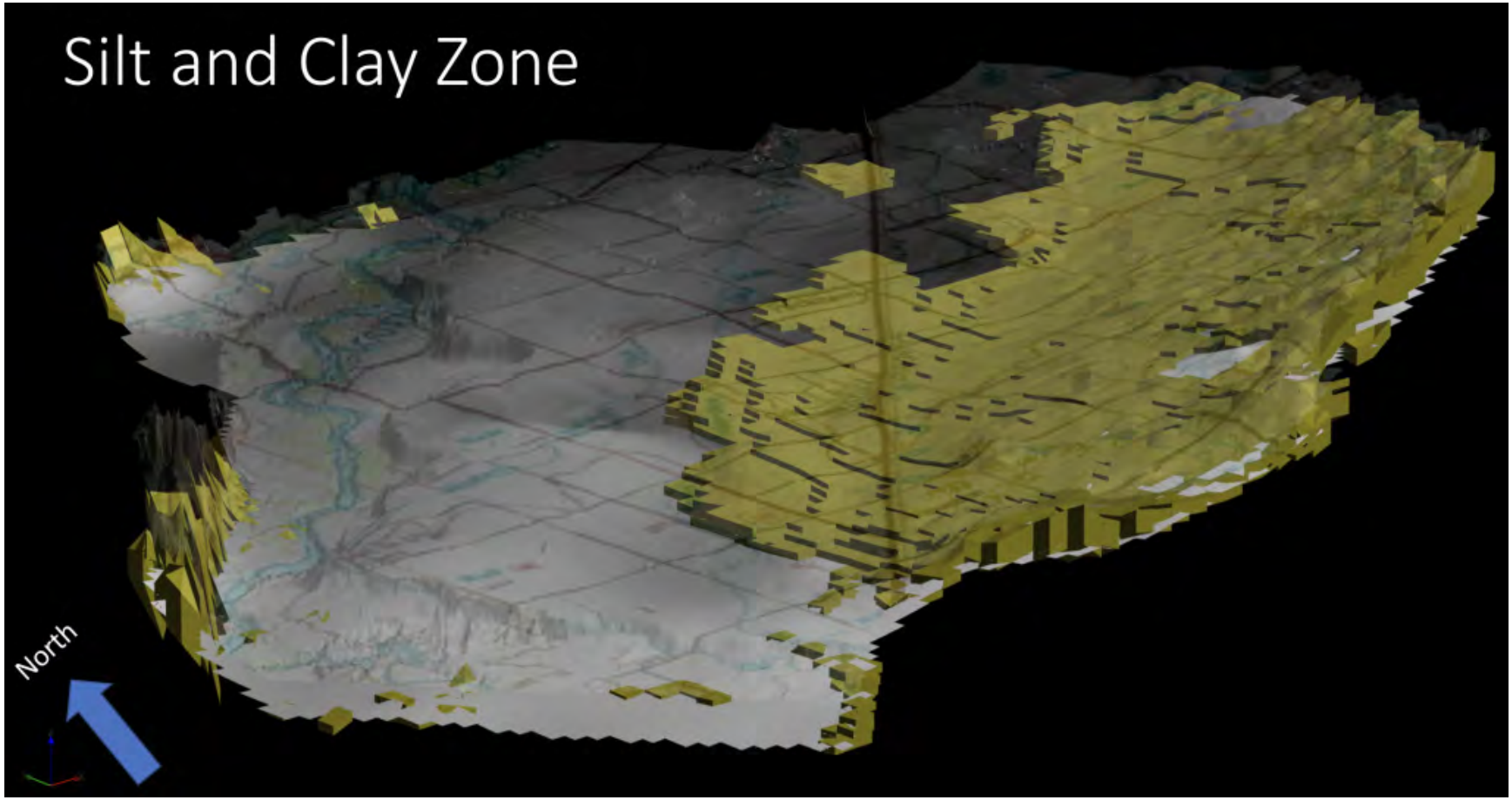

Figure 5-34. 3D map of the Quaternary silt and clay lithology class, a nearly continuous layer in the south section of the Gilcrest survey area, looking down river from the confluence of the South Platte River and Saint Vrain creek. The gray shaded surface is the bedrock. A transparent image of the surface elevation is overlain by the 100K USGS topography map for reference. Projection is NAD83 UTM Zone 13 North (meters), NAVD88 (feet) vertical exaggeration 1:5.

Five selected wells were identified in the CO-DWR records as having confined characteristics when completed in the aquifers below the silt and clay layer (Figure 5-35). Four of these wells were included in the CGS study (Barkmann et al., 2014) and one was added during this investigation from the CO-DWR database. This silt and clay unit impacts the area hydrologically by blocking or slowing down water movement to and from the land surface. When considering that groundwater lies above and below this layer, which creates a restriction to water movement across this zone, impacting recharge from meteoric, applied irrigation, and recharge facility waters by stopping, slowing, or redirecting subsurface flows. The areas that are not affected by this silt and clay are unconfined and are recharged by the available surface water (meteoric, irrigation and storage). Figure 5-36 shows a fence diagram of the ***Q*** unconsolidated materials in relation to the 3D silt and clay layer with the CCWCD recharge projects indicated as blue outlines. In the southeastern portion of the survey area the aquifer is composed of two zones separated by the silt and clay layer. The interpretation of line L202703, which is perpendicular to the valley just east of the town of Gilcrest, shows the silt and clay layer extending off the southern edge of the ***Kl*** out toward the South Platte River (Figure 5-37). The unconsolidated ***Q*** materials of the Gilcrest AEM survey area contain zones of saturated thickness up to >102 ft based on the AGF interpreted water table constructed for this report (Figure 5-38). Unsaturated Q materials range in thickness from 0 to >32 ft across the survey area (Figure 5-39). The thinnest unsaturated thickness is near the South Platte River and the thickest area is on the terraces and the hills on the south side of the river within the paleochannel region. Appendix 1 contains interpreted 2D profiles that illustrate the details of the Quaternary in the Gilcrest AEM survey area. Appendix 2 contains 3D images of the Gilcrest AEM survey area that have been rotated around various angles to allow viewing of the overall distribution of materials.

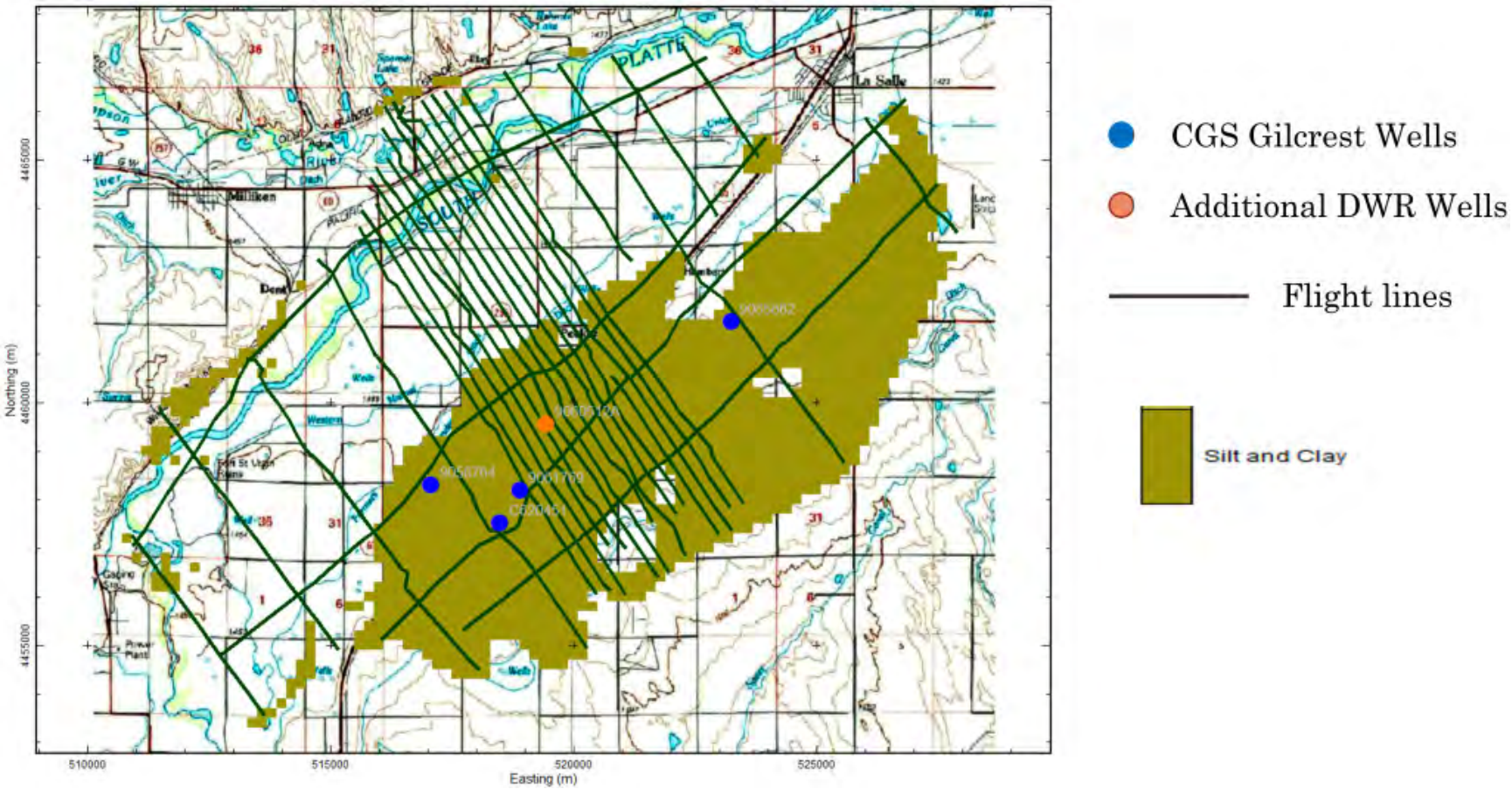

Figure 5-35. Map of selected wells in the area that exhibit semi-confining/confining characteristics plotted on the spatial extent of the Quaternary silt and clay lithology on the south side of the survey area. Labeled wells indicate Colorado Department of Water Resources Receipt Number. Flight lines are indicated by dark green lines. Base map is the 100K USGS topography map. Projection is NAD83 UTM Zone 13 North (meters).

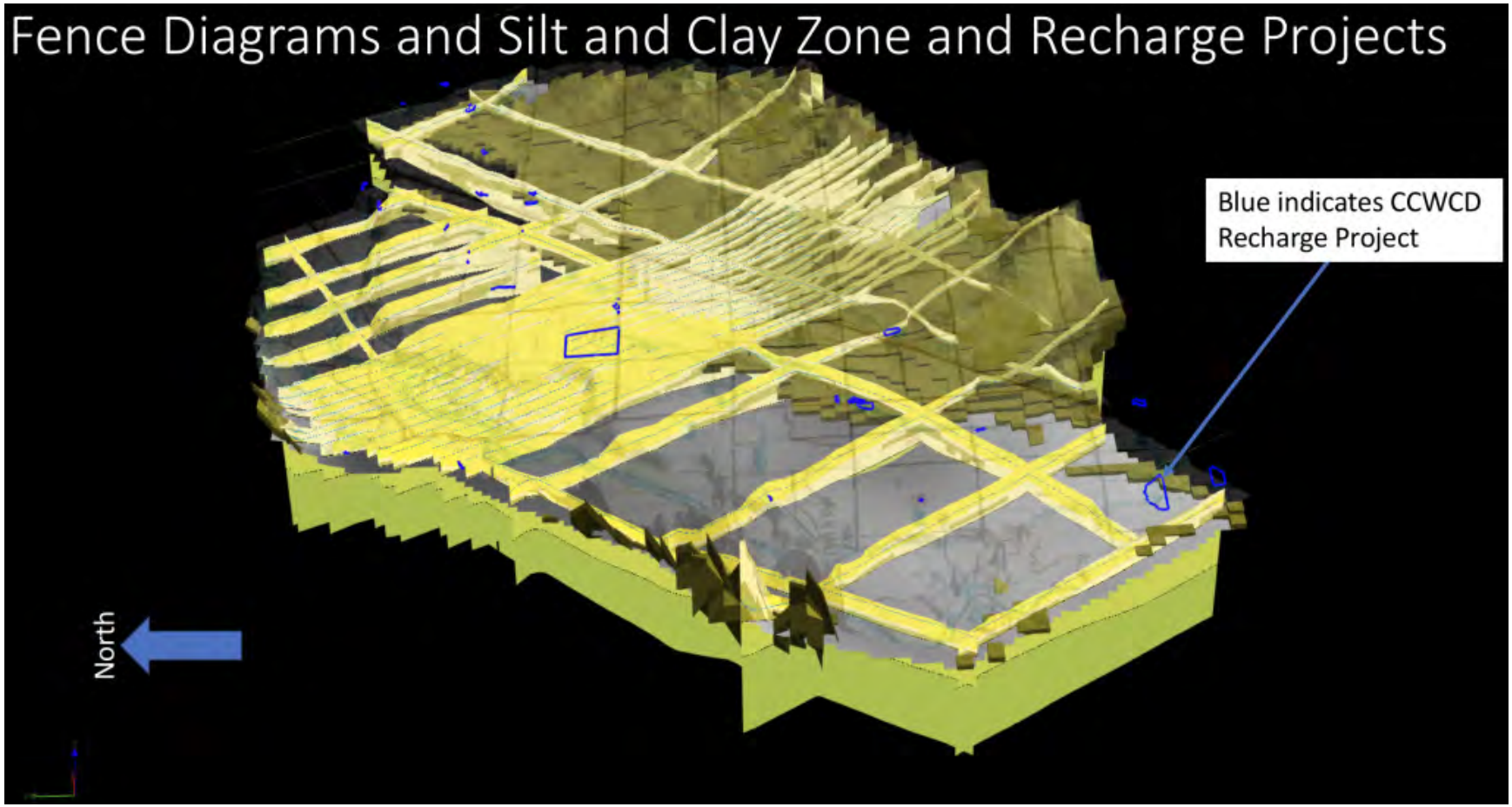

Figure 5-36. 3D fence diagram of the interpreted AEM profiles and the relation to the voxel model of the silt and clay layer. The gray-shaded surface is the bedrock. A transparent image of the surface elevation is overlain by the 100K USGS topography map for reference. The CCWCD recharge projects are indicated by the blue outlines. Projection is NAD83 UTM Zone 13 North (meters), NAVD88 (feet) vertical exaggeration 1:5.

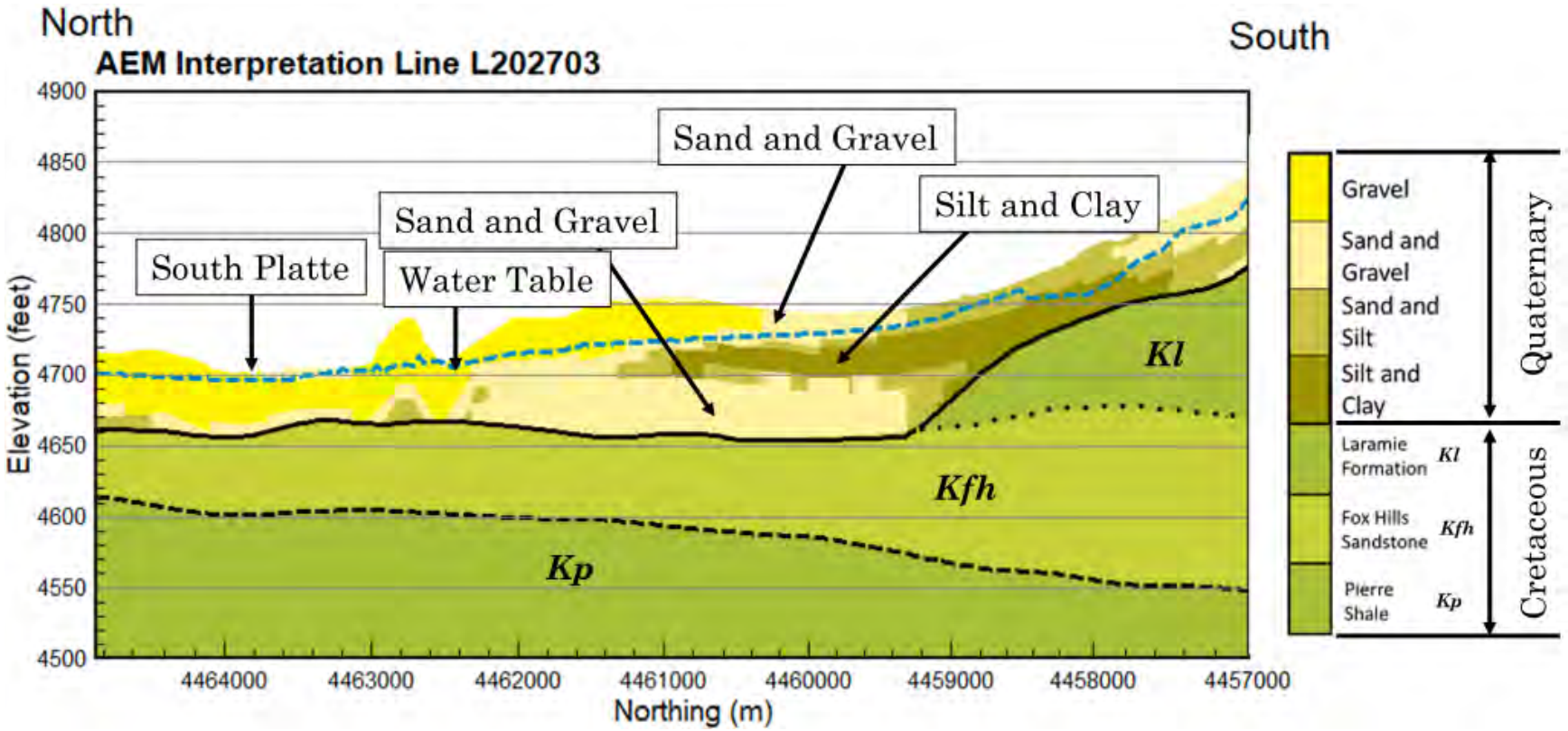

Figure 5-37. 2D interpreted profile of Line L202703 showing the silt and clay layer extending from the south out into the valley toward the South Platte River. The dashed blue line is the water table, the solid black line is the Quaternary (*Q*) and Cretaceous Fox Hills Sandstone (*Kfh*) contact, and the dashed black lines are the Cretaceous Laramie Formation (*Kl*) and *Kfh contact as well as the Kfh* and Pierre Shale (*Kp*) contact. Projection is NAD83 UTM Zone 13 North (meters), NAVD88 (feet).

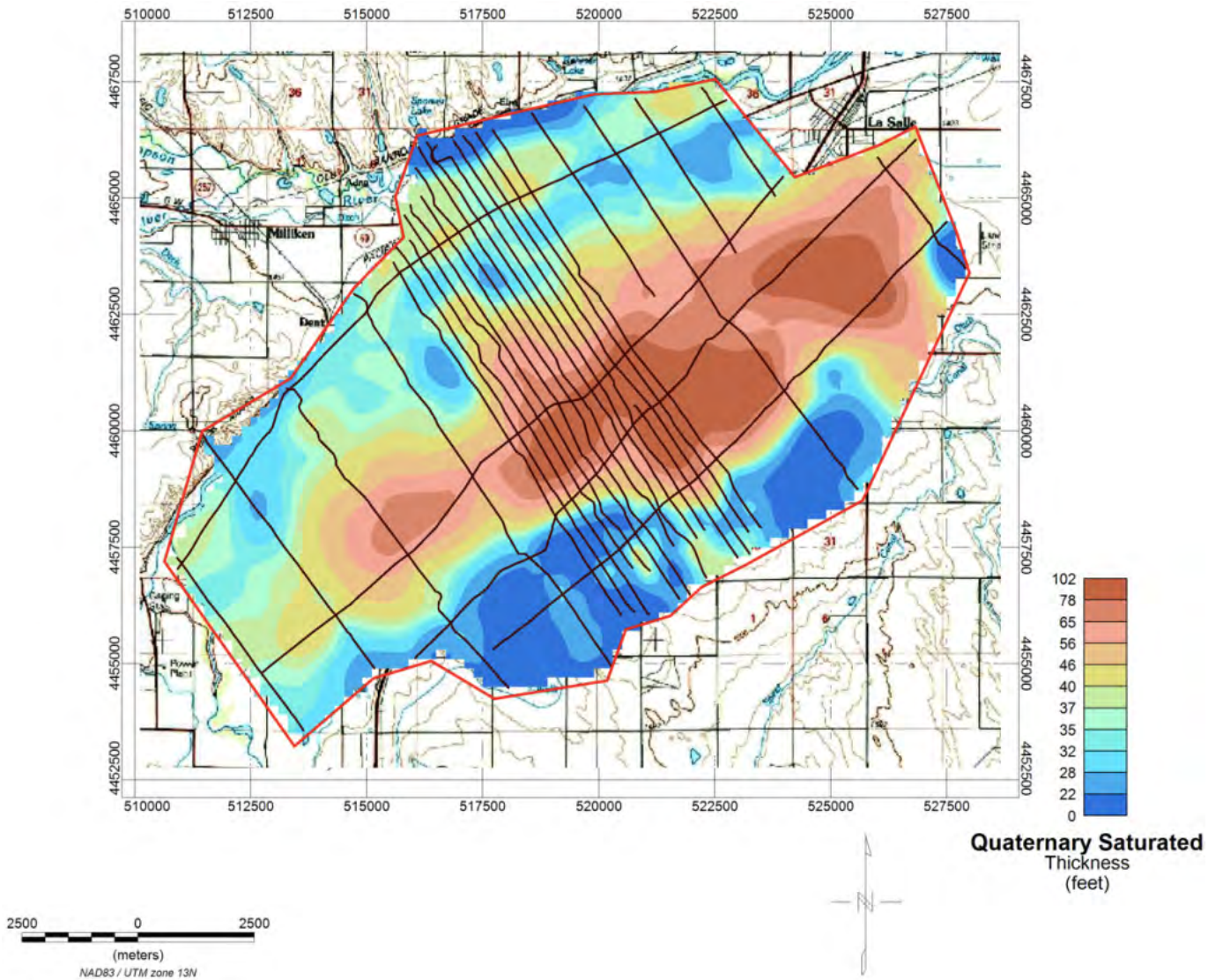

Figure 5-38. Map of the saturated Quaternary (*Q*) materials in the Gilcrest survey area. The thickest saturated area is associated with the paleochannel in the center of the survey area. Flight lines are indicated by brown lines. Red line indicated AEM survey area. Base map is the 100K USGS topography map.

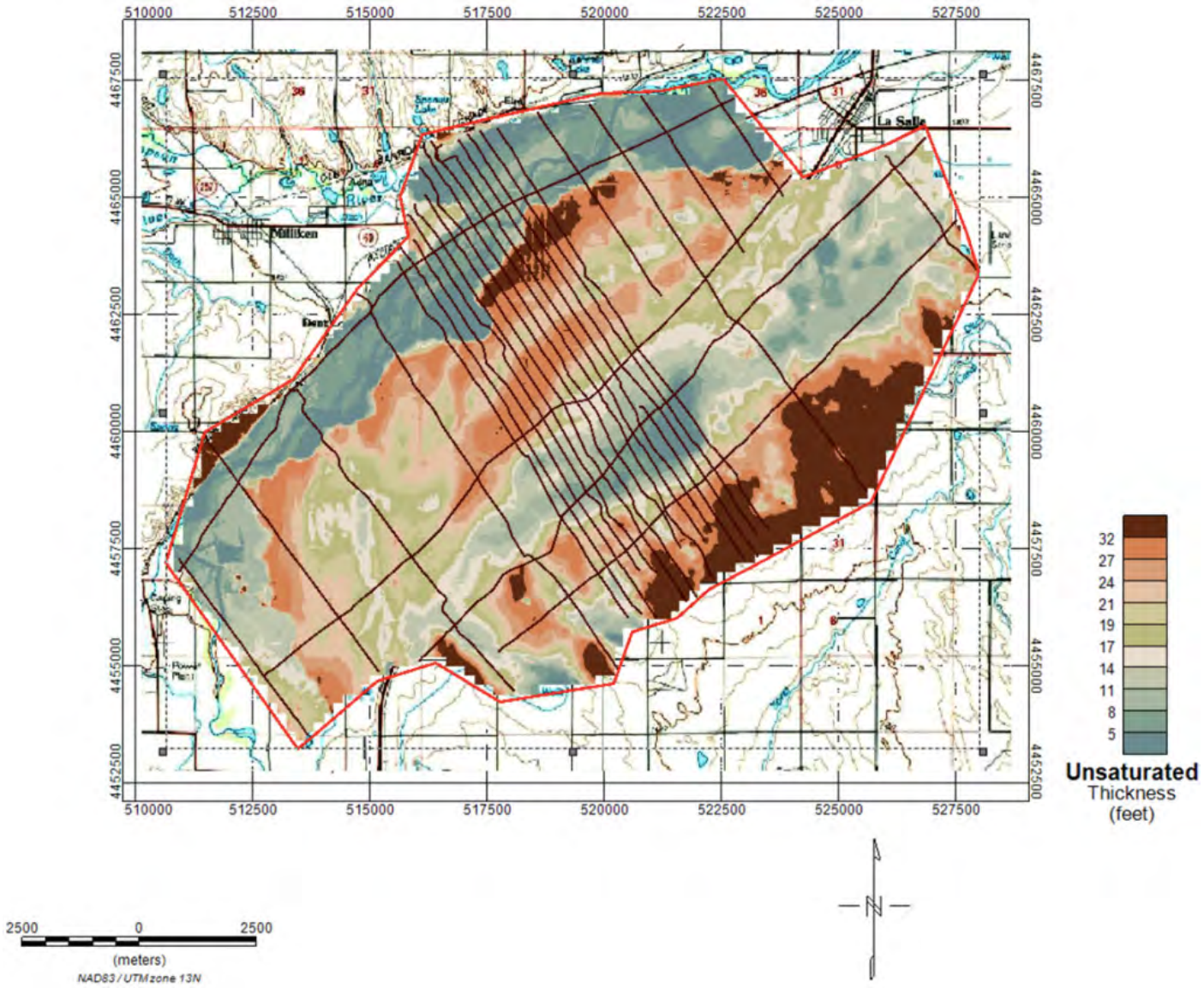

Figure 5-39. Map of unsaturated Quaternary (*Q*) materials in the Gilcrest survey area. Note the thicker sections are near the terraces. . Flight lines are indicated by brown lines. Red line indicated AEM survey area. Base map is the 100K USGS topography map.

5.2.2 The Cretaceous Bedrock Units

The Cretaceous bedrock is made up of the Cretaceous Laramie Formation (***Kl***) on southern side of the Gilcrest AEM survey area and is shown in Figure 5-40. This is likely more ***Kl*** on the north side of the river, but the AEM survey lines did not extend in that area adequately to resolve the ***Kl***. The remaining bedrock is the Cretaceous Fox Hills Sandstone (***Kfh***). Figure 5-41 presents the elevation of the ***Kfh*** and shows that the unit has been eroded in areas beneath the ***Q*** materials by the paleo-South Platte River. Even though the ***Kfh*** is eroded and thinned in the area of the valley and current South Platte River, the unit extends throughout the survey area. Below the ***Kfh***, the Cretaceous Pierre Shale is continuous throughout the survey area (Figure 5-42) and exhibits the general structural configuration that would be expected for the area based on previous published material (see Section 2.1). A geologic map of the bedrock units within the Gilcrest survey area is presented in Figure 5-43.

The ***Kfh*** exists throughout the project area and can be aquifer material as the ***Kfh*** has a hydrologic connection to the ***Q*** sediments in much of the area. The interaction of the ***Kfh*** with the ***Q*** sediments can be a source of water to the South Platte River based on the AEM mapping in the Gilcrest survey area. A map of the of the resistive (> 18 ohm-m) portion of the Cretaceous Fox Hills Sandstone (***Kfh***) within the Gilcrest survey area is presented in Figure 5-44. A profile of Line L101701 shows the Gravel, and Sand and Gravel lithology classes in contact with the resistive portions of the ***Kfh*** (Figure 5-45).

While the bottom of the ***Kp*** was not imaged with the AEM system that was selected to map the near-surface materials of the Gilcrest area, there are indications of areas within the ***Kp*** that have elevated resistivities (Figure 5-46). These areas may be related to coarse zones within the ***Kp*** that have been identified by others (Topper et al., 2017).

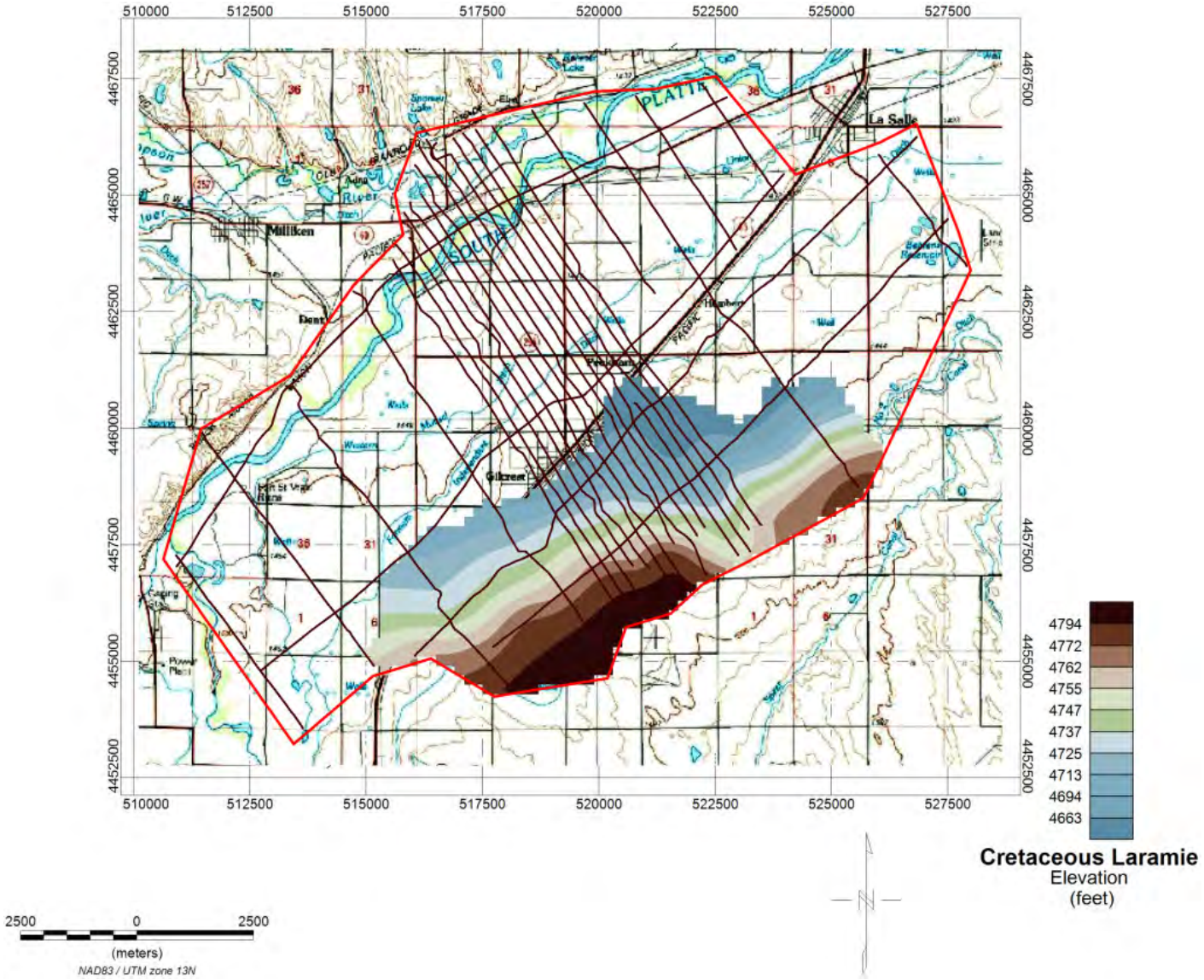

Figure 5-40. Map of the elevation of the Cretaceous Laramie Formation (*Kl*) bedrock unit within the Gilcrest AEM survey area. Flight lines are indicated by brown lines. Red line indicated AEM survey area. Base map is the 100K USGS topography map.

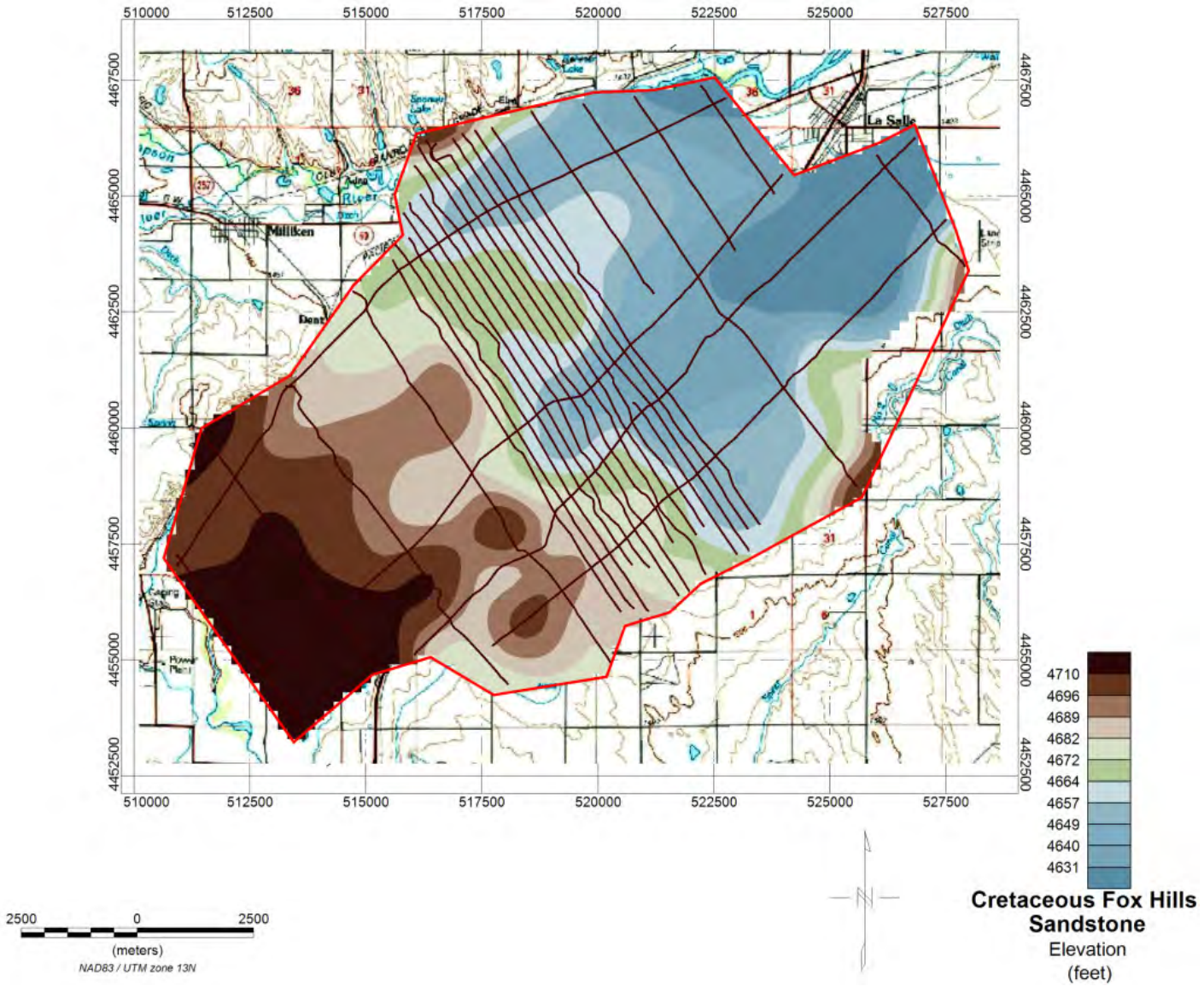

Figure 5-41. Map of the elevation of the Cretaceous Fox Hills Sandstone (*Kfh*) bedrock unit within the Gilcrest AEM survey area. Flight lines are indicated by brown lines. Red line indicated AEM survey area. Base map is the 100K USGS topography map.

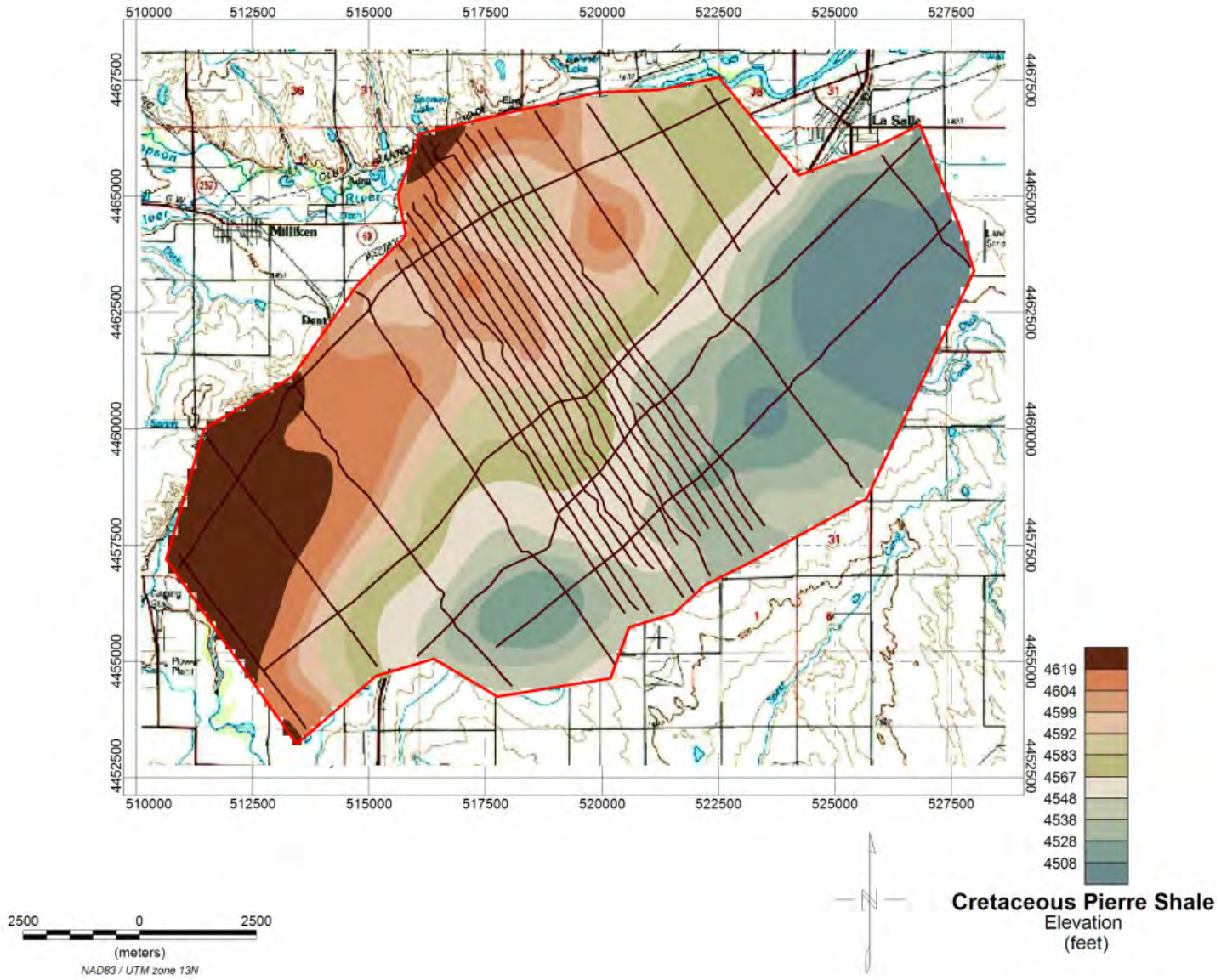

Figure 5-42. Map of the elevation of the Cretaceous Pierre Shale (*Kp*) bedrock unit within the Gilcrest AEM survey area. Flight lines are indicated by brown lines. Red line indicated AEM survey area. Base map is the 100K USGS topography map.

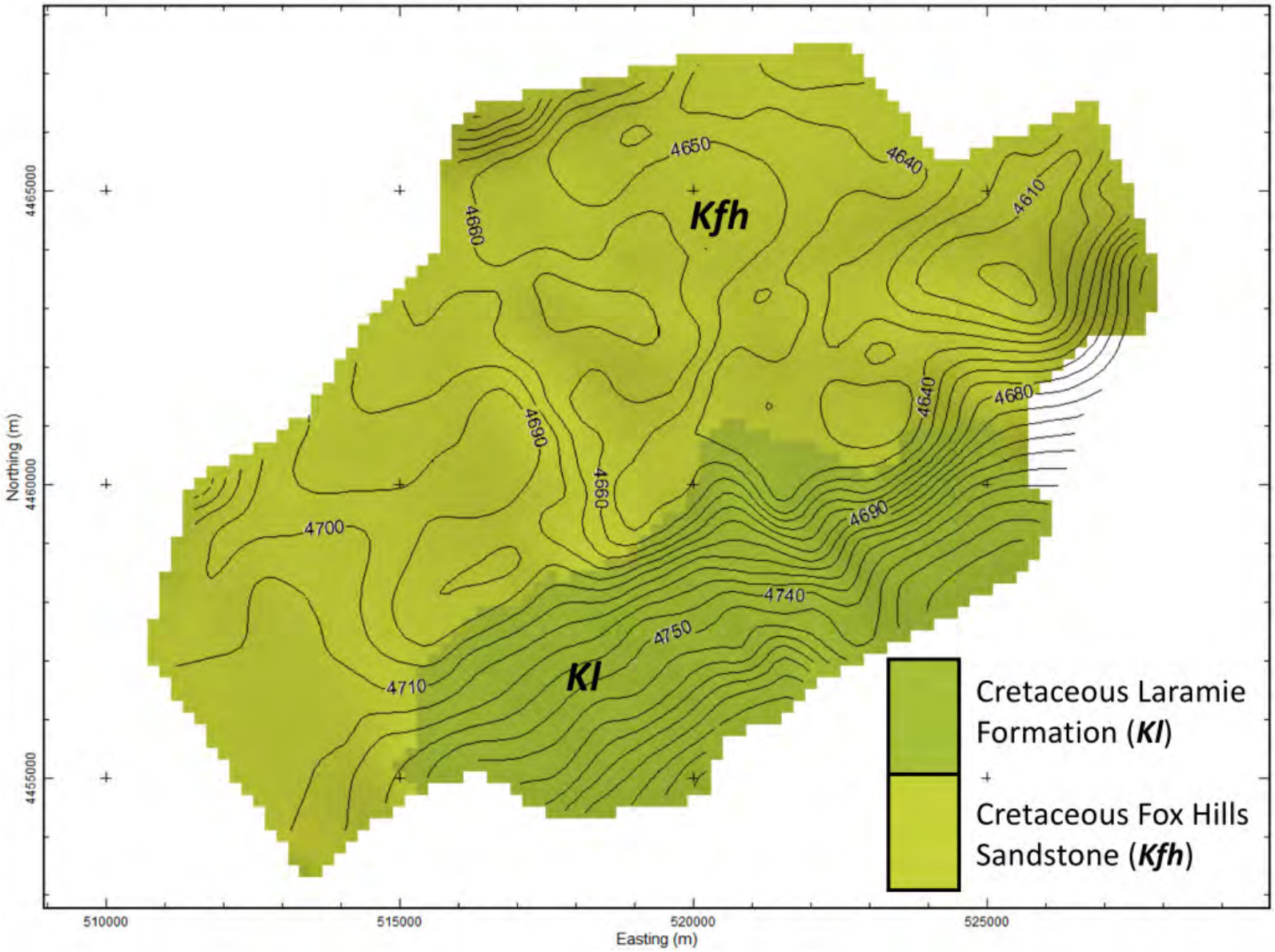

Figure 5-43. Geological map of the bedrock units within the Gilcrest survey area.

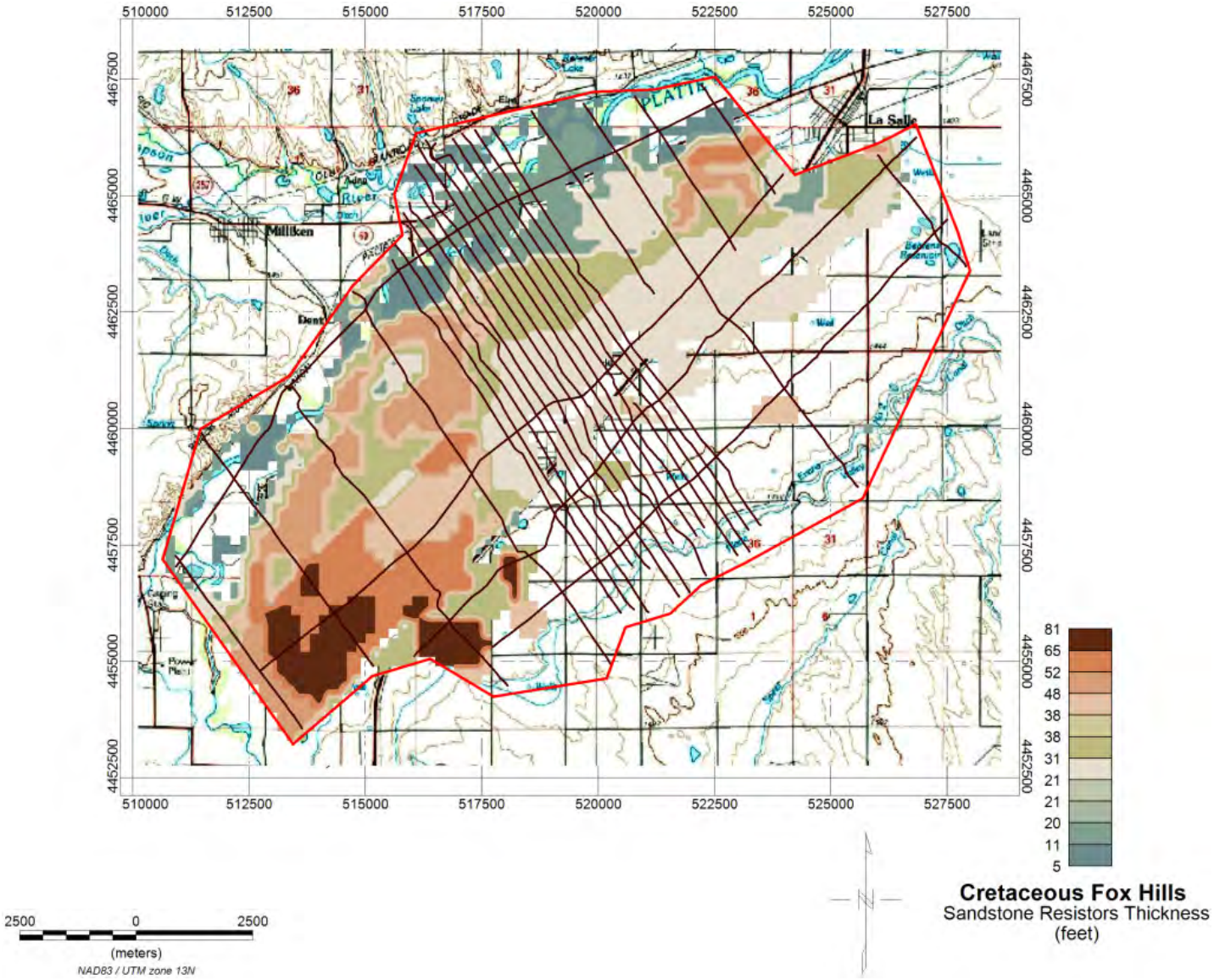

Figure 5-44. Map of the resistive (> 18 ohm-m) portion of the Cretaceous Fox Hills Sandstone (*Kfh*) within the Gilcrest survey area. Flight lines are indicated by brown lines. Red line indicated AEM survey area. Base map is the 100K USGS topography map.

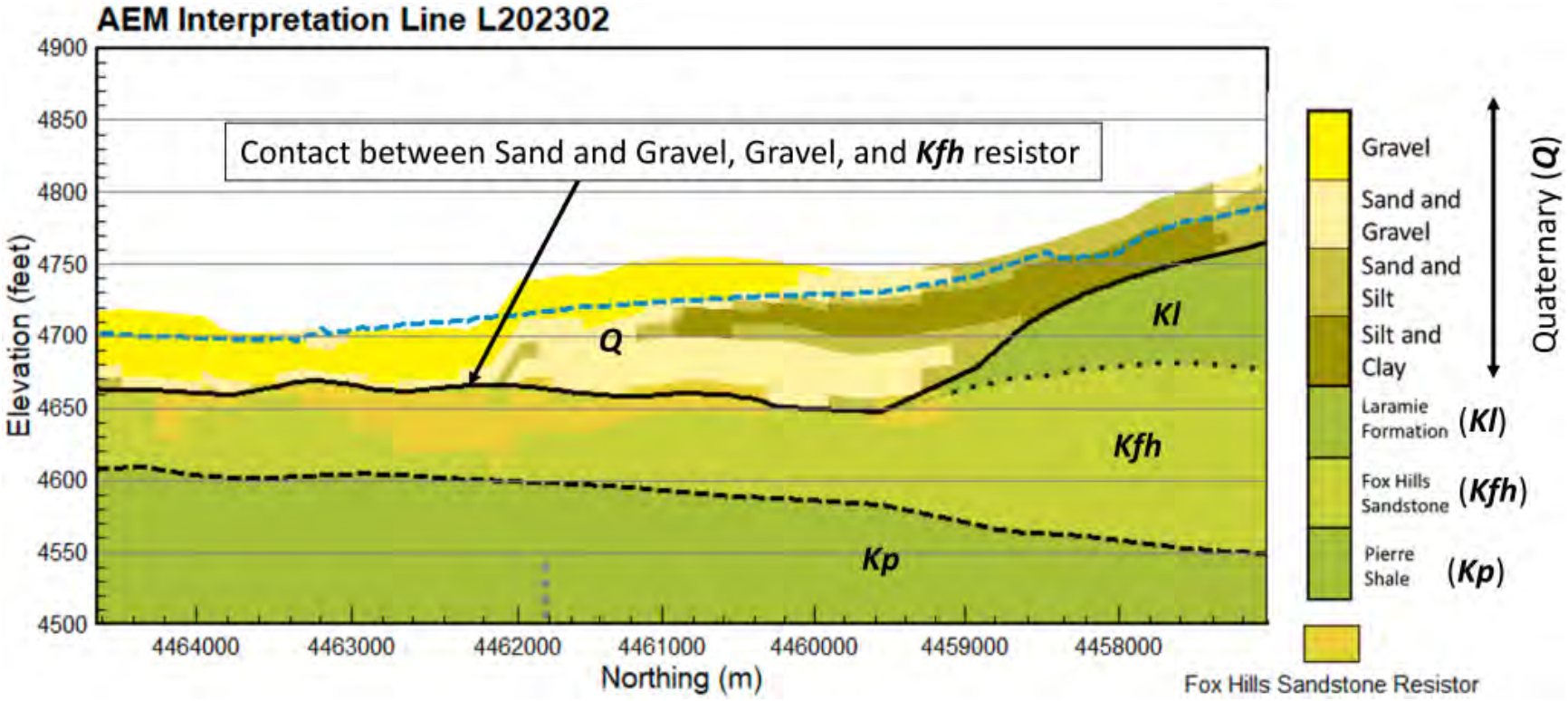

Figure 5-45. Profile L101701 of the interpreted lithologies and bedrock units for the Gilcrest AEM survey area. Dark yellow area indicates the location of the resistive *Kfh*. This may be a zone of potential hydrologic connection between the Cretaceous Fox Hills Sandstone (*Kfh*) and the Quaternary (*Q*) sediments. The dashed blue line is the water table, the solid black line is the Quaternary (*Q*) and Cretaceous Fox Hills Sandstone (*Kfh*) contact, and the dashed black lines are the Cretaceous Laramie Formation (*Kl*) and *Kfh contact as well as the Kfh* and Pierre Shale (*Kp*) contact. Projection is NAD83 UTM Zone 13 North (meters), NAVD88 (feet)

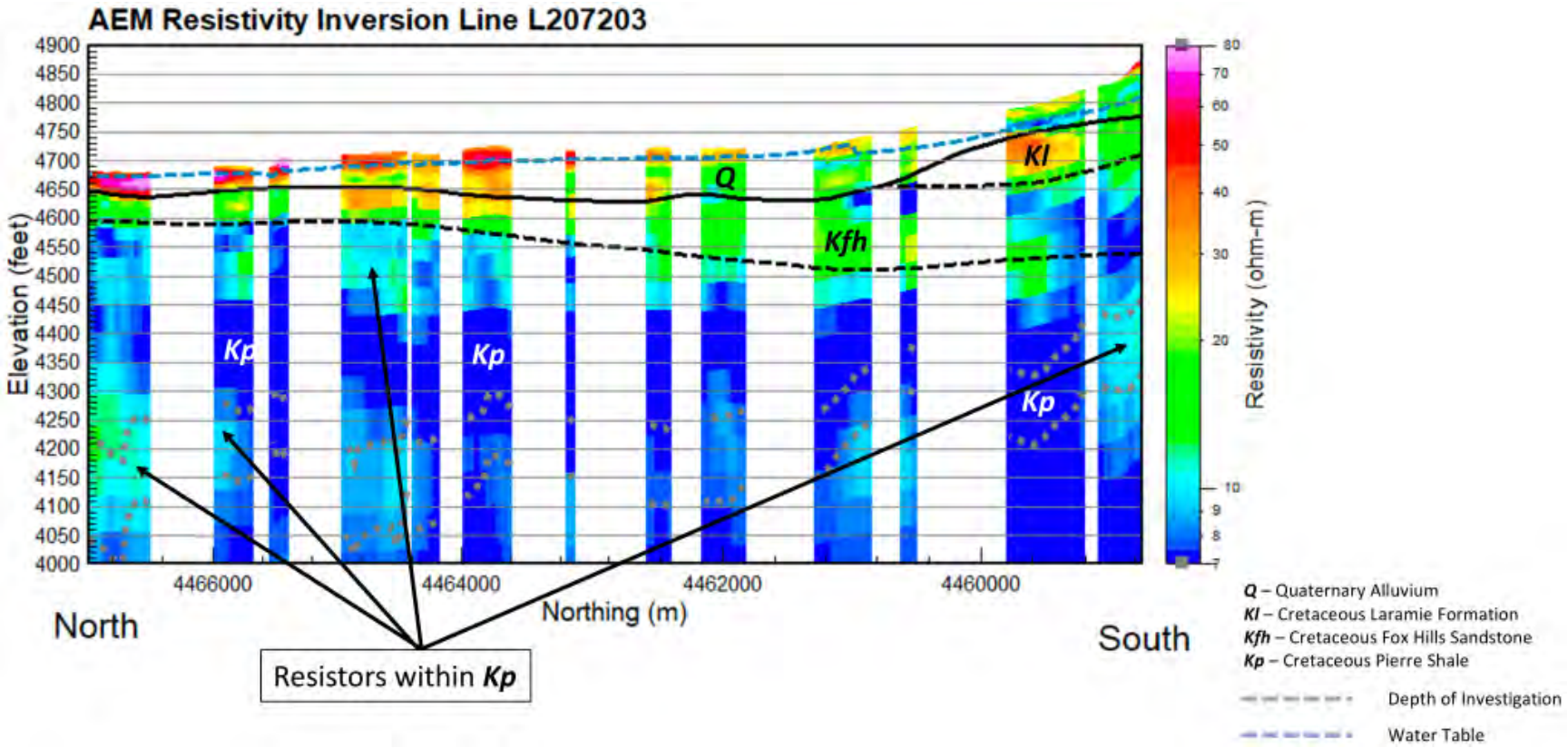

Figure 5-46. Profile of the resistivity on Line L207203 showing the resistive zones within the Cretaceous Pierre Shale (*Kp*). Projection is NAD83 UTM Zone 13 North (meters), NAVD88 (feet).

5.3 Recharge within the Gilcrest AEM Survey Area

3D representations of the subsurface resulting from the AEM method illustrate areas of aquifer and the lithology classes from the bedrock up to the land surface. The interpreted aquifer lithologies for the Gilcrest AEM survey area are presented in this report. From these data a new series of near-surface maps, which includes the interval from 0 to 26 feet, were constructed. The interval of 0-26 feet is noteworthy because this is the first six layers of the inverted AEM resistivity earth model. Remember from the discussion around Table 4-5 that each model layer represents an average of the earth's resistivities within the bounds of each layer, based on the physics behind the electromagnetic exploration technique. These first layer maps show all lithology classes including: 1) silt and clay; 2) sand and silt; 3) sand and gravel; and 4) gravel. These maps indicate the areas at the land surface that can potentially transmit water to the groundwater aquifers in the area. The coarse Quaternary (***Q***) materials (gravel; sand and gravel) transmit the largest volume of water. The silt and clay lithology class being the least able to transmit water. The sand and silt is in-between providing a marginal ability to transmit water. These groups do overlap at the ends of the lithology classes.

The lithology classes at the land surface are presented in Figure 5-47. Note the variability of the full range of materials from gravel to silt and clay. The area for greatest potential recharge is from near the center of the survey area and north across the river. The least amount of potential recharge is in the area of silt and clay deposits in the south. A Google Earth image of the first layer of the AEM earth model is presented in Figure 5-48. The kmz used in this image can be found in Appendix 3-Deliverables\KMZ\Recharge. The Google Earth kmz's have been found to be useful as they allow the reader to locate a property or area of interest and get an idea of its potential recharge ability.

The layers in the inverted resistivity earth model (Table 4-5) that can have the greatest impact on the recharge include layers one through six. These layers are provided in figures 5-47 through 5-58 including 0 to ~3 feet (map in Figure 5-47, Google Earth image in Figure 5-48), ~3 ft to ~7 ft (map in Figure 5-49, Google Earth image in Figure 5-50) , ~7 ft to ~11 ft (map in Figure 5-51, Google Earth image in Figure 5-52) , ~11 ft to ~16 ft (map in Figure 5-53, Google Earth image in Figure 5-54) , ~16 ft to ~21 ft (map in Figure 5-55, Google Earth image in Figure 5-56) , ~21 ft to ~26 ft (map in Figure 5-57, Google Earth image in Figure 5-58). By using the maps, the 3D voxels, and the kmz's, a greater understanding of the potential recharge in the AEM survey area and the paths to the groundwater system can be better understood. These maps are an effective way to best site any recharge structures for the CCWCD. The best information for this is where the flight lines are closely spaced as there is a greater number of soundings in close proximity to each other providing greater detail.

An estimate of the unsaturated thickness in the Gilcrest area is provided in Figure 5-59. By looking at the thickness of the gravel/sand and gravel lithology classes within the zone of unsaturated thickness (Figure 5-60), an understanding of the areas where recharge could flow can be estimated. Figure 5-60 also provides a good look the geometry of the terrace deposits within the Gilcrest survey area.

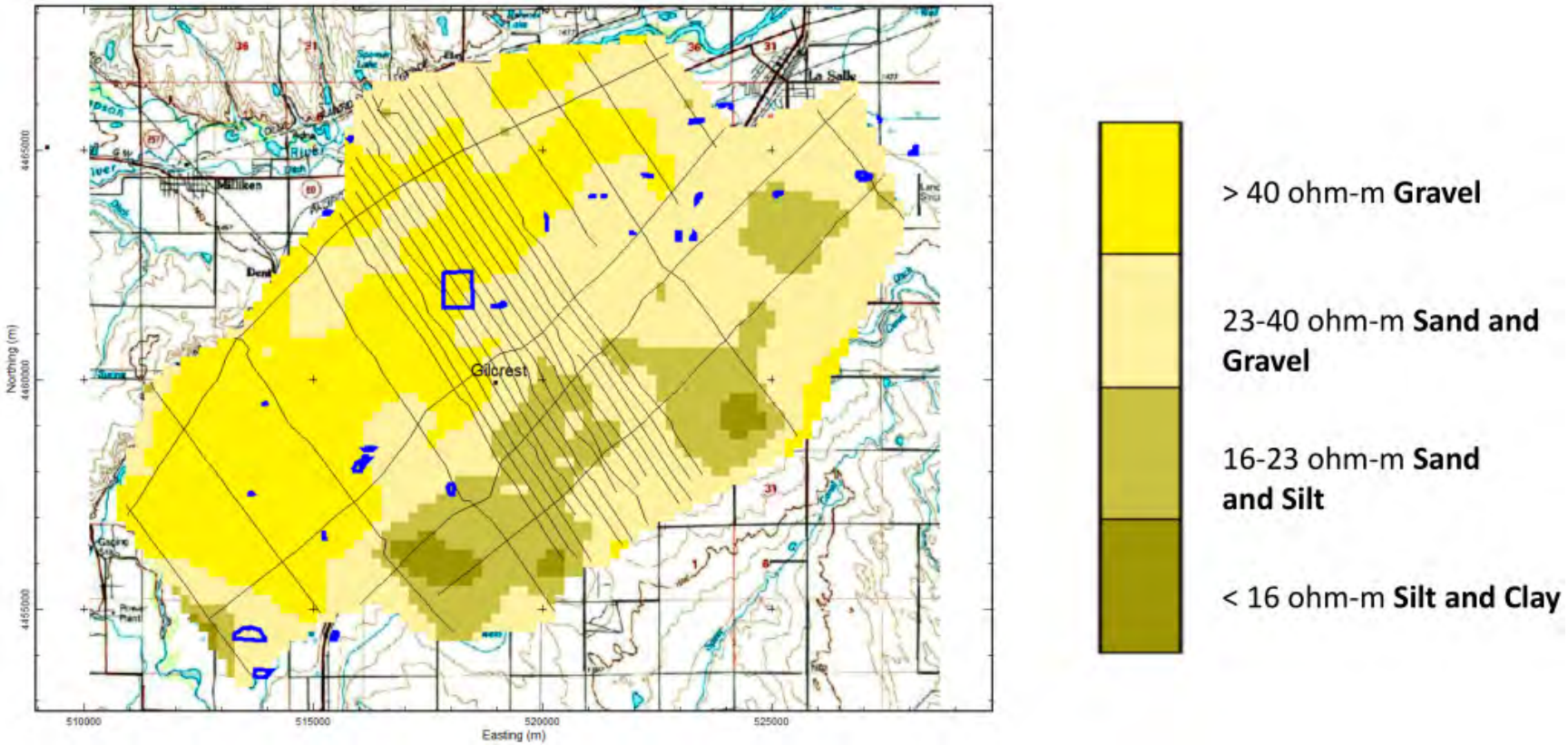

Figure 5-47. Map of the interpreted lithologies for the layer from 0 to ~3 feet in depth for the Gilcrest AEM survey area. Blue areas indicate current CCWCD recharge projects. Flight lines are indicated by black lines. Base map is the 100K USGS topography map. Projection is NAD83 UTM Zone 13 North (meters).

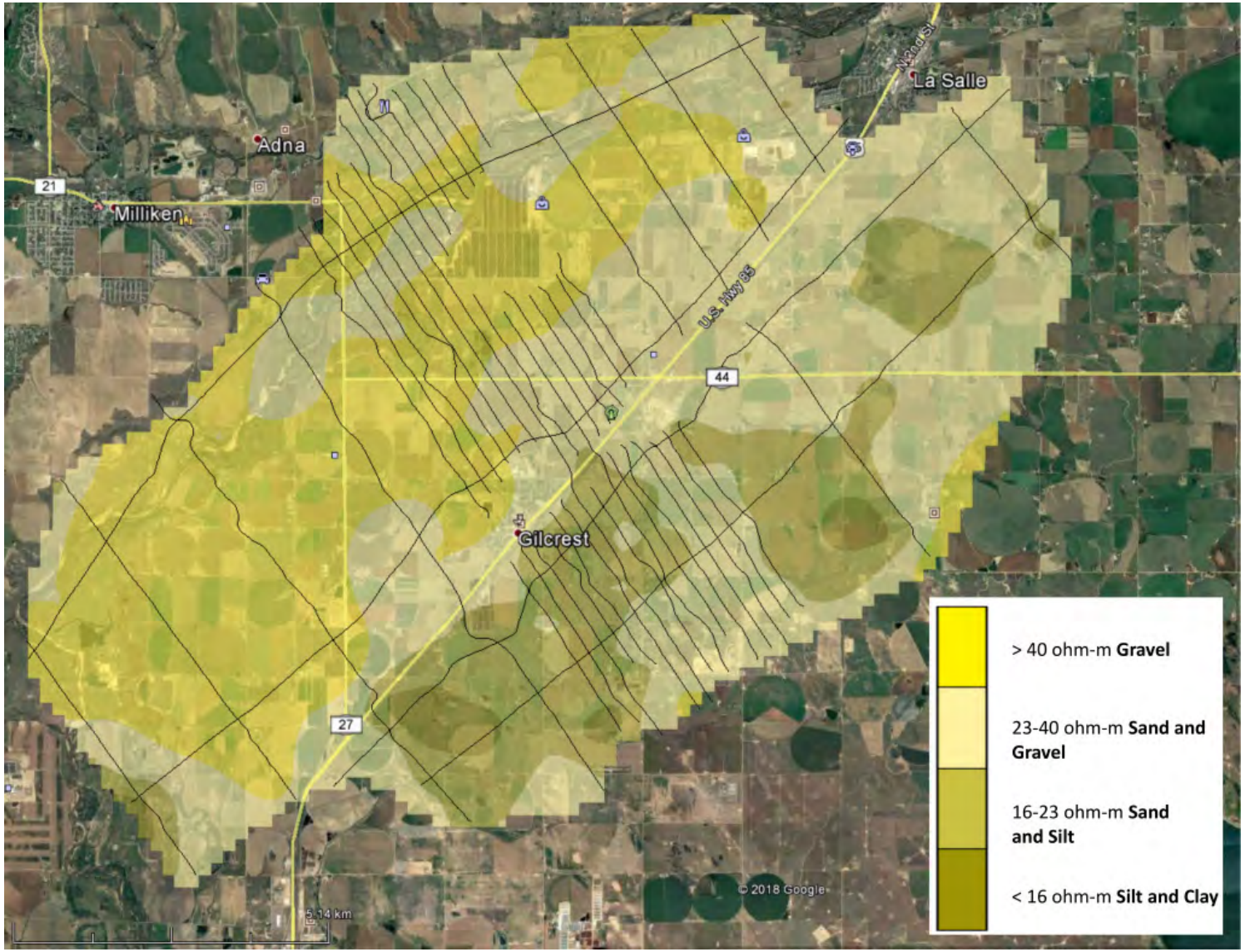

Figure 5-48. Google Earth image of the 0 ft to ~3 ft depth recharge zone for the Gilcrest AEM survey area. This kmz is in Appendix 3-Deliverables\KMZ\Recharge.

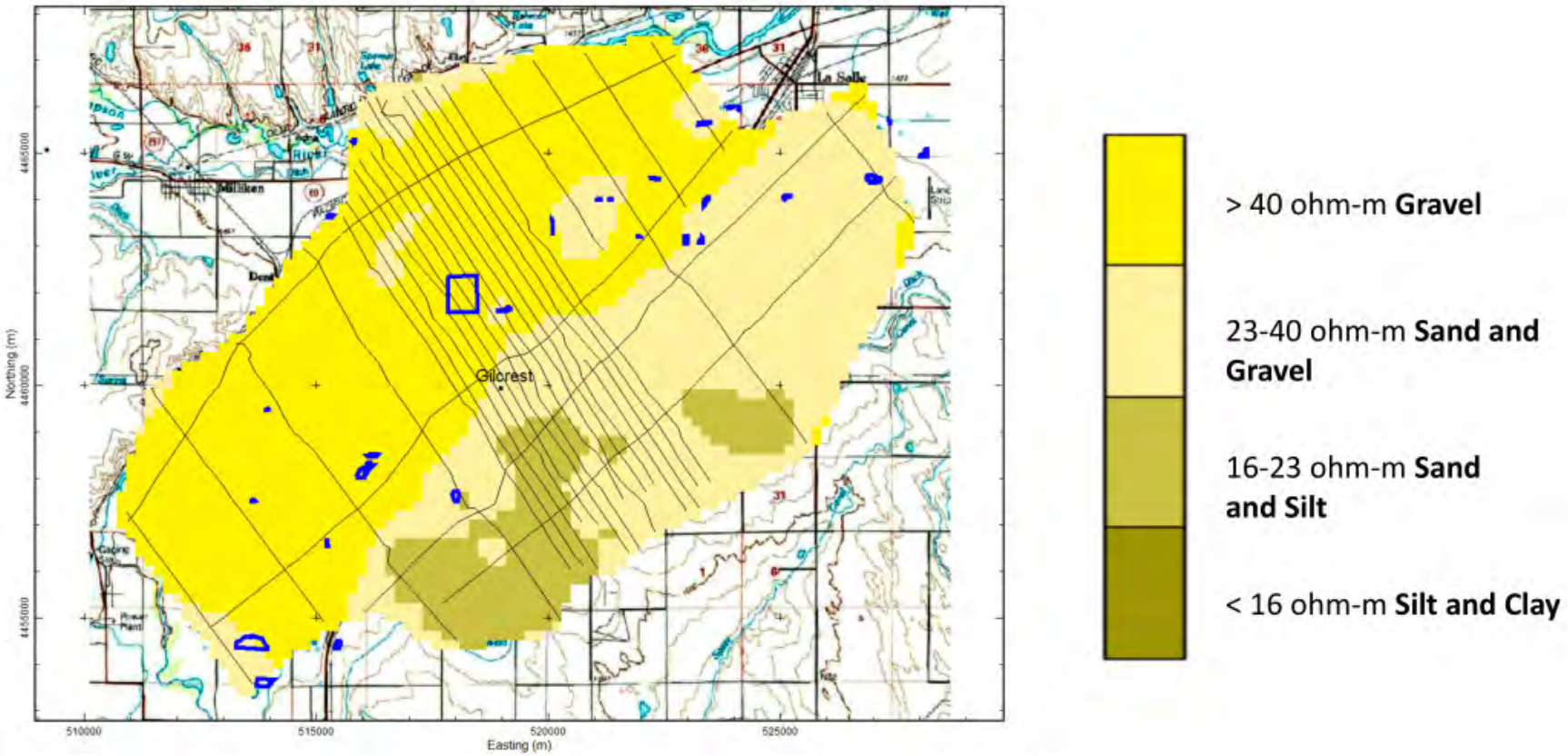

Figure 5-49. Map of the interpreted lithologies for the layer from ~3 to ~7 feet in depth for the Gilcrest AEM survey area. Blue areas indicate current CCWCD recharge projects. Flight lines are indicated by black lines. Base map is the 100K USGS topography map. Projection is NAD83 UTM Zone 13 North (meters).

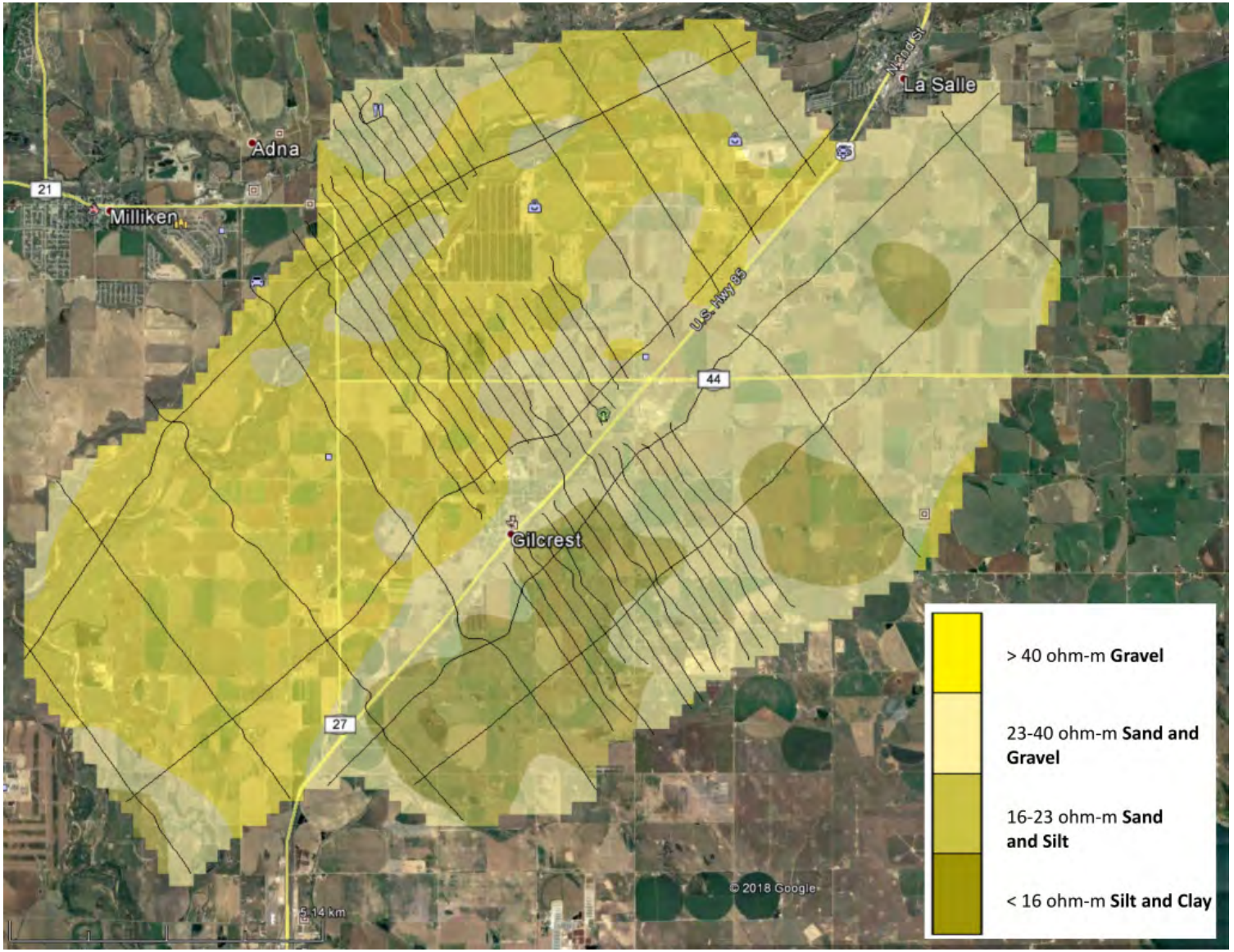

Figure 5-50. Google Earth image of the ~3 ft to ~7 ft depth recharge zone for the Gilcrest AEM survey area. This kmz is in Appendix 3-Deliverables\KMZ\Recharge.

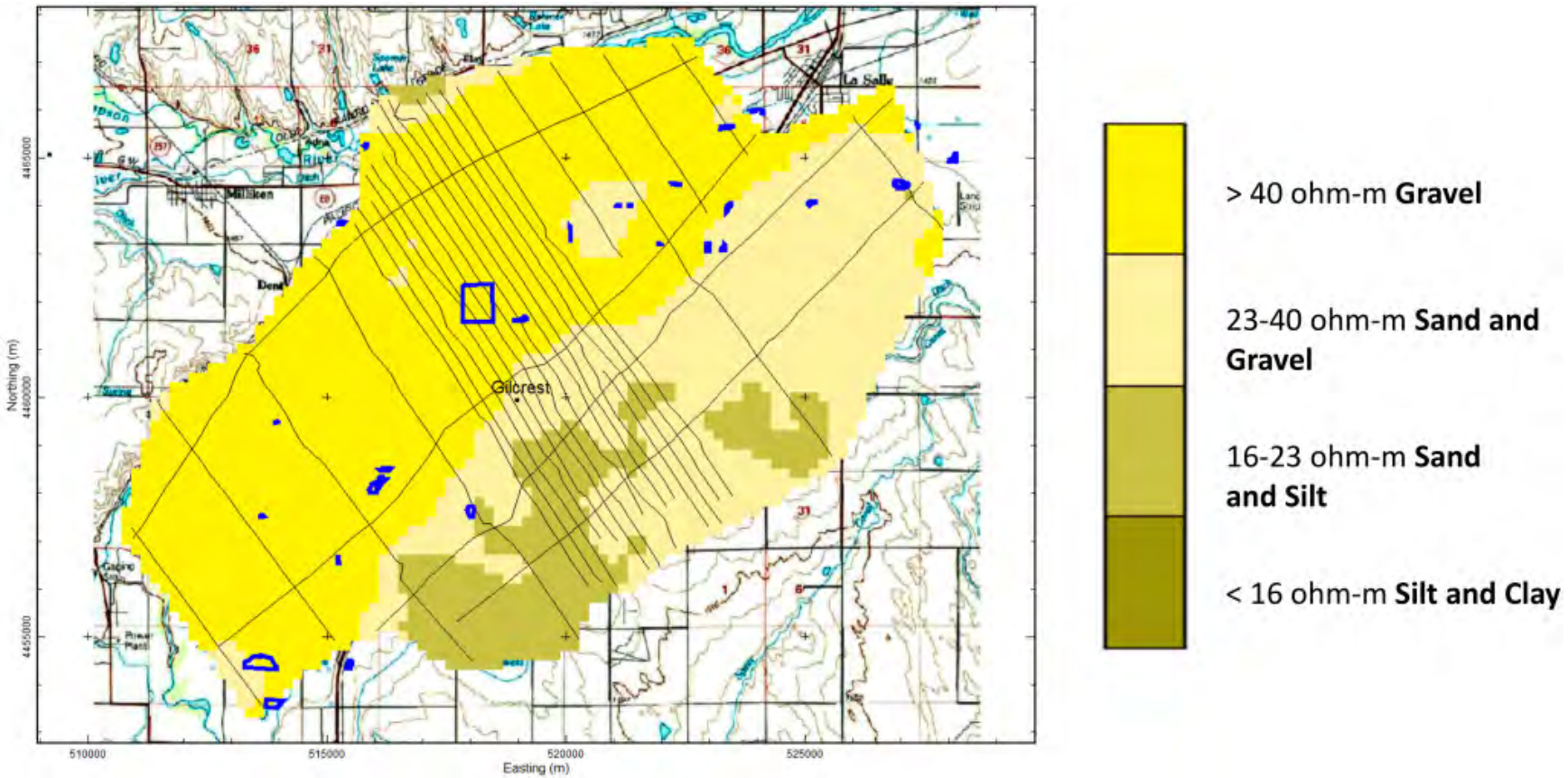

Figure 5-51. Map of the interpreted lithologies for the layer from ~7 to ~11 feet in depth for the Gilcrest AEM survey area. Blue areas indicate current CCWCD recharge projects. Flight lines are indicated by black lines. Base map is the 100K USGS topography map. Projection is NAD83 UTM Zone 13 North (meters).

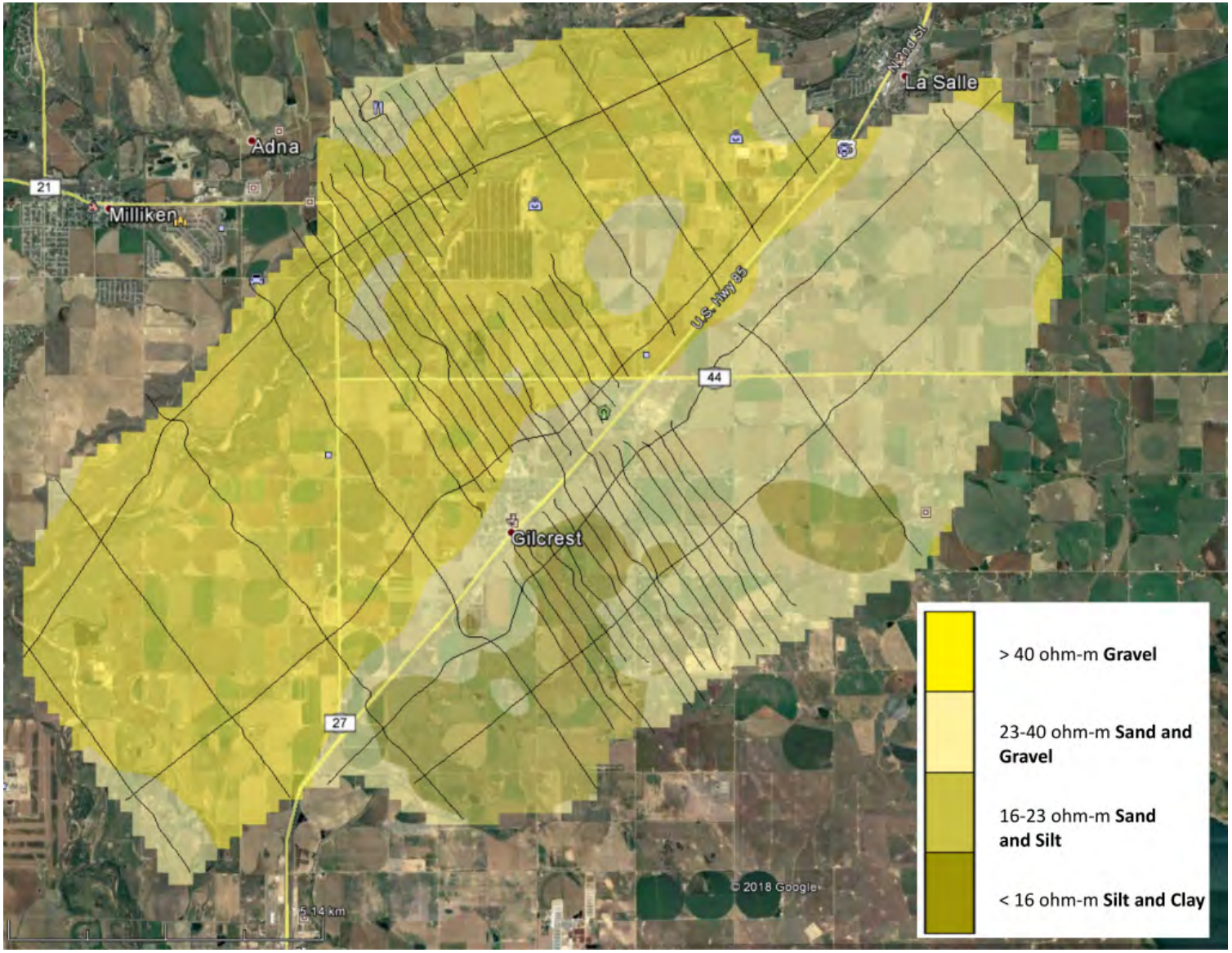

Figure 5-52. Google Earth image of the ~7 ft to ~11 ft depth recharge zone for the Gilcrest AEM survey area. This kmz is in Appendix 3-Deliverables\KMZ\Recharge.

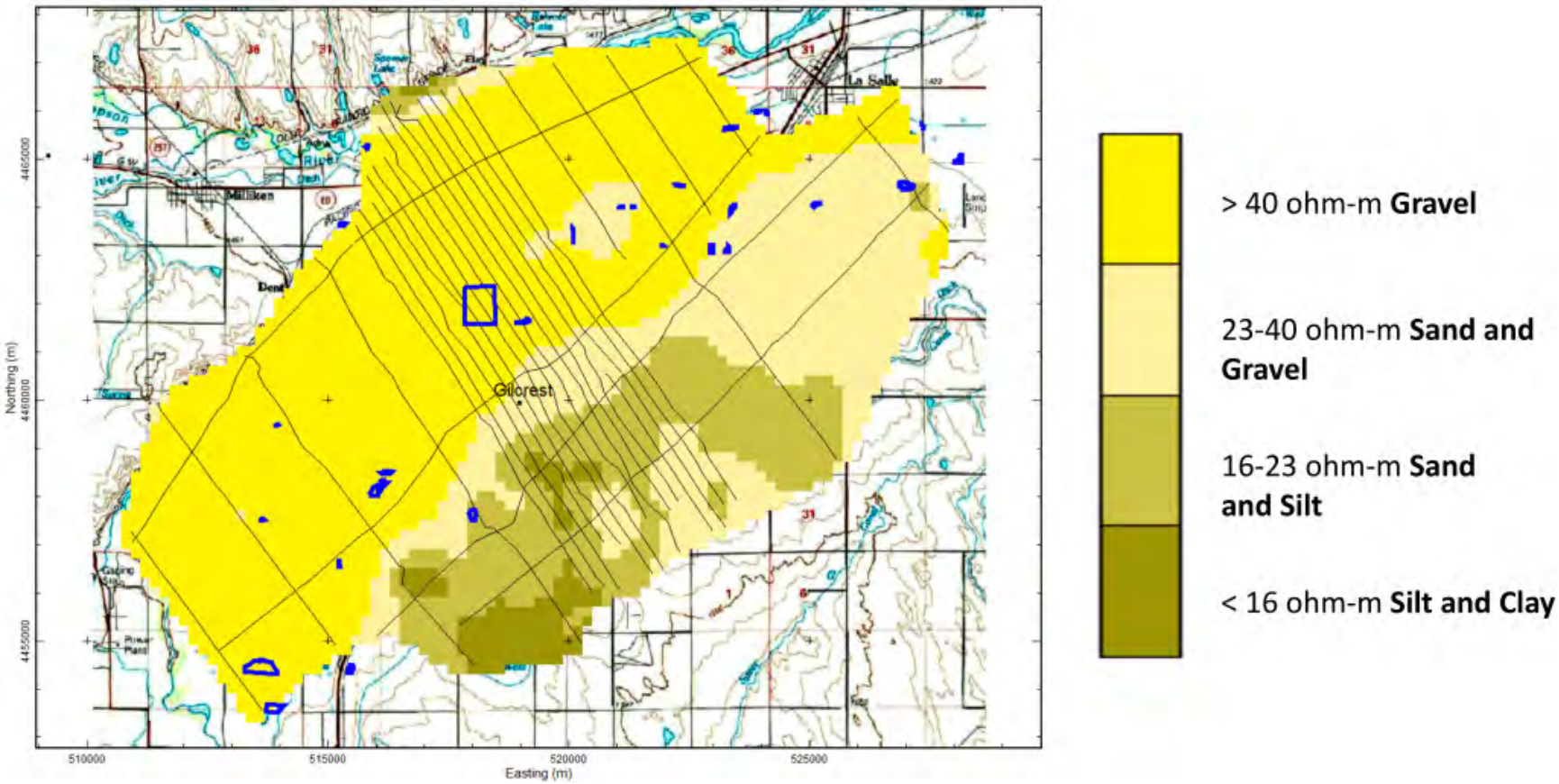

Figure 5-53. Map of the interpreted lithologies for the layer from ~11 to ~16 feet in depth for the Gilcrest AEM survey area. Blue areas indicate current CCWCD recharge projects. Flight lines are indicated by black lines. Base map is the 100K USGS topography map. Projection is NAD83 UTM Zone 13 North (meters).

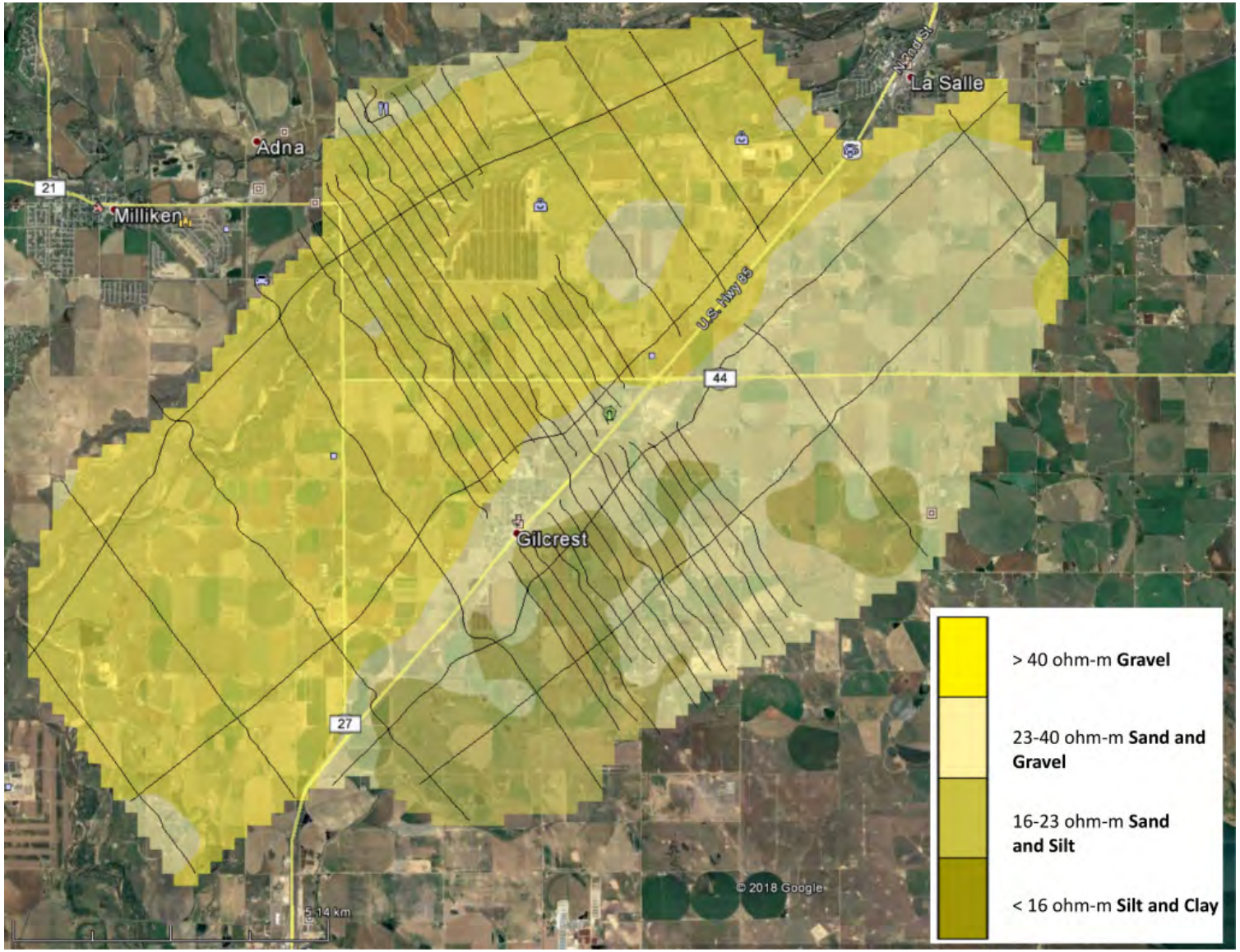

Figure 5-54. Google Earth image of the ~11 ft to ~16 ft depth recharge zone for the Gilcrest AEM survey area. This kmz is in Appendix 3-Deliverables\KMZ\Recharge.

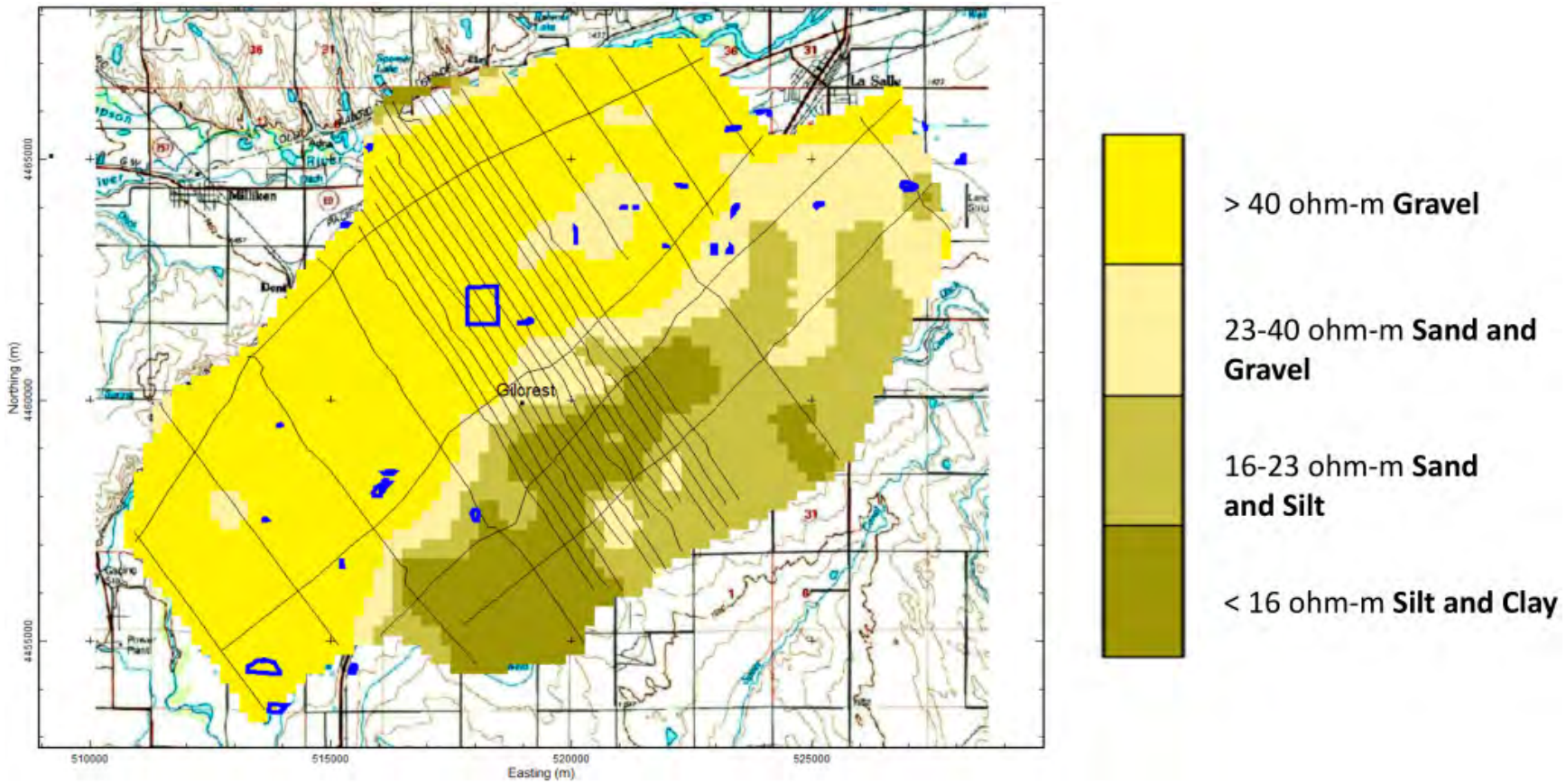

Figure 5-55. Map of the interpreted lithologies for the layer from ~16 to ~21 feet in depth for the Gilcrest AEM survey area. Blue areas indicate current CCWCD recharge projects. Flight lines are indicated by black lines. Base map is the 100K USGS topography map. Projection is NAD83 UTM Zone 13 North (meters).

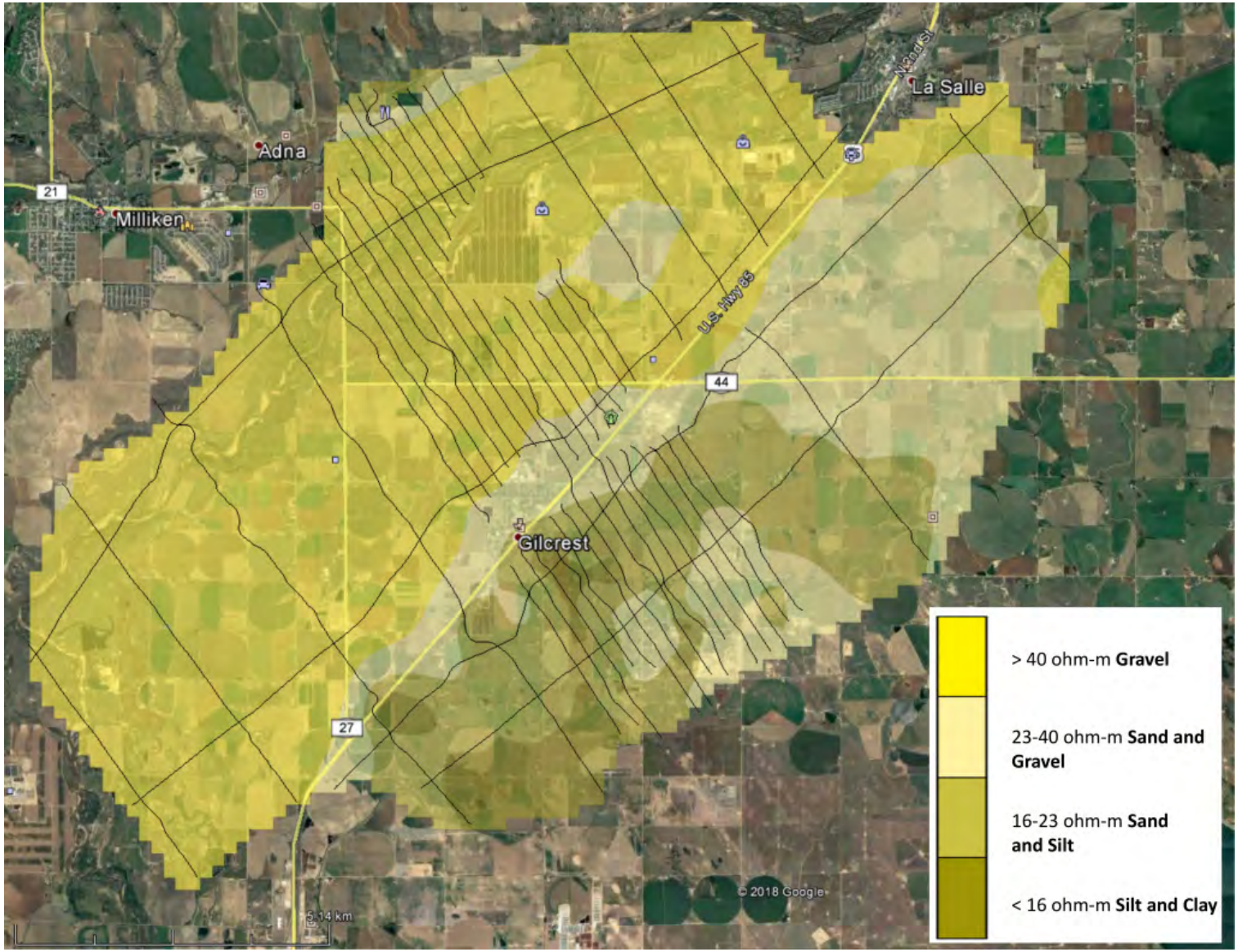

Figure 5-56. Google Earth image of the ~16 ft to ~21 ft depth recharge zone for the Gilcrest AEM survey area. This kmz is in Appendix 3-Deliverables\KMZ\Recharge.

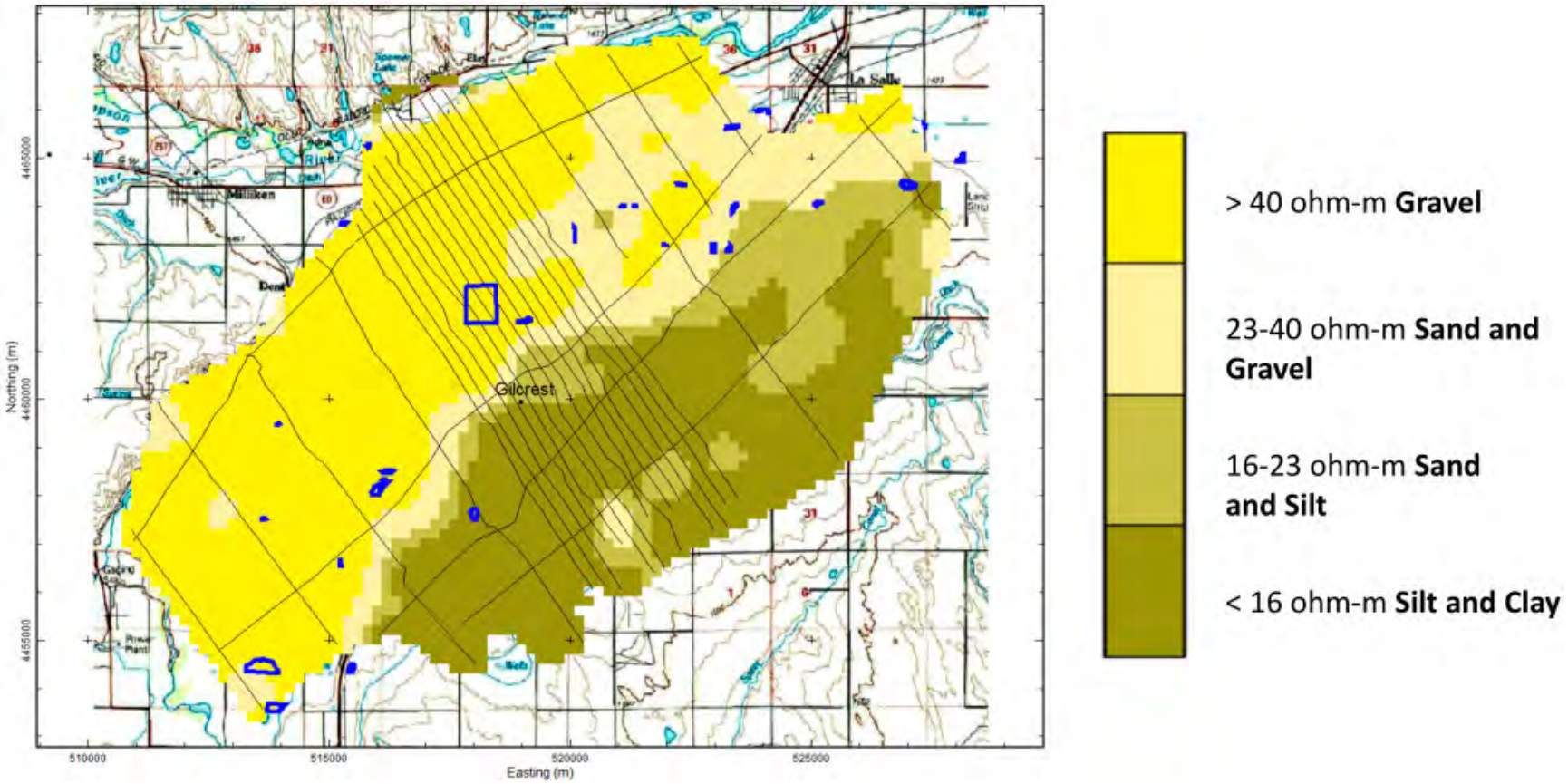

Figure 5-57. Map of the interpreted lithologies for the layer from ~21 to ~26 feet in depth for the Gilcrest AEM survey area. Blue areas indicate current CCWCD recharge projects. Flight lines are indicated by black lines. Base map is the 100K USGS topography map. Projection is NAD83 UTM Zone 13 North (meters).

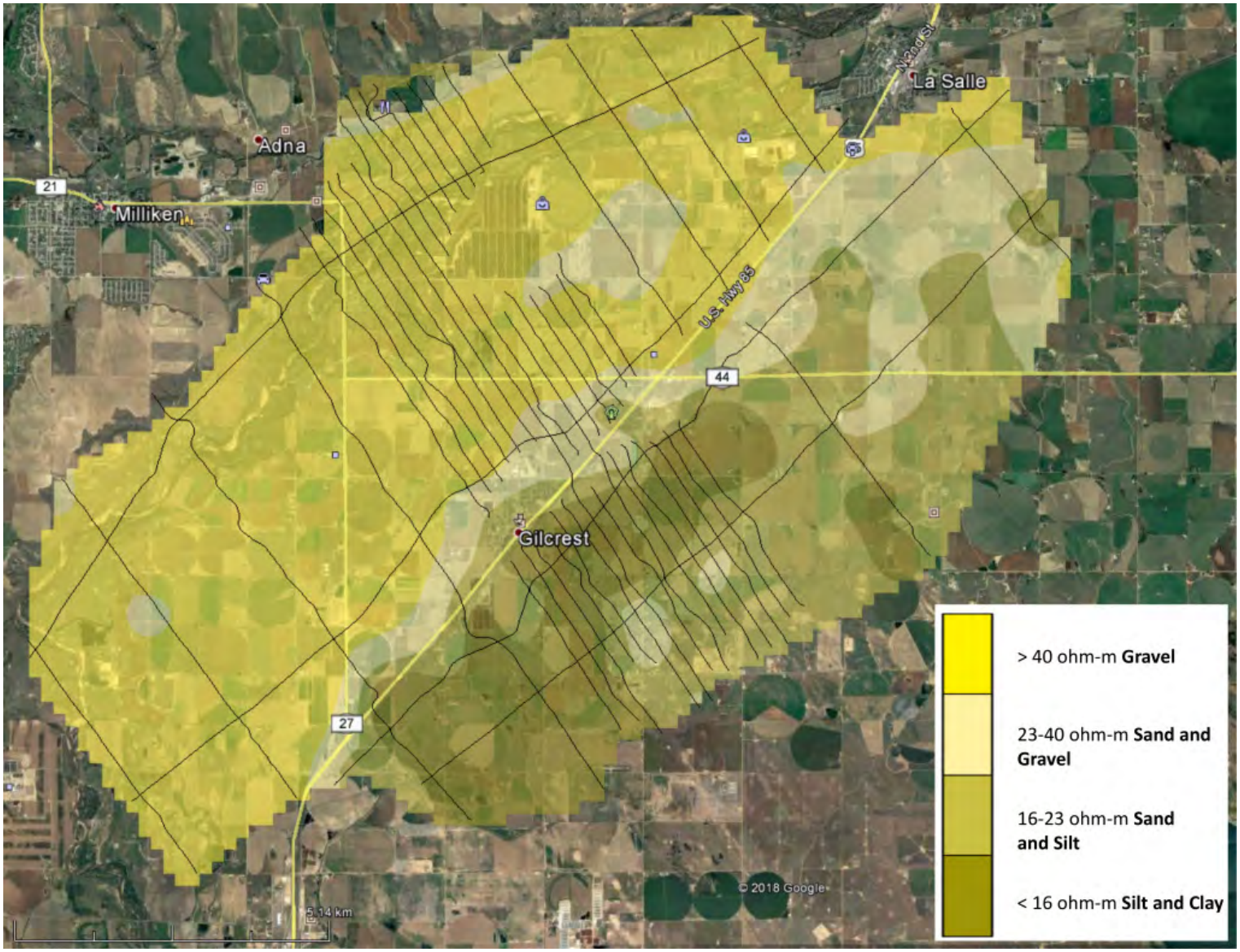

Figure 5-58. Google Earth image of the ~21 ft to ~26 ft depth recharge zone for the Gilcrest AEM survey area. This kmz is in Appendix 3-Deliverables\KMZ\Recharge.

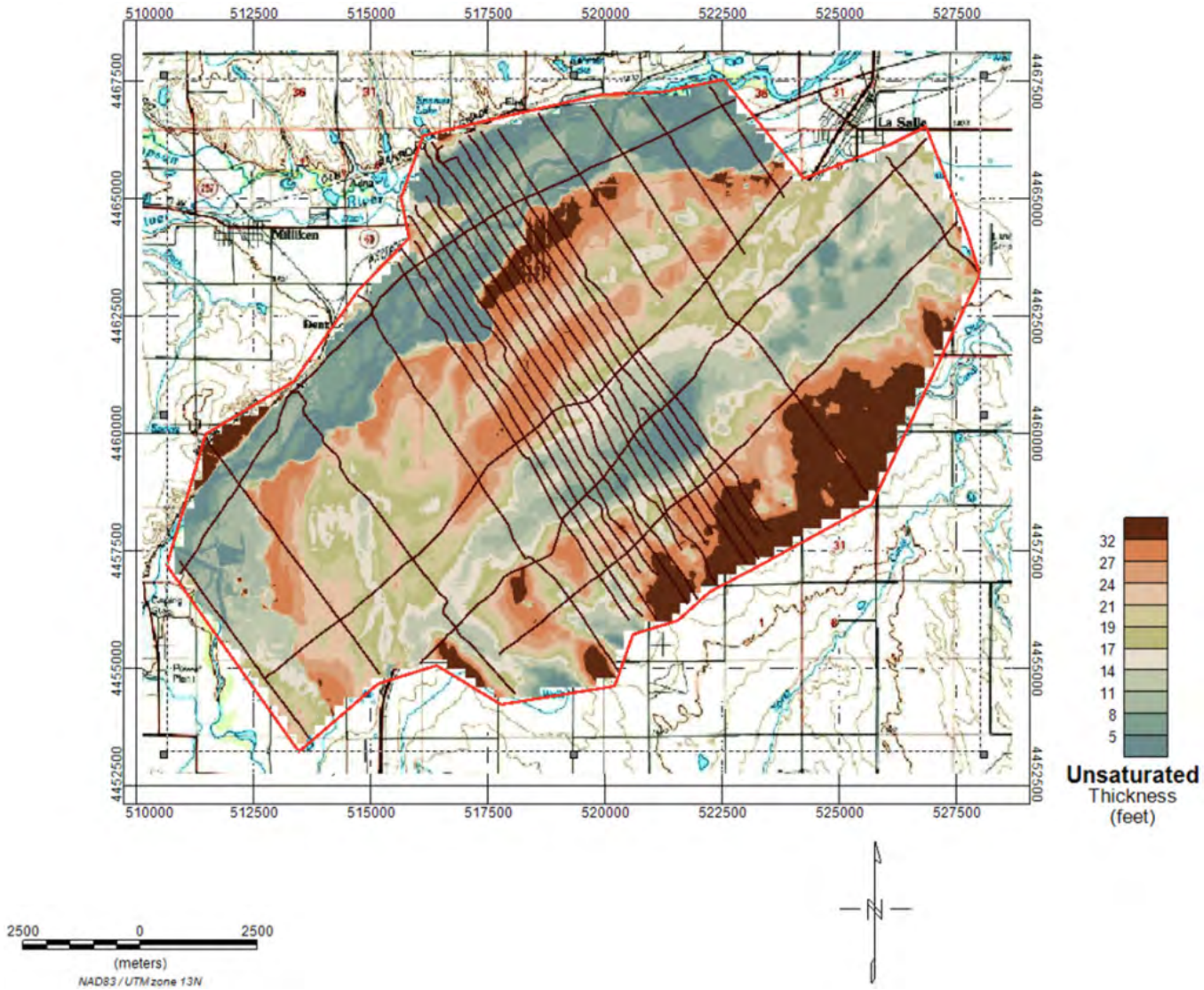

Figure 5-59. Map of unsaturated thickness within the Gilcrest survey area. Note the thicker sections are near the terraces and the south side of the survey area. Flight lines are indicated by brown lines. Red line indicated survey area. Base map is the 100K USGS topography map. Projection is NAD83 UTM Zone 13 North (meters).

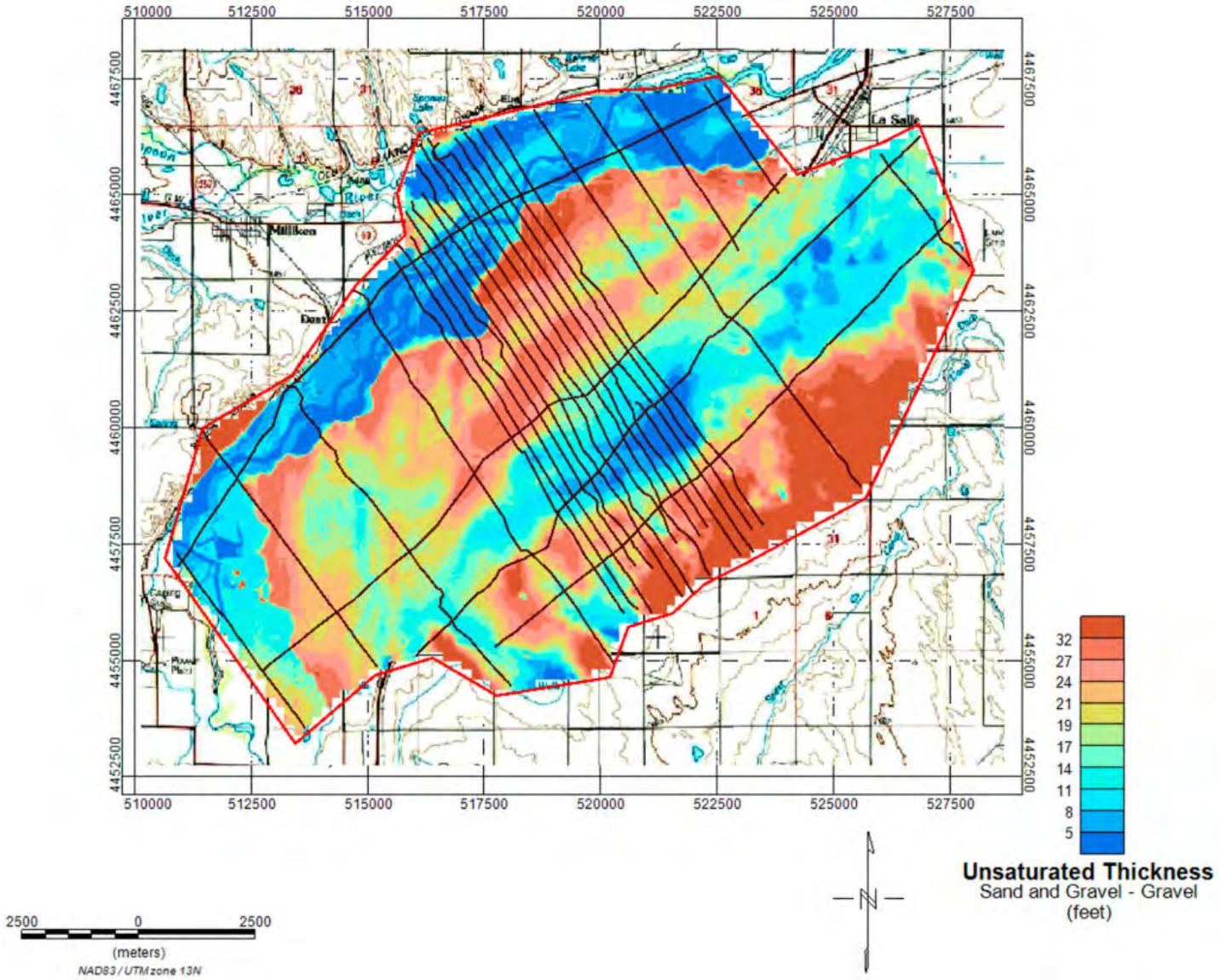

Figure 5-60. Map of unsaturated Gravel/Sand and Gravel within the Gilcrest survey area. Flight lines are indicated by brown lines. Red line indicated survey area. Base map is the 100K USGS topography map. Projection is NAD83 UTM Zone 13 North (meters).

5.4 Key Findings from the AEM Investigation

5.4.1 Boreholes

The borehole information was gathered from two sources: 1) CGS Gilcrest/LaSalle Pilot Project Hydrogeologic Characterization Report which contains information on 432 boreholes which the CGS has inspected and summarized lithologies; and 2) 62 additional wells from the CO-DWR database. In some cases, wells were extended into the bedrock units by reexamining the well information from the CO-DWR database. No boreholes within the AEM study area contained usable geophysical logs that were within the Quaternary materials. Some oil and gas wells had geophysical logs but logs were acquired below the depth of interest for this study.

5.4.2 Digitizing Interpreted Geological Contacts

Characterization and interpretation of the subsurface was performed in cross-section and derived surface grid formats. Contacts between the geologic units were digitized in 2D including: Quaternary (***Q***) and Cretaceous Laramie Formation (***Kl***), Cretaceous Fox Hills Sandstone (***Kfh)*** and Cretaceous Pierre Shale ***(Kp)***. The interpretive process benefited from the use of CGS and CO-DWR borehole logs. Surface grids of the interpreted geologic formations were then produced. Each flight line profile with interpretation, including the ***Q*** aquifer lithology classes and ***Kl***, ***Kfh,*** and ***Kp*** are included in the appendices as well as interpretative surface grids.

5.4.3 Resistivity/Lithology Relationship

Assessment of the sediment character in the ***Q*** deposits was conducted to determine the overall composition of the major categories used to define the aquifer and aquitards in the Gilcrest AEM survey area. Resistivity thresholds were used to characterize silt and clay (<16 ohm-m), sand and silt (16-23 ohm-m), sand and gravel (23-40 ohm-m), and gravel (>40 ohm-m). This allowed for the characterization of the ranges of resistivities present in the ***Q*** deposits.

5.4.4 Hydrogeological Framework of the Gilcrest AEM Survey Area

The AEM reveals considerable variability in the ***Q*** deposits across the Gilcrest survey area. The subsurface distribution of materials in the ***Q*** can be generally characterized in aquifer materials made up of mostly alluvial gravel, sand and gravel, and sand and silt with non-aquifer material made up of silt and clay. Due to an extensive silt and clay layer in the southern part of the study area which splits the ***Q*** deposits horizontally, an area of semi confined to confined conditions exist that affect wells in that area. The ***Q*** aquifer of the Gilcrest AEM survey area is potentially hydrologically connected to the Cretaceous units present in the area, most likely the ***Kfh*** units; the ***Kp*** acts as a deeper bedrock aquiclude for the area in most areas.

5.4.5 Potential Recharge Zones within the Gilcrest AEM Survey Area

Each Gilcrest AEM flight line was interpreted for potential aquifer recharge material at the first model layer (0-3 ft) as well as the following layers: 3-7 ft, 7-11 ft, 11-16 ft, 16-21 ft, and 21-26 ft. These layers are the most useful for understanding the potential for recharge from the land surface downward to the aquifers. Areas of gravel material will have the highest potential to transmit the largest amount of water to the groundwater system, with sand and gravel potentially transmitting slightly less water from whatever source, downward, as both units are permeable. Sand and silt zones will have lower potential to transmit water downward and the silt and clay will transmit minimal to no water to the groundwater aquifer. The best information for illustrating this concept is where the flight lines are closely spaced, as there is a greater number of soundings in close proximity to each other providing greater detail.

5.5 Recommendations

Recommendations provided to the CCWCD in this section are based on the interpretation and understanding gained from the addition of the AEM data to existing information and from discussions with the CCWCD about their management challenges.

5.5.1 Additional AEM Mapping

The aquifer maps provided in this report represent the detailed hydrogeologic framework developed for the Gilcrest survey area. The detail provided in the hydrogeological interpretation of the survey area allowed for confident development of a hydrogeologic framework. The interpretations match well with the boreholes and the historic work in the area. While no additional high resolution AEM information is needed within survey area to resolve questions of resource management, it is recommended that additional areas of closely spaced lines or "block flights" be collected to develop detailed frameworks as needed in other areas. This would be particularly important if a detailed understanding of the near surface for recharge infrastructure or well field development is necessary. Surface geophysical, specifically EM or electrical, data acquisition could also be used to gain a detailed understand of the near surface in small areas.

5.5.2 Update the Water Table Map

The groundwater data used in the analyses presented in this report use the 2017 water table map from the CGS. Additional water level measurement locations would improve the water table map if the mapped area is expanded to include all of the Gilcrest survey area and beyond. This is especially true on the north, west and south sides of survey area. Additional monitoring wells added to the network to understand the semi-confined and confined nature of the aquifers under the silt and clay layer on the south side would be beneficial.

5.5.3 Siting new test holes and production wells

The AEM framework maps and profiles provided in this report provide insight in 3D on the relationship between current boreholes and production groundwater wells. At the time of this report, the currently available lithology data for the Gilcrest area was used in building the framework maps and profiles. It is recommended that the results from this report be used to site new test holes and monitoring wells. Often test holes are sited based on previous work that is regional in nature. By utilizing the maps in this report, new drilling locations can be sited in optimal locations. The location of new water supply wells can also use the results in this report to guide development of sites. Planners should locate wells in areas of greatest saturated thickness with the best understanding of how the well production will be used in groundwater management related to CCWCD activities. Additional monitoring wells added to the network to understand the semi-confined and confined nature of the aquifers under the silt and clay layer on the south side would be beneficial.

5.5.4 Aquifer testing and borehole logging

Aquifer tests are recommended to improve estimates of aquifer characteristics. A robust aquifer characterization program is highly recommended at the state, District's and smaller entity levels. Aquifer tests can be designed based on the results of AEM surveys and existing production wells could be used in conjunction with three or more installed water level observation wells. Additional test holes with detailed, functional, and well calibrated geophysical logging for aquifer characteristics are highly recommended. The lack of test holes with geophysical logs in the Gilcrest survey area did provide added complexity and uncertainty to the interpretation. Borehole geophysical logs would have made this investigation more robust. Examples of additional logging would be flow meter logs and geophysical logs including gamma, neutron, electrical, and induction logs. Detailed aquifer characteristics can be accomplished with nuclear magnetic resonance logging (NMR). This is a quick and effective way to characterize porosity and water content, estimates of permeability, mobile/bound water fraction, and pore-size distributions with depth. This is very cost effective when compared to traditional aquifer tests.

5.5.5 Recharge Zones

The Gilcrest hydrogeologic framework in this report provides a focus upon areas of recharge from the ground surface to the groundwater aquifer. The block flights of AEM data acquisition provide the most detailed information for understanding recharge throughout the Gilcrest survey area. It is recommended that additional AEM data be collected, or surface geophysical data utilizing closely-spaced lines for near-surface resolution as needed related to CCWCD activities. It is further recommended that future work integrate new soils maps with the results of this study to provide details on soil permeability, slope, and water retention to provide a more complete understanding of the transport of water from the land surface to the groundwater aquifer.

5.5.6 Managed Aquifer Recharge

The area which lies out of the silt and clay layer on the south side of Gilcrest may have the best potential for managed aquifer recharge. The unsaturated thickness map provided in the report is the best guide to looking for optimal sites when combined with the other information provided within the report. Detailed analysis for this purpose would need to be done to determine if this is a viable opportunity for the CCWCD. Additional AEM mapping within CCWCD would also locate similar locations. These detailed maps will benefit the CCWCD in locating and developing Managed Aquifer Recharge sites and would be beneficial for siting areas to provide storage and release of water for stream flow and other uses.

6 Description of Data Delivered

6.1 Tables Describing Included Data Files

Table 6-1 describes the data columns in the ASCII EM_MAG *.xyz files for the CCWCD AEM survey area as well as the Geosoft database files *_EM_MAG.gdb. These files contain the electromagnetic raw data, plus the magnetic and navigational data, as supplied directly from SkyTEM.

The results of the SCI are included in Gilcrest_SCI_Inv_v1.gdb and .xyz and the data columns of these files are described in Table 6-2.

The borehole data used in the interpretation of the inversion results for the CCWCD survey are included in the files listed in Table 6-3. Each type of borehole information has both a collar file containing the location of each of the wells, and a second file containing the borehole data for the individual wells. The data column descriptions for the collar files are listed in Table 6-4. Table 6-5 describes the channels in all the borehole data files as well as indicates which type of data contains each channel.

Table 6-6 describes the raw airborne data files included in Appendix 3_Deliverables \Raw_Data. As discussed above, four (4) flights were required to acquire the CCWCD (Figure 4-3) AEM data. Grouped by flight date, there are four (4) data flies included in Appendix_3_Deliverables\Raw_Data for each flight. These files have extensions of "*.sps" and "*.skb". The "*.sps" files include navigation and DGPS location data and the "*.skb" files include the raw AEM data that have been PFC-corrections (discussed in Section 4.9). Two additional files are used for all the flights. These are the system description and specifications file (with the extension "*.gex") in the GEO subdirectory and the 'mask' file (with the extension "*.lin"), in the MASK subdirectory, which correlates the flight dates, flight numbers, and assigned line numbers.

The various interpretation results are included in data files CCWCD_InterpSurfaces_v1 in gdb and ASCII xyz formats. Table 6-7 describes the data columns of those files.

ESRI Arc View Binary Grids and equivalent Geosoft grids of the surfaces that were used in the interpretation (DEM, water table) and derived from the interpretation (top of geological units) of the AEM and borehole are listed in Table 6-8. And stored in Appendix 3_Deliverables\Grids.

Voxel grids were completed for the CCWCD AEM survey area of the ***Q*** and ***Kl, Kfh, Kp*** units as well as lithological units (Gravel, Sand and Gravel, Sand and Silt, and Silt and Clay). The voxel grids were made using a 250 ft grid cell size and the model layer thickness (Table 4-5). Table 6-9 is a list of the channel names in both ASCII *.xyz and Geosoft *.gdb format for the voxel files.

In summary, the following are included as deliverables:

- Raw EM Mag data Geosoft database and ASCII *.xyz
- SCI inversion Geosoft database and ASCII *.xyz
- Borehole Geosoft databases and ASCII *.xyz
- Interpretations Geosoft database and ASCII *.xyz
- Raw Data Files - SkyTEM files *.geo, *skb, *.lin
- ESRI ArcView and Geosoft grid files – surface, topo, etc.
- 3D fence diagrams of the CCWCD survey lines.
- 3D voxel models as ASCII *.xyz and *.gdb for the Gilcrest AEM survey areas

KMZs for the Gilcrest AEM survey (Discussed in Section 6.2)

Table 6-1: Channel name, description, and units for Gilcrest_EM_MAG Geosoft *.gdb and *.xyz with EM, magnetic, DGPS, Inclinometer, altitude, and associated data.

Parameter	Description	Unit
Fid	Unique Fiducial Number	
Line	Line Number	
Flight	Name of Flight	yyyymmdd.ff
DateTime	DateTime Format	Decimal days
Date	DateTime Format	yyyymmdd
Time	Time UTC	hhmmss.sss
AngleX	Angle (in flight direction)	Degrees
AngleY	Angle (perpendicular to flight direction)	Degrees
Height	Filtered Height Measurement	Meters [m]
Lon	Longitude, WGS84	Decimal Degrees
Lat	Latitude, WGS84	Decimal Degrees
E_UTM13N_M	Easting, NAD83 UTM Zone 13N	Meters [m]
N_UTM13N_M	Northing, NAD83 UTM Zone 13N	Meters [m]
DEM_M	Digital Elevation	Meters [m]
Elevation_FT	Elevation, 100 ft grid of NED DEM NAVD88	Feet (ft)
Alt	DGPS Altitude above sea level	Meters [m]
GDSpeed	Ground Speed	Kilometers/hour [km/h]
Curr_LM	Current, Low Moment	Amps [A]
Curr_HM	Current, High Moment	Amps [A]
LM_Z_G01 [Gates 0-27]	Normalized (PFC-Corrected) Low Moment Z-RxCoil value	pV/(m^4*A)
HM_Z_G01 [Gates 0-36]	Normalized (PFC-Corrected) High Moment Z-RxCoil value	pV/(m^4*A)
LM_X_G01 [Gates 0-27]	Normalized (PFC-Corrected) Low Moment X-RxCoil value	pV/(m^4*A)
HM_X_G01 [Gates 0-36]	Normalized (PFC-Corrected) High Moment X-RxCoil value	pV/(m^4*A)
PLNI_60Hz_Intensity	Power Line Noise Intensity monitor	
bmag_raw	Raw Base Station Mag Data filtered	nanoTesla [nT]
Diurnal	Diurnal Mag Data	nanoTesla [nT]
Mag_raw	Raw Mag Data	nanoTesla [nT]
Mag_cor	Mag Data Corrected for Diurnal Drift	nanoTesla [nT]
RMF	Residual Magnetic Field	nanoTesla [nT]
TMI	Total Magnetic field Intensity	nanoTesla [nT]

Table 6-2: Channel name, description, and units for Gilcrest_SCI_Inv_v1 Geosoft gdb and xyz files with EM inversion results.

Parameter	Description	Unit
LINE	Line Number	Feet [ft]
Easting_M	Easting NAD83, UTM Zone 13	Meters [m]
Northing_M	Northing NAD83, UTM Zone 13	Meters [m]
DEM_M	DEM from survey	Meters [m]
DEM_FT	DEM from 100 ft grid NED NAVD88	Feet [ft]
FID	Unique Fiducial Number	
TIME	Date Time Format	Decimal days
ALT_M	Altitude of system above ground	Meters [m]
INVALT_M	Inverted Altitude of system above ground	Meters [m]
INVALTSTD	Inverted Altitude Standard Deviation of system above ground	Meters [m]
DELTAALT	Change in Altitude of system above ground	Meters [m]
RESDATA	Residual of individual sounding	
RESTOTAL	Total residual for inverted section	
DOI_UPPER_M	More conservative estimate of DOI	Meters [m]
DOI_LOWER_M	Less conservative estimate of DOI	Meters [m]
DOI_UPPER_FT	More conservative estimate of DOI	Feet [ft]
DOI_LOWER_FT	Less conservative estimate of DOI	Feet [ft]
RHO_I_0 THROUGH RHO_I_28	Inverted resistivity of each later	Ohm-m
RHO_STD_0 THROUGH RHO_STD_28	Inverted resistivity standard deviation	
SIGMA_I_0 THROUGH SIGMA_I_28	Conductivity	S/m
DEP_TOP_0_FT THROUGH DEP_TOP_28_FT	Depth to the top of individual layers	Feet [ft]
DEP_BOT_0_FT THROUGH DEP_BOT_28_FT	Depth to the bottom of individual layers	Feet [ft]
THK_0_FT THROUGH THK_28_FT	Thickness of individual layers	Feet [ft]
DEP_TOP_0_M THROUGH DEP_TOP_28_M	Depth to the top of individual layers	Meters [m]
DEP_BOT_0_M THROUGH DEP_BOT_28_M	Depth to the bottom of individual layers	Meters [m]
THK_0_M THROUGH THK_28_M	Thickness of individual layers	Meters [m]

Table 6-3: Files containing borehole information for the Gilcrest AEM survey.

Database (*.xyz, *.gdb)	Description
RegWellLith_Collar	432 wells with lithology identified in the CGS Gilcrest/LaSalle Pilot Project Hydrogeologic Characterization Report (Barkmann et al., 2014)
RegWellLith _Data	
NewRegWellLith _Collar	62 wells from the CO-DWR database (CODWR, 2018)
NewRegWellLith _Lith	

Table 6-4: Channel name, description, and units for collar files.

Parameter	Description	Unit
DH_Hole	Name of individual boreholes (CO-DWR Receipt Number)	
DH_East	Easting of boreholes, NAD83, UTM Zone 13	Feet [ft]
DH_North	Northing of boreholes, NAD83, UTM Zone 13	Feet [ft]
DH_RL	Elevation of top of borehole	Feet [ft]
DH_Dip	Dip of borehole	Degrees
DH_Azimuth	Azimuth of borehole	Degrees
DH_Top	Depth to top of borehole	Feet [ft]
DH_Bottom	Depth to bottom of borehole	Feet [ft]
DH_ZMin	Minimum elevation in borehole	Feet [ft]
DH_ZMax	Maximum elevation in borehole	Feet [ft]

Table 6-5: Channel name description and units for borehole data.

Parameter	Description	Unit	Type of Log
DH_East	Easting of boreholes, NAD83, UTM Zone 13	Feet [ft]	All
DH_North	Northing of boreholes, NAD83, UTM Zone 13	Feet [ft]	All
DH_RL	Elevation in borehole	Feet [ft]	All
DH_From	End of interval	Feet[ft]	Strat, Lith
DH_To	Start of interval	Feet [ft]	Strat, Lith
Lithcode	Lithology description associated with 30 categories		

Table 6-6: Raw SkyTEM data files

Folder	File Name	Description
Data	..NavSys.sps, …PaPc.sps, ...RawData_PFC.skb, …DPGS.sps	Raw data files included for each flight used in importing to Aarhus Workbench
Geo	20170606_337m2_Cal_DualWaveform_60Hz.gex	304M System Description
Mask	20170602_418_USA_Gilcrest.lin	Production file listing dates, flights, and assigned line numbers

Table 6-7: Channel name description and units for the interpretation results files Gilcrest_InterpSurfaces_v1 "gdb" and "xyz" files.

Parameter	Description	Unit
Line	Flight Line Number	
Easting_M	Easting NAD83, UTM Zone 13	Meters [m]
Northing_M	Northing NAD83, UTM Zone 13	Meters [m]
DEM_ft	Topography at 100ft sampling (NAVD 1988)	Feet [ft]
RHO[0] through RHO[28]	Array of Inverted model resistivities of each later	Ohm-m
RHO_STD[0] through RHO_STD[28]	Array of standard deviations of inverted model resistivities of each layer	
RESDATA	Inversion model residuals of each individual sounding	
RESTOTAL	Average of all model inversion residuals	
DEP_TOP_ft[0] through DEP_TOP_ft[28]	Depth to the top of individual layers	Feet [ft]
DEP_BOT_ft[0] through DEP_BOT_ft[28]	Depth to the bottom of individual layers	Feet [ft]
DOI_UPPER_FT	More conservative estimate of DOI from Workbench	Feet [ft]
DOI_LOWER_FT	Less conservative estimate of DOI from Workbench	Feet [ft]
WaterTable_Interp	Elevation of the top of the water table from Barkmann et al. (2014) and Sebol and Barkmann (2017).	Feet [ft]
SedimentType[0] through SedimentType[28]	Array of Sediment types: 0 - Bedrock; 1 – Silt and Clay; 2 – Sand and Silt; 3 – Sand and Gravel; 4 - Gravel	Integer Array
Top_Silt_and_Clay	Elevation of top of Silt and Clay Material (< 16 ohm-m)	Feet [ft]
Bottom_Silt_and_Clay	Elevation of bottom of Silt and Clay Material (< 16 ohm-m)	Feet [ft]
Top_Sand_and_Silt	Elevation of top of Sand and Silt Material (16-23 ohm-m)	Feet [ft]
Bottom_Sand_and_Silt	Elevation of bottom of Sand and Silt Material (16-23 ohm-m)	Feet [ft]
Top_Upper_Sand_and_Gravel	Elevation of top of Upper Sand and Gravel Material (23-40 ohm-m)	Feet [ft]
Bottom_Upper_Sand_and_Gravel	Elevation of bottom of Upper Sand and Gravel Material (23-40 ohm-m)	Feet [ft]
Top_Lower_Sand_and_Gravel	Elevation of top of Lower Sand and Gravel Material (23-40 ohm-m)	Feet [ft]
Bottom_Lower_Sand_and_Gravel	Elevation of bottom of Lower Sand and Gravel Material (23-40 ohm-m)	Feet [ft]
Top_Gravel	Elevation of top of Gravel Material (> 40 ohm-m)	Feet [ft]
Bottom_Gravel	Elevation of bottom of Gravel Material (> 40 ohm-m)	Feet [ft]
Bedrock	Elevation of top of Bedrock	Feet (ft)
Kl	Elevation of the top of the Cretaceous Laramie Formation.	Feet [ft]
Kfh	Elevation of the top of the Cretaceous Fox Hills Formation	Feet [ft]
Kp	Elevation of the top of the Cretaceous Pierre Formation	Feet [ft]
*	No data or unit not detected	

Table 6-8. Files containing ESRI ArcView Binary Grids *.flt and Geosoft Grids *.grd (NAD 83 UTM Zone 13 North (meters)

Grid File Name	Description	Grid Cell Size (meters)
Gilcrest_DEM	Grid of the Digital Elevation Model; NAVD88 (feet)	30
Gilcrest_Bedrock_AGF	Grid of the Elevation of the Bedrock; NAVD88 (feet)	150
Gilcrest_Watertable_AGF	Grid of the Elevation of the water table as derived by AGF; NAVD88 (feet)	200
Gilcrest_Kl	Grid of the elevation of the top of the Cretaceous Laramie Formation (***Kl***); NAVD88 (feet)	200
Gilcrest_Kfh	Grid of the elevation of the top of the Cretaceous Fox Hills Sandstone (***Kfh***); NAVD88 (feet)	200
Gilcrest_Kp	Grid of the elevation of the top of the Cretaceous Fox Hills Sandstone (***Kp***); NAVD88 (feet)	200
Gilcrest_Quaternary	Grid of the thickness of the Quaternary (***Q***) (feet)	200
Gilcrest_QSaturated	Grid of the thickness of the Saturated Quaternary (***Q***) (feet)	200
Gilcrest_Q_Silt_Clay	Grid of the thickness of the Quaternary (***Q***) Silt and Clay (feet)	200
Gilcrest_Q_Sand_Silt	Grid of the thickness of the Quaternary (***Q***) Sand and Silt (feet)	200
Gilcrest_Q_Sand_Gravel	Grid of the thickness of the Quaternary (***Q***) Sand and Gravel (feet)	200
Gilcrest_Q_Gravel	Grid of the thickness of the Quaternary (***Q***) Gravel (feet)	200
Gilcrest_Q_SandGravel_Gravel	Grid of the thickness of the Quaternary (Q) Sand and Gravel combined with the Gravel (feet)	200
Gilcrest_Q_SiltClay_SandSilt	Grid of the thickness of the Quaternary (Q) Silt and Clay combined with the Sand and Silt (feet)	200
Gilcrest_Unsaturated	Grid of the thickness of the unsaturated Quaternary (Q) (feet)	200
Gilcrest_Unsaturated_SandGravel_Gravel	Grid of the thickness of the unsaturated Quaternary (Q) Sand and Gravel combined with the Gravel (feet)	200
Gilcrest_Kfh_Res	Grid of the thickness of the Cretaceous Fox Hills Sandstone (***Kfh***) over 18 ohm-m (feet)	200

Table 6-9. Channel name, description, and units for Gilcrest_Quaternary_Voxel_Litholgy; Gilcrest_Kl_Voxel; Gilcrest_Kfh_Voxel; and Gilcrest_Kp_Voxel as*.csv and *.gdb..

Parameter	Description	Unit
X	Easting NAD83, UTM Zone 13 North	meter
Y	Northing NAD83, UTM Zone 13 North	meter
Z	Elevation of Voxel Node	NAVD88 [ft]
Resistivity	Voxel cell resistivity value of the Quaternary (***Q***) resistivity	Ohm-m
LithCode	For the Quaternary only (1 = Silt and Clay; 2 = Sand and Silt; 3 = Sand and Gravel; and 4 = Gravel)	NA
Lithology	For the Quaternary only (Silt and Clay; Sand and Silt; Sand and Gravel; and Gravel)	NA

6.2 Description of Included Google Earth KMZ Data and Profiles

In addition to the data delivered in .xyz format, Google Earth .KMZ files were generated to view the geophysical AEM flight line locations and interpreted geologic data. KMZ files for all "*As-Flown*" flight lines and data "*Retained*" for inversion after editing are included in the folder "*Appendix_3_Deliverables\KMZs\FlightLines*".

KMZ files of the potential recharge zones for the CCWCD survey area are included in the folder "*Appendix_3_Deliverables\KMZs\Recharge*".

Unique KMZ files were created for each individual flight line. Within these specialized KMZ files, the AEM flight line is shown as well as place marks at each location where there are interpreted geologic results. The attribute data for each unique place mark contains location information plus the elevations of tops and bottoms of the silt and clay, sand and silt, sand and gravel, and gravel materials as well as bedrock, the interpreted water table, and the elevations of the tops of the Cretaceous Laramie Formation (***Kl***), the Cretaceous Fox Hills Formation (***Kfh***), and the Cretaceous Pierre Shale (***Kp***). These KMZ files are located within the "*Appendix_3_Deliverables\KMZs\Interpretation* folder. Also in the profile folder is a "*GoogleE_Readme.pdf*" file that provides instructions in regards to the "*Settings*" changes that need to be made in Google Earth, and how to use the KMZ files in Google Earth including a legend of what attributes are displayed when an AEM sounding location is clicked. This Readme file is repeated below as a convenience. An example of the CCWCD KMZ is presented in Figure 6-1.

6.2.1 Included README for the CCWCD Interpretation KMZ's

README for:

CCWCD_Interpretation_v1.kmz

Data Files – Within the folder "*CCWCD_Interpretation_Profiles*" is the folder "*CCWCD_Profiles*". Please copy the folder *CCWCD_Profiles* to your C:\ drive. Do not rename any of the files or directories within the folder.

Google Earth Instructions:

STEP 1: In Google Earth, click "*Tools*", then "*Options*".

STEP 2: In the Google Earth Options box, click the "*General*" tab.

STEP 3: Under "*Placemark balloons*", make sure the box is checked to allow access to local files (the profiles).

STEP 4: Under "*Display*", make sure the box is checked to show web results in external browser.

STEP 5: The *CCWCD_Interpretation_v1.kmz* file within the folder named *CCWCD_Interpretation_Profiles* can now be opened and viewed in Google Earth.

Data:

Easting (m) – Easting coordinate in NAD83, UTM 14N, in meters

Northing (m) – Northing coordinate in NAD83, UTM 14N, in meters

Elevation (ft) – DEM elevation in feet

WaterTable Elev (ft) – Water Table elevation, in feet.

Top Gravel (ft) – Elevation of the Top of the Gravel zone, in feet

Bottom Gravel (ft) – Elevation of the Bottom of the Gravel zone, in feet

Top Upper Sand and Gravel (ft) – Elevation of the Top of the Upper Sand and Gravel zone, in feet

Bottom Upper Sand and Gravel (ft) – Elevation of the Bottom of the Upper Sand and Gravel zone, in feet

Top Lower Sand and Gravel (ft) – Elevation of the Top of the Lower Sand and Gravel zone, in feet

Bottom Lower Sand and Gravel (ft) – Elevation of the Bottom of the Lower Sand and Gravel zone, in feet

Top Sand and Silt (ft) – Elevation of the Top of the Sand and Silt zone, in feet

Bottom Sand and Silt (ft) – Elevation of the Bottom of the Sand and Silt zone, in feet

Top Silt and Clay (ft) – Elevation of the Top of the Silt and Clay zone, in feet

Bottom Silt and Clay (ft) – Elevation of the Bottom of the Silt and Clay zone, in feet

Elevation Bedrock (ft) – Elevation of the top of Bedrock, in feet

Elevation Kl (ft) – Elevation of the Top of the Cretaceous Laramie Formation, in feet

Elevation Kfh (ft) – Elevation of the Top of the Cretaceous Fox Hills Formation, in feet

Elevation Kp (ft) – Elevation of the Top of the Cretaceous Pierre Shale Formation, in feet

Profile – Link to Interpreted AEM profile images

Legend – Link to this write-up describing data channels listed here

NOTE – The user may find that some top and bottom elevations of sand and gravel, sand and silt, and silt and clay overlap. This is due to the interbedded nature of these units when the beds are quite thin.

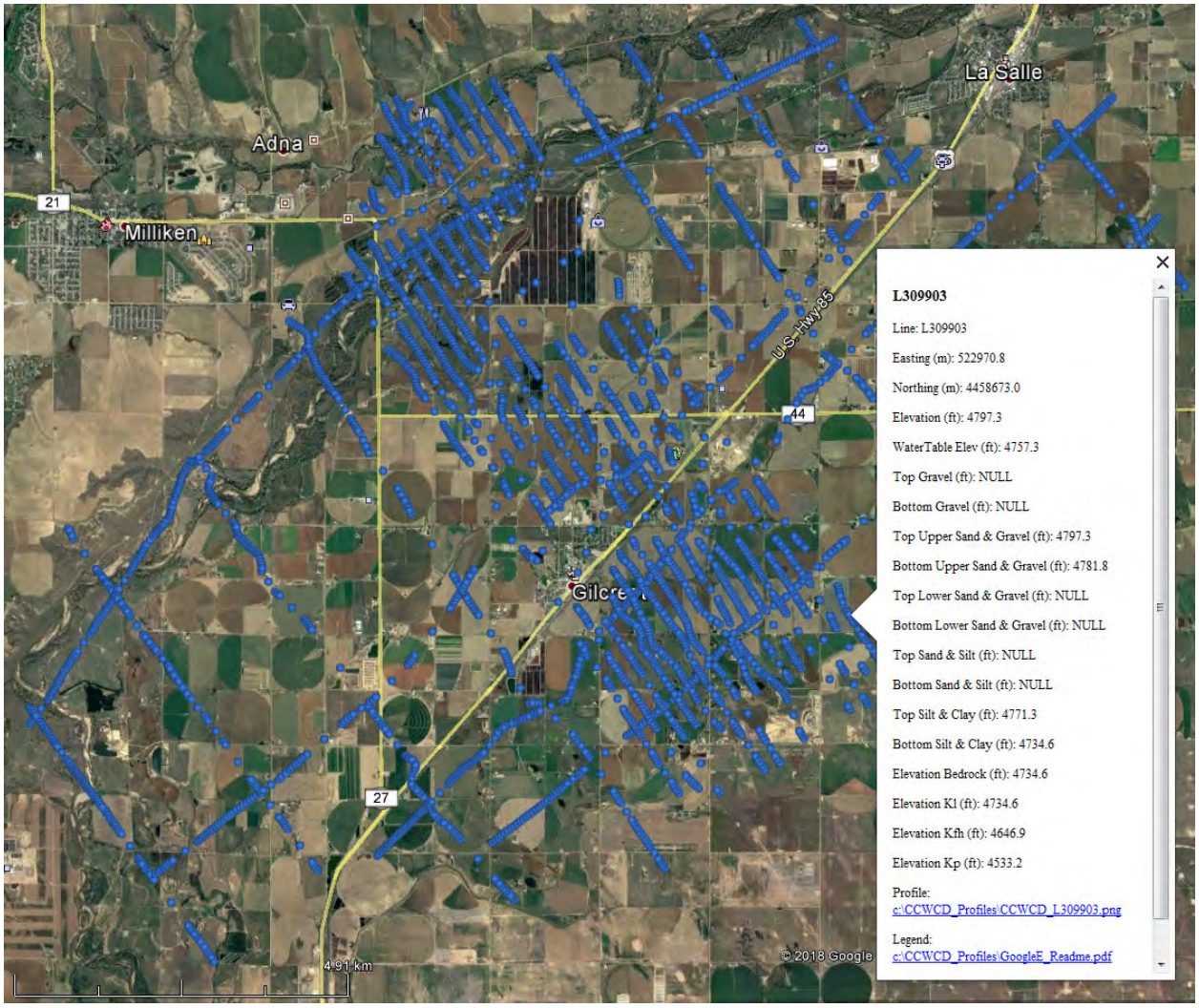

Figure 6-1. Example Google Earth image for the CCWCD Interpretation kmz.

7 References

Abraham, J.D., Cannia, J.C., Bedrosian, P.A., Johnson, M.R., Ball, L.B., and Sibray, S.S., 2011, Airborne electromagnetic mapping of the base of aquifer in areas of western Nebraska. U.S. Geological Survey, Scientific Investigations Report 2011-5219. https://pubs.er.usgs.gov/publication/sir20115219 (accessed April 16, 2018).

AGF, 2017, Hydrogeologic Framework of Selected Areas in the Twin Platte and Central Platte Natural Resources Districts, Prepared for the Central Platte and Twin Platte Natural Resources Districts: by Aqua Geo Frameworks, LLC, Mitchell, Nebraska. https://www.dropbox.com/s/re4rzd96e7g8t55/TPNRD-CPNRD_AEM_Hydrogeologic_Report_AGF_28Dec2017_v1.pdf?dl=0 (accessed April 14, 2018)

Andersen, K. R., Christiansen, A. V., Auken, E., and Nyboe, N. S., 2018 (submitted) Modeling and inversion of the TEM response during transmitter ramp-down, Geophysics, 25 p.

Asch, T.H., Abraham, J.D., and Irons, T., 2015, "A discussion on depth of investigation in geophysics and AEM inversion results", Presented at the Society of Exploration Geophysicists Annual Meeting, New Orleans.

Barkmann, P.E., Dechesne, M., Wickham, M.E., Carlson, J., Formalo, S., 2011, Cross-sections of the fresh-water-bearing strata of the Denver Basin between Greeley and Colorado Springs, Colorado: Colorado Geological Survey.

Barkmann, P.E., Horn, A., Morre, A., Pike, J., and Curtiss, W., 2014, Gilcrest/LaSalle pilot project hydrogeologic characterization report: Colorado Geological Survey, Report, Golden, CO, 253p.

Carney, C.P., Abraham, J.D., Cannia, J.C., and Steele, G.V., 2015, Airborne Electromagnetic Geophysical Surveys and Hydrogeologic Framework Development for Selected Sites in the Lower Elkhorn Natural Resources District: prepared for the Lower Elkhorn Natural Resources District by Exploration Resources International Geophysics LLC, Vicksburg, MS. http://www.enwra.org/LENRD2014AEMDataDownload.html

CDM Smith, 2013. South Platte Decision Support System Alluvial Groundwater Model Report, Prepared by CDM Smith for Colorado Water Conservation Board, April 2013.

Christiansen, A. V., and E. Auken, 2012, "A global measure for depth of investigation." *Geophysics,Vol. 77, No. 4* WB171-177.

Christensen, N. B., Reid, J. E., and Halkjaer, M., 2009, "Fast, laterally smooth inversion of airborne time-domain elecromagnetic data." *Near Surface Geophysics* 599-612.

Colorado Division of Water Resources (CO-DWR), 2018, Well permits and related lithologic logs accessed from DWR websites:(http://dwr.state.co.us/wellpermitsearch) , HydroBase, (http://water.state.co.us/DataMaps/DataSearch)

Colorado Water Conservation Board (CWCB), 2013, South Platte Decision Support System Alluvial Aquifer GIS data set: accessed from CWCB website, (http://cdss.state.co.us/GIS/Pages/Division1SouthPlatte.aspx).

Colorado Oil and Gas Conservation Commission, 2018, Website for downloads, GIS: http://cogcc.state.co.us/data2.html#/downloads

DatamineDiscover, 2017, Datamine Discover Profile Analyst, https://www.dataminediscover.com/discover (accessed on April 12, 2018)

Dechesne, M., Raynolds, R.G., Barkmann, P.E., and Johnson, K.R., 2011, Notes on the Denver Basin Geologic Maps: Bedrock Geology, Structure, and Isopach Maps of the Upper Cretaceous to Paleogene Strata in the Denver Basin between Greeley and Colorado Springs, Colorado. Colorado Geological Survey

Foged, Nikolaj, Esben Auken, Anders Vest Christiansen, and Kurt Ingvard Sorensen, 2013, "Test-site calibration and validation of airborne and ground based TEM systems." *Geophysics* 78, No.2: E95-E106.

Geosoft, 2018, Oasis montaj, v9.3.2, http://www.geosoft.com/products/geosoft-release-93

HydroGeophysics Group, Aarhus University, 2010, "Validation of the SkyTEM system at the extended TEM test site." Aarhus, Denmark.

HydroGeophysics Group, Aarhus University, 2011, "Guide for processing and inversion of SkyTEM data in Aarhus Workbench, Version 2.0."

Hobza C.M., Abraham, J.D., Cannia, J.C., Johnson, M.R., and Sibray, S.S., 2014. Base of Principal Aquifer for Parts of the North Platte, South Platte and Twin Platte Natural Resources Districts, Western, Nebraska. U.S. Geological Survey Scientific Investigations Map 3310. https://pubs.usgs.gov/sim/3310/ (accessed April 10, 2018).

Hurr, R.T., Schneider, P.A., Hofstra, W.E., Devenish, T.G., and Albin, D.R., 1972, Hydrogeologic characteristics of the valley-fill aquifer in the Greeley reach of the South Platte River valley, Colorado: U.S. Geological Survey, Open-File Report OF-73-124, scale 1:62,500.

Lindsey, D.,A., Langer, W., H., Knepper, D.,H., 2005, Stratigraphy, Lithology, and Sedimentary Features of Quaternary Alluvial Deposits of the South Platte River and Some of its Tributaries East of the Front Range, Colorado: U.S. Geological Survey Professional Paper 1705.

Robson, S.G., Heiny, J.S. and Arnold, L.R., 2000a, Geohydrology of the shallow Aquifers in the Fort Lupton-Gilcrest Area, Colorado USGS Hydrologic Investigations Atlas HA-746C.

Robson, S., G., Arnold, L., R., and Heiny, J., S., 2000b. Geohydrology of the shallow aquifers in the Greeley-Nunn Area, Colorado. Colorado USGS Hydrologic Investigations Atlas HA-746A.

Schamper, C., Auken, E., and Sorensen, K., 2014, *Coil response inversion for very early time modelling of helicopter-borne time-domain electromagnetic data and mapping of near-surface Geologic Layers.* European Association of Geoscientistis & Engineers, Geophysical Prospecting, v. 62, Issue 3, p. 658–674.

Sebol, L.A., and Barkmann, P.E., 2017, Addendum to the Gilcrest/LaSalle pilot project hydrogeologic characterization report: Colorado Geological Survey, Technical Memorandum, Golden, CO, 18p.

SkyTem Airborne Surveys Worldwide, 2018, SkyTEM304M. http://skytem.com/tem-systems/ (accessed April 16, 2018)

Smith, R.O., Schneider, P.A., Petri, L.R., 1964, Ground-Water resources of the South Platte River Basin in western Adams and southwestern Weld Counties Colorado: U.S. Geological Survey Water Supply Paper 1658.

Topper, R, Spray, K., L., Bellis, W.H., Hamilton, J., L., Barkmann, P., E., 2003, Groundwater Atlas of Colorado: Colorado Geological Survey, Special Publication 53

Topper, R., Meyer, R., Haworth, C.D., Donegan, M., Banks, K.C., Bandler, H., Flor, A., and Sares, M.A., 2017, The Upper Pierre Aquifer of the Cheyenne Basin, Northeastern Colorado, Geologic Cross Sections: Colorado Division of Water Resources, Water Resources Investigation 2017-1a

U.S. Geological Survey (USGS), 2016, The National Map, 2016, 3DEP products and services: The National Map, 3D Elevation Program Web page, http://nationalmap.gov/3DEP/3dep_prodserv.html (accessed March 3, 2018)

Viezzoli, A., Christiansen, A. V. , Auken, E., and Sorensen, K., 2008, "Quasi-3D modeling of airborne TEM data by spatially constrainted inversion." *Geophysics Vol. 73 No. 3* F105-F11

Wellman, T.P., 2015, Evaluation of groundwater levels in the South Platte River alluvial aquifer, Colorado, 1953–2012, and design of initial well networks for monitoring groundwater levels: U.S. Geological Survey Scientific Investigations Report 2015–5015, 67 p., http://dx.doi.org/10.3133/sir20155015.